GLUCOSE METABOLISM IN THE OUTER SEGMENTS OF PHOTORECEPTOR CELLS: ITS INVOLVEMENT IN THE PHOTOTRANSDUCTION PROCESS

by

SHU-CHAN HSU

B.Sc., University of British Columbia, 1988

A THESIS SUBMITTED IN PARTIAL FULFILLMENT OF

THE REQUIREMENTS FOR THE DEGREE OF

DOCTOR OF PHILOSOPHY

in

THE FACULTY OF GRADUATE STUDIES

DEPARTMENT OF BIOCHEMISTRY

UNIVERSITY OF BRITISH COLUMBIA

We accept this thesis as conforming

to the required standard

THE UNIVERSITY OF BRITISH COLUMBIA

April, 1993

© Shu-Chan Hsu,1993

In presenting this thesis in partial fulfilment of the requirements for an advanced degree at the University of British Columbia, I agree that the Library shall make it freely available for reference and study. I further agree that permission for extensive copying of this thesis for scholarly purposes may be granted by the head of my department or by his or her representatives. It is understood that copying or publication of this thesis for financial gain shall not be allowed without my written permission.

(Signature)

Department of BIOCHEMISTRY

The University of British Columbia
Vancouver, Canada

Date April 16, 1993

DE-6 (2/88)

ABSTRACT

The existence and function of glucose metabolism in the outer segments of photoreceptor cells were investigated using biochemical and immunocytochemical approaches. The presence of glycolytic enzymes in photoreceptor outer segments was detected by enzyme activity assays, Western blotting, and immunofluorescence microscopy. Activities of six glycolytic enzymes including hexokinase, phosphofructokinase, aldolase, glyceraldehyde-3-phosphate dehydrogenase, phosphoglycerate kinase, pyruvate kinase, and lactate dehydrogenase, were found to be present in purified rod outer segment preparations in quantities similar to that found in human red blood cells. Immunofluorescence microscopy of bovine and chicken retina sections labeled with monoclonal antibodies against glyceraldehyde-3-phosphate dehydrogenase, phosphoglycerate kinase, and lactate dehydrogenase have confirmed that these enzymes are present in rod and cone outer segments and are not simply contaminants from the inner segments or other retinal cells. One of these glycolytic enzymes, glyceraldehyde-3-phosphate dehydrogenase, was found to make up approximately 2 % of the total rod outer segment protein and over 11 % of the plasma membrane protein. It has been purified by affinity chromatography on a NAD^+-agarose column and shown to associate reversibly and electrostatically with a specific protein in the rod outer segment plasma membrane.

The rod outer segment plasma membrane was also found to contain a GLUT-1 type glucose transporter of M_r 45K as detected by 3-O-methylglucose uptake and exchange studies and Western blot analyses using type-specific glucose transporter antibodies. Solid-phase radioimmune competitive inhibition studies indicated that the rod outer segment plasma membrane contained 15 % the number of glucose transporters found in human red blood cell membranes and had an estimated density of 400 glucose transporter per $u m^2$ of rod outer segment plasma

membrane. Immunofluorescence microscopy indicated that both rod and cone outer segments have a GLUT-1 type glucose transporter.

The involvement of glucose metabolism in supporting the phototransduction process was studied by measuring the activities of glycolytic and hexose monophosphate pathways in isolated rod outer segments by spectrophotometric and radiometric enzyme assays. Glucose metabolism in rod outer segments was found to produce both ATP and NADPH required for the maintenance of phototransduction. ATP produced by glycolysis at a rate of 35-44 nmol/min/mg rod outer segment protein can potentially support cGMP regeneration, one of the most energy-consuming processes in phototransduction, under dark but not light conditions. NADPH produced by the hexose monophosphate pathway at a maximal rate of 40 nmol/min/mg ROS protein is sufficient to support the reduction of all-*trans*-retinal to all-*trans*-retinol in rod outer segments occurring at a rate of 1.2 nmol/min/mg ROS protein. A high hexose monophosphate pathway capacity suggests that the pathway may also be involved in supporting the glutathione redox cycle to protect rod outer segments from oxidative stress.

In summary, photoreceptor outer segments contain enzymes involved in glucose metabolism and a GLUT-1 type glucose transporter for glucose supply. Glucose metabolism in this organelle can potentially function to maintain a constant ROS cGMP concentration in dark, to buffer against sudden changes in cytoplasmic ATP concentration upon visual excitation and to supply NADPH required for visual recovery.

TABLE OF CONTENTS

CHAPTER 2

IDENTIFICATION OF A MAJOR PROTEIN ASSOCIATED WITH THE PLASMA MEMBRANE OF RETINAL PHOTORECEPTOR OUTER SEGMENTS AS GLYCERALDEHYDE-3-PHOSPHATE DEHYDROGENASE

CHAPTER 3

DETECTION OF GLYCOLYTIC ENZYMES AND A GLUT-1 GLUCOSE TRANSPORTER IN THE OUTER SEGMENTS OF ROD AND CONE PHOTORECEPTOR CELLS

CHAPTER 4

GLUCOSE METABOLISM IN THE OUTER SEGMENTS OF RETINAL PHOTORECEPTOR CELLS: ITS INVOLVEMENT IN THE MAINTENANCE OF THE PHOTOTRANSDUCTION PROCESS

LIST OF TABLES

LIST OF FIGURES

LIST OF ABBREVIATIONS

ADP ..... adenosine 5'-diphosphate

ALD ..... aldolase

ATP..... adenosine 5'-triphosphate

BCA ..... bicinchoninic acid

cGMP..... guanosine 3':5'-cyclic monophosphate

CTAB..... cetyltrimethylammonium bromide

EDTA.... ethylenediamine tetraacetate

FITC..... fluorescein isothiocyanate

G3PD..... glyceraldehyde-3-phosphate dehydrogenase

GDP..... guanosine 5'-diphosphate

GMP ..... guanosine 5'-monophosphate

GTP..... guanosine 5'-triphosphate

HEPES .. (N-[2-hydroxyethyl]piperazine-N'-[2-ethanesulfonic acid])

HK..... hexokinase

HMP ..... hexose monophosphate pathway

Ig..... immunoglobulin

LDH..... lactate dehydrogenase

M_r ..... molecular weight

NAD..... nicotinamide adenine dinucleotide

NADP.... nicotinamide adenine dinucleotide phosphate

PBS..... phosphate buffered saline

PFK..... phosphofructokinase

PGK..... phosphoglycerate kinase

PK..... pyruvate kinase

RBC ..... red blood cells

ROS..... rod outer segments

SDS ..... sodium dodecyl sulphate

TCA ..... tricarboxylic acid cycle

Tris ..... (Tris[hydroxymethyl]aminomethane)

w/v ..... weight per volume

ACKNOWLEDGEMENT

I would like to thank Dr. Robert Molday for his excellent supervision and support throughout my stay in his lab. I would also like to extend my gratitude to Laurie Molday, Dr. Greg Connell, Dr. Delyth Wong, Dr. Dale Laird, Dr. Jim Richards, Dr. Andy Goldberg and Sue Curtis for their patience in teaching me many biochemical, immunochemical, photographic and computer management techniques used in my studies. Much appreciation is also extended to my graduate student advisory committee (Dr. Philip Bragg, Dr. Roger Brownsey and Dr. Sid Katz) for their encouragement, helpful advice and letters of reference. I am also grateful to Drs. Ann Milam and Greg Hageman for disucussions relating to immunofluorescence microscopy of retina, to Dr. Gustav Lienhard for information about glucose transporter antibodies and to Drs. Langxing Pan and Peter G. Isaacson for their generous gift of Mab65 against lactate dehydrogenase, to Dr. Alison Buchan for the use of her Zeiss Microscope and to Andrea Dose, Michelle Illing, Orson Moritz and Dr. Andy William for enjoyable discussion sessions. Finally, I would like to thank my parents and my brother Yi-Te Hsu for their support and interest in my work.

CHAPTER 1

INTRODUCTION

1.1. RETINA

The neural retina is a highly specialized extension of the central nervous system responsible for light detection. In vertebrates, the retina is composed of six types of neurons: rod photoreceptors, cone photoreceptors, bipolar cells, horizontal cells, amacrine cells, and ganglion cells (Fig. 1). Light entering the eye first passes through the ganglion cell layer and finally reaches the photoreceptor cells where the phototransduction process, or the conversion of light energy to electrical potential, occurs. The photosignals in the form of electrical impulses are relayed from the photoreceptor cells to the ganglion cells and finally to the visual cortex in the brain.

1.2. PHOTORECEPTOR CELLS

In vertebrates, rod and cone photoreceptor cells are the light-sensitive cells of the retina. Rod photoreceptor cells mediate black-and-white vision under dim light. In humans, they have a diameter of 1-3 um and a length of 40-60 um and are primarily located in the peripheral region of the retina. The cone photoreceptor cells are responsible for color vision in daylight. In humans, they are 1-1.5 um in diameter and 75 um in length and are found in the macular (central) region of the retina (Shichi, 1983). Both types of photoreceptor cells can be divided into four compartments: an outer segment, an inner segment, a cell body and a synaptic terminus (Fig. 2). The outer segment, which is connected to the inner segment by a thin, nonmotile cilium junction, is a specialized organelle where the phototransduction process takes place. The inner segment and the adjacent cell

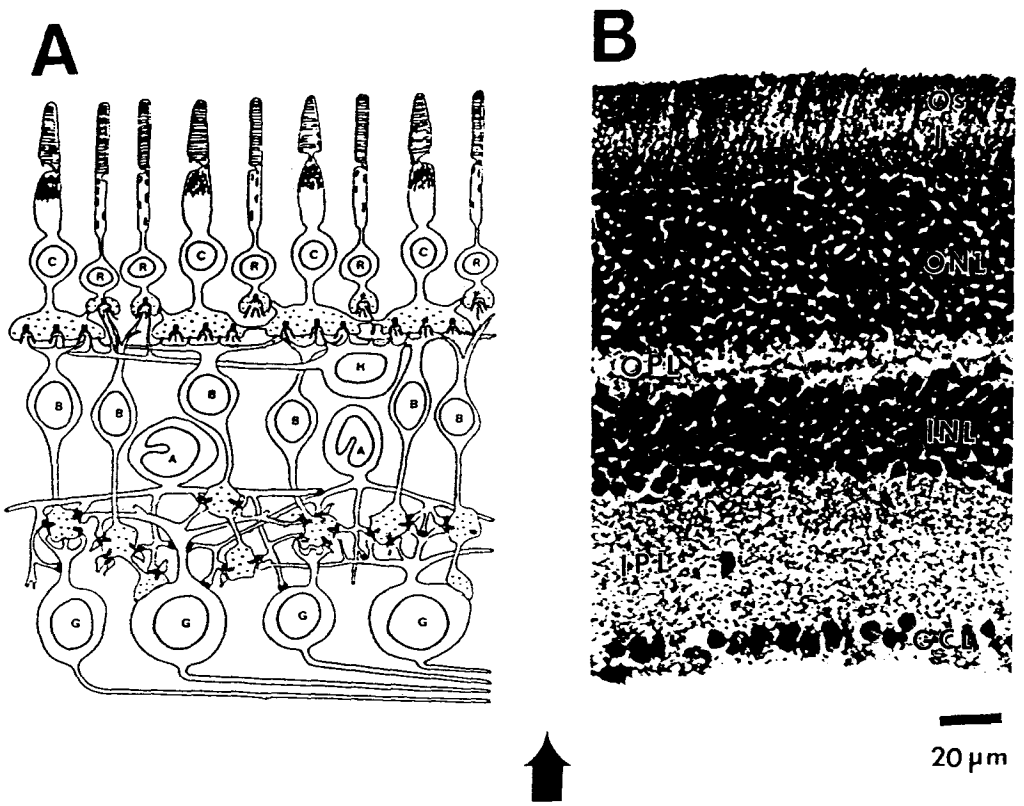

Fig. 1: **Synaptic connections of neural retina.**

Schematic diagram (**A**) and light micrograph stained with hematoxylin and eosin (**B**) showing layers of vertebrate retina. **Os**, outer segments of cone (C) and rod (R) photoreceptor cells; **Is**, photoreceptor inner segments; **ONL**, outer nuclear layer containing cell bodies of photoreceptor cells; **OPL**, outer plexiform layer containing synaptic connections among photoreceptor, bipolar (B) and horizontal (H)) cells; **INL**, inner nuclear layer containing cell bodies of bipolar, horizontal and amacrine (A) cells; **IPL**, inner plexiform layer containing synaptic connections among bipolar, amacrine and ganglion (G) cells; **GCL**, ganglion cell layer. The arrow indicates the direction of light entering the eye (diagram adapted from Shichi, 1983 and light micrograph adapted from Johnson and Blanks, 1984).

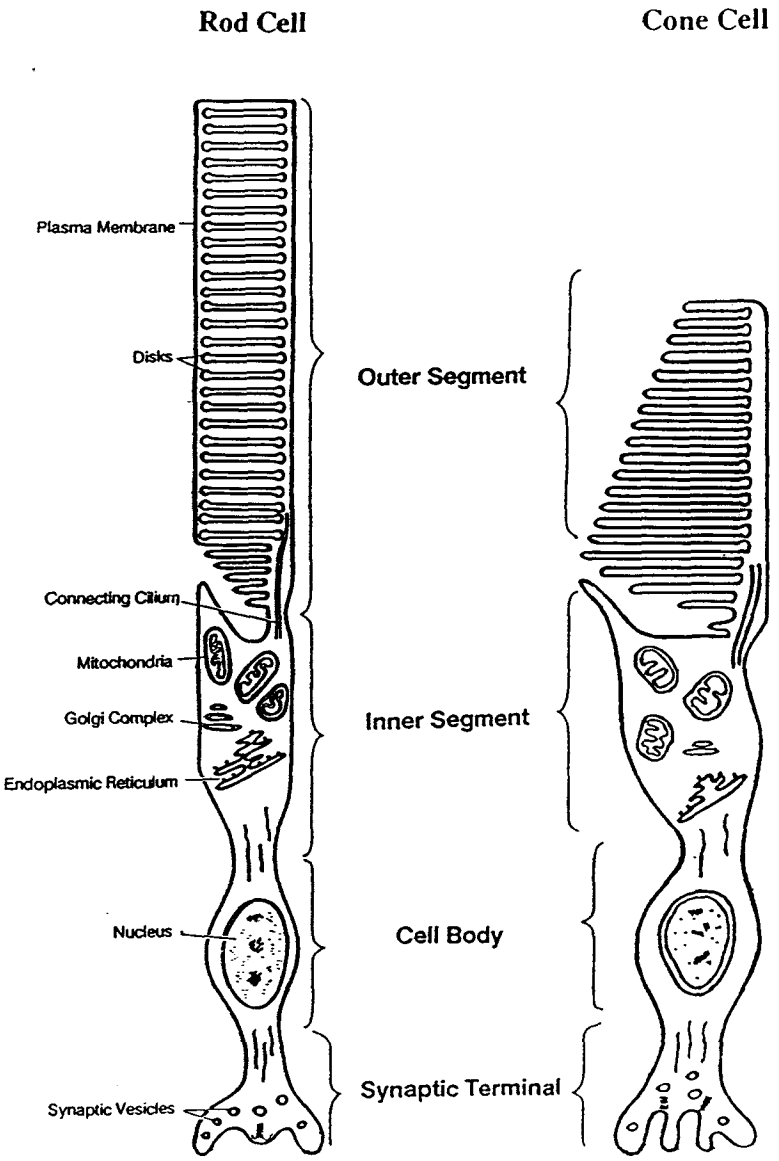

Fig. 2: **Schematic diagram of rod and cone photoreceptor cells.**
Both rod and cone photoreceptor cells can be divided into four compartments: the outer segment, the inner segment, the cell body and the synaptic terminus. The outer segment is connected to the inner segment by a cilium junction (diagram provided by Dr. Robert S. Molday).

body contain the primary metabolic (mitochondria) and biosynthetic machinery (endoplasmic reticulum, ribosomes, Golgi apparatus and nucleus) of the photoreceptor cell. The synaptic terminus modulates the secretion of neurotransmitters to the bipolar and horizontal cells.

1.3. PHOTORECEPTOR OUTER SEGMENTS

1.3.1. Structure

Cone and rod outer segments consist of a highly ordered array of about 2000 flattened disks surrounded by a plasma membrane (Fig. 2). In the cone outer segment, the disk membrane is continuous with the plasma membrane. In the rod outer segment, the disks are separate from each other and from the plasma membrane except at the proximal end of the outer segment where new disks are formed from evagination of the plasma membrane (Steinberg *et al.*, 1980). New disk and plasma membranes are constantly synthesized at the base of the outer segment to replace distal outer segment tips phagocytized by retinal pigment epithelial cells.

1.3.2. Protein composition

Because the cilium junction between the inner and outer segments of the rod photoreceptor cell is very fragile, rod outer segments (ROS) can be readily broken off from the retina and isolated by sucrose density centrifugation for biochemical studies (McConnell, 1965; Papermaster and Dreyer, 1974). Recently, the disk and plasma membranes of ROS have been separated from each other using a ricin-gold-dextran affinity density perturbation method (Molday and Molday, 1987) and shown to have different protein compositions. Protein compositional analysis of these two membranes indicates that with the exception of rod visual protein, rhodopsin, which is found in both disk and plasma membranes, ROS proteins are preferentially sorted

to either the plasma or disk membranes (Fig. 3). Known major disk and plasma membrane proteins are listed in Table I.

1.4. PHOTOTRANSDUCTION

Phototransduction is the process in which light initiates a cascade of events leading to the hyperpolarization of the photoreceptor cell. In rod photoreceptor cells, this process can be divided into three phases: dark state, visual excitation and visual recovery (Reviews: Kaupp and Koch, 1986; Yau and Baylor, 1989; Lolley and Lee, 1990; Pugh and Lamb, 1990; and Stryer, 1986,1991).

1.4.1. Dark state

In dark the resting membrane potential of a rod photoreceptor cell is maintained at -30 to -40mV. A steady state current (also called dark current) of 25 - 71 pA or 1.5 - 4.3 x 10^8 monovalent charges/sec/ROS has been detected flowing outward from the inner segment and inward into the outer segment of the rod photoreceptor cell (Fig. 4, refs. Hagins *et al.*, 1970; Baylor *et al.*, 1979a,b; Stryer, 1986). The inward current is carried by Na^+ (80-85 %), Ca^{2+} (10-15 %) and Mg^{2+} (3 %) entering the outer segment through a cGMP-gated cation channel (Yokishima and Hagins, 1970; Fesenko *et al.*, 1985; Yau and Nakatani, 1985; Hodgkin *et al.*, 1985; Nataki and Yau, 1988a; Cook and *et al.*, 1987,1989). The balancing outward current is carried by K^+ from the inner segment. Na^+ entering the outer segment is pumped out by a Na^+/K^+ ATPase in the inner segment (Sillmann *et al.*, 1969; Hagins *et al.*, 1970; Stirling and Lee, 1980). This pump maintains the Na^+ and K^+ gradients across the photoreceptor plasma membrane required for the perpetuation of the dark current. Ca^{2+} entering the outer segment is extruded by an electrogenic Na^+/Ca^{2+}-K^+ exchanger in the outer segment (Yau and Nataki, 1984; Schroder and Fain, 1984; Cook and Kaupp, 1988). Extrusion of

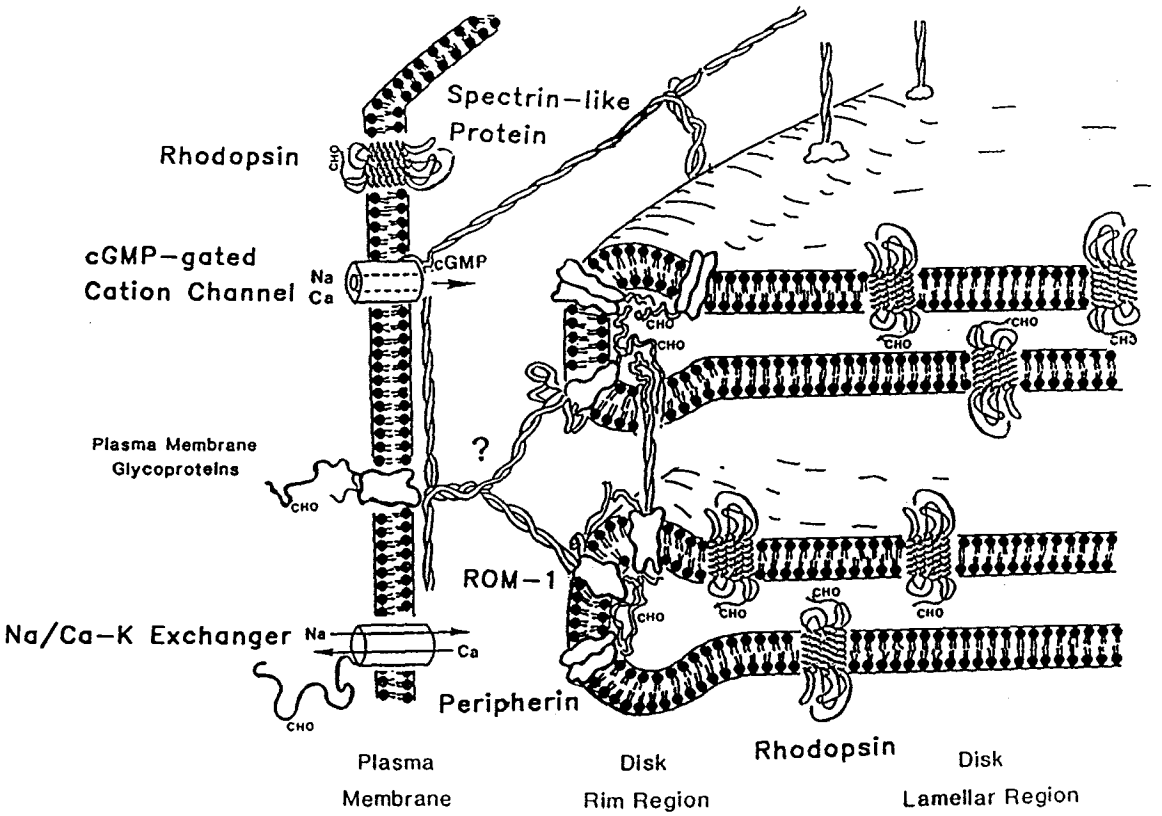

Fig. 3: **Differential protein composition in the plasma and disk membranes of rod photoreceptor outer segments.**

A proposed model for the localization of major disk membrane-specific proteins such as peripherin and ROM-1 and plasma membrane-specific proteins such as the spectrin-like protein, the cGMP-gated cation channel and the Na/Ca-K exchanger in rod photoreceptor outer segments. **CHO** denotes carbohydrate (diagram adapted from Dr. Robert S. Molday).

Table I
Major Proteins of Bovine ROS Disk and Plasma Membranes

Protein	MW (kDa)	Function
Disk membrane		
rhodopsin[a]	38	photon receptor[a]
peripherin	39	disk rim structure maintenance[b]
ROM-1	37	disk rim structure maintenance (interacts with peripherin)[c]
rim protein	220	unknown
Plasma membrane		
rhodopsin	38	photon receptor
G3PD[d]	34	glycolysis
cGMP-gated cation channel	69	allows Na^+ and Ca^{2+} to enter ROS
spectrin-like protein	240	associates with the cGMP-gated cation channel complex
Na^+/Ca^{2+}-K^+ exchanger	230	extrudes Ca^{2+} and K^+ in exchange for Na^+ entry into ROS

[a] *Rhodopsin is the only known protein found in both ROS plasma and disk membranes. It constitutes about 50 % of total plasma membrane protein and up to 90 % of total disk membrane protein.*
[b] *Hypothesized function; ref. Connell and Molday, 1991.*
[c] *Hypothesized function; ref. Bascom et al., 1992.*
[d] *Associated with the ROS plasma membrane under hypotonic conditions.*

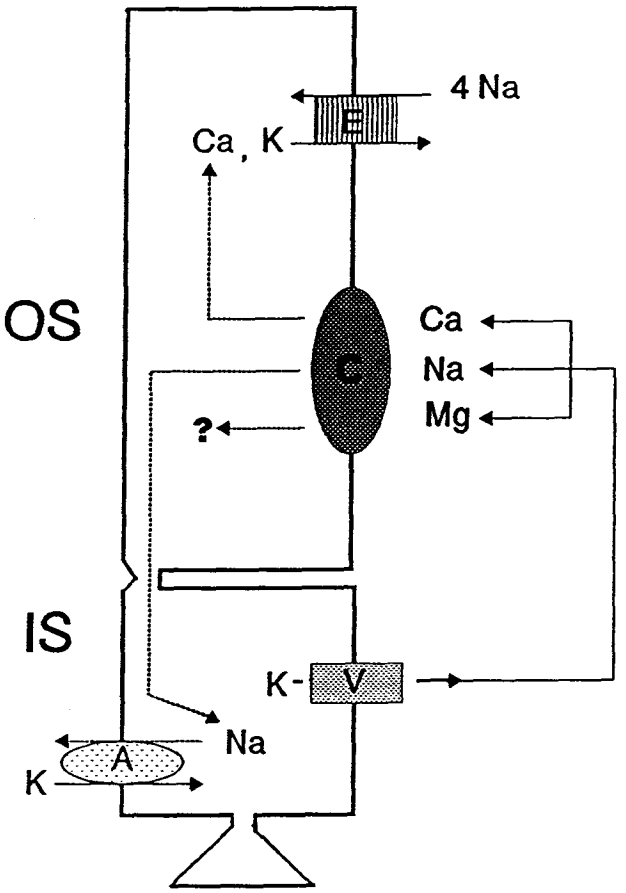

Fig. 4: **Dark current in the rod photoreceptor cell.**

The dark current consists of an outward current carried by K^+ from a voltage-gated K^+ channel (**V**) in the inner segment (IS) and an inward current carried by Na^+, Ca^{2+} and Mg^{2+} into the outer segment (OS) through a cGMP-gated cation channel (**C**). Na^+ entering the outer segment is eventually pumped out of the photoreceptor cell by a Na^+/K^+ ATPase (**A**) in the inner segment. Ca^{2+} entering the outer segment is extruded by a Na^+/Ca^{2+}-K^+ exchanger (**E**) in the outer segment. The extrusion mechanism of Mg^{2+} is still not known.

each Ca^{2+} is coupled to the influx of four Na^{+} and the efflux of one K^{+} (Schnetkamp, 1986; Cervetto *et al.*, 1989). The mechanism of Mg^{2+} extrusion is still unknown.

1.4.2. Visual Excitation

The process of visual excitation is a G protein mediated signal transduction pathway analogous to that initiated by hormones epinephrine and glucagon. In the case of visual excitation, light is the signal whose interaction with its receptor rhodopsin results in the activation of an effector enzyme (cGMP-phosphodiesterase) through a G protein (transducin). This process is illustrated in Fig. 5 and briefly described below:

1. Upon absorption of a photon, the 11-*cis*-retinyl chromophore of rhodopsin isomerizes to all-*trans*-retinal through a series of unstable intermediates leading to the release of all-*trans*-retinal from the rhodopsin apoprotein or opsin (review. Shichi, 1983). One intermediate, metarhodopsin II, formed within 1 msec after rhodopsin photobleaching, activates transducin (Emeis *et al.*, 1982 and Bennett *et al.*, 1982). This is the first amplification step in the visual cascade. One photoactivated rhodopsin can activate as many as 500 transducin molecules (Fung *et al.*, 1981).

2. Each transducin molecule has three subunits; α (39 kDa), β (36 kDa) and γ (8 kDa). Metarhodopsin II activates transducin by catalysing the exchange of GDP for GTP bound at the α subunit of transducin (Fung and Stryer, 1980; Kühn *et al.*, 1981; Fung, 1983). The α subunit with its bound GTP then dissociates from the $\beta\gamma$ subunits. The ease of α subunit dissociation from the $\beta\gamma$ subunits has been postulated to be modulated by the type of fatty acyl chain covalently linked to the amino terminus of the α subunit (Kokame *et al.*, 1992; Neubert *et al.*, 1992).

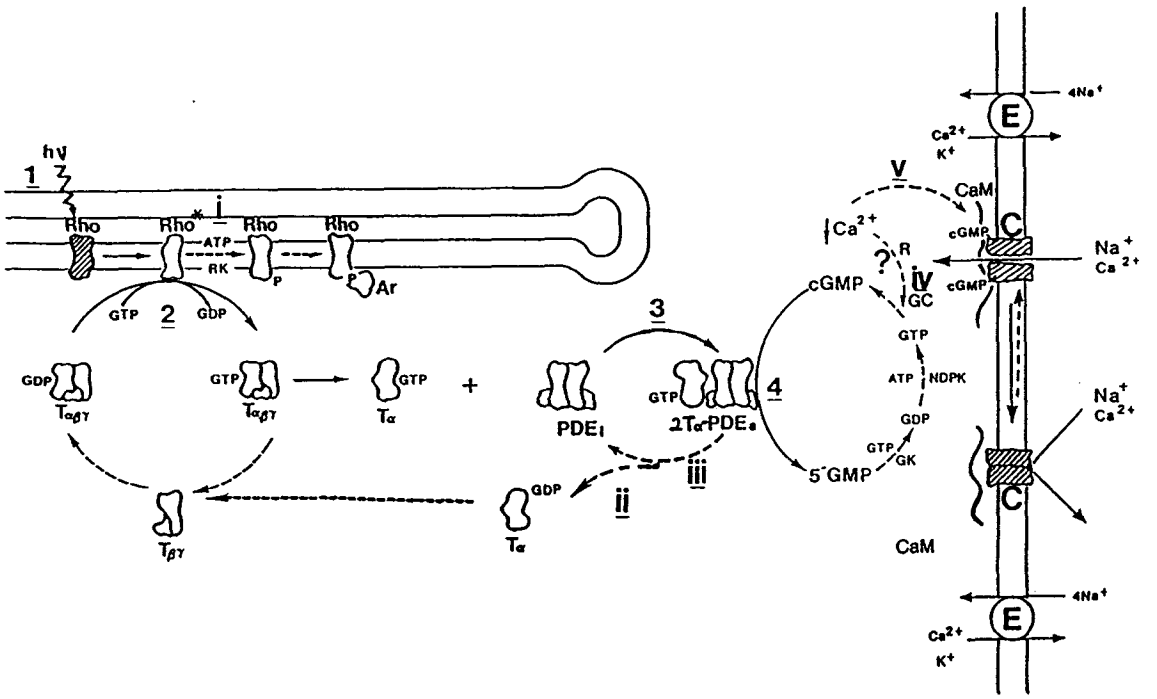

Fig. 5: **Visual excitation and recovery in the rod photoreceptor cell.**
This diagram illustrates the visual excitation (⟶) and recovery (- - -▸) pathways. These processes are described in more detail in sections 1.4.1, 1.4.2, and 1.4.3 (diagram adapted from Dr. R.S. Molday).

In the **visual excitation process**:
(1) Light activates rhodopsin (rho).
(2) Activated rhodopsin activates transducin (T).
(3) The α subunit of activated transducin then activates the cGMP-phosphodiesterase (PDE).
(4) Hydrolysis of cGMP to 5'GMP by PDE results in the closure of the cGMP-gated cation channel (C), preventing cations from entering the outer segment.

In the **visual recovery process**:
(i) Rhodopsin is inactivated by rhodopsin kinase (RK) and arrestin (AR).
(ii) Transducin α subunit is inactivated by GTP hydrolysis and reassociates with transducin $\beta\gamma$ subunits.
(iii) PDE is inactivated upon dissociation from transducin.
(iv) A decrease in the intracellular Ca^{2+} concentration due to a continuous extrusion of Ca^{2+} ions by the Na^+/Ca^{2+}-K^+ exchanger (E) results in the activation of guanylate cyclase possibly by recoverin (R). Cyclic GMP is resynthesized from GMP by guanosine monophosphate kinase (GK), nucleoside diphosphate kinase (NDK) and guanylate cyclase (GC).
(v) A low intracellular Ca^{2+} allows a calmodulin-mediated facilitated reopening of the cation channel.

The dissociated α subunit activates cGMP-phosphodiesterase (PDE), the effector enzyme in this signal transduction pathway.

3. Each PDE molecule consists of an α (88 kDa), a β (84 kDa) and two γ (11 kDa) subunits. Transducin activates PDE by relieving the inhibitory effect of PDE γ subunits on PDE $\alpha\beta$ subunits. It is still not clear whether this transducin α subunit-mediated relief of PDE inhibition is carried out by dissociating the inhibitory PDE γ subunits from the catalytic PDE $\alpha\beta$ subunits (Fung and Griswold-Prenner, 1989; Wensel and Stryer, 1990; Yamazaki *et al.*, 1990) or by changing the interaction between the PDE γ and $\alpha\beta$ subunits (Arshavsky and Bownds, 1992). Once activated, one PDE molecule can hydrolyze approximately 10^5 cGMP to 5'-GMP per second (Wheeler and Bitensky, 1977; Yee and Liebman, 1978; Woodruff and Bownds, 1979; Liebman and Pugh, 1980). This is the second amplification step in the visual excitation process.

4. In ROS, although the concentration of total cGMP is approximately 60 *u*M, the majority of cGMP is bound at the non-catalytic cGMP-binding site of PDE and is not readily available for binding to the cGMP-gated cation channel or for hydrolysis by PDE (Yamazaki *et al.*, 1980; Charbonneau *et al.*, 1990). An estimated concentration of 4-10 *u*M free cGMP maintains approximately 1-5 % of the total ROS cGMP-gated channel in their opened state in the dark (Nataki and Yau, 1988b). Since the cGMP-gated cation channel requires bound cGMP to remain open, a reduction in the free ROS cytoplasmic cGMP concentration due to cGMP hydrolysis by PDE upon illumination results in channel closure (Fesenko *et al.*, 1985; Koch and Kaupp, 1985). Closure of the channel decreases the permeability of ROS plasma membrane to cations, preventing the influx of Na^+, Ca^{2+} and Mg^{2+} into ROS (thus the inward dark current is decreased). A continual efflux of K^+ from the inner segment results in the hyperpolarization of the rod cell.

Unlike other neurons which have a threshold of stimulation, rod cells undergo a spatially limited hyperpolarization in response to the absorption of even one photon (Baylor *et al.*, 1979b). Amplification of the visual cascade in response to one photon can result in the hydrolysis of 10^5 cGMP and lead to a 0.2-1.5 pA decrease in the dark current or an average reduction of the influx of 5.3 x 10^6 Na^+ per second (due to closure of 300-400 channels or about 4% of the total opened cation channels, ref. Baylor *et al.*, 1979b; reviews, Stryer, 1986; Lolley and Lee, 1990). The magnitude of hyperpolarization is directly proportional to the number of rhodopsin molecules activated, to a maximum of about 10 rhodopsin activations per rod cell (Penn and Hagins, 1972; Baylor *et al.*, 1979a,b; Lamb *et al.*, 1981).

5. In the dark, neurotransmitters are continuously secreted from the synaptic terminus of rod photoreceptor cells. Hyperpolarization of the rod cell decreases the neurotransmitter secretion through an unknown mechanism. Subsequent events leading to the perception of vision are not well understood. The mechanism of the visual excitation in cone outer segments has not yet been extensively studied at the molecular level. However, it has been observed that cone photoreceptor cells are much less sensitive (25-100 times) and have a faster electrical response (several fold) to light than rod photoreceptor cells (review: Yau *et al.*, 1988).

1.4.3. Visual recovery (Fig. 5): Restoration of bleached ROS to the dark state requires the deactivation of proteins involved in the visual excitation process, reopening of the cGMP-gated cation channel to restore the dark current and regeneration of rhodopsin.

Quenching of visual cascade

Rhodopsin: Activated rhodopsin is deactivated 2-3 seconds after photoactivation, long before the spontaneous decay of metarhodopsin II to opsin

and all-*trans*-retinal (10^3 seconds at 20 °C). This inactivation results from phosphorylation of metarhodopsin II by rhodopsin kinase (Kühn and Dreyer, 1972; Miller *et al.*, 1986) and the binding of arrestin to phosphorylated rhodopsin (Wilden and Kühn, 1982; Kühn *et al.*, 1984; Zuckerman *et al.*, 1985). These reactions inhibit the interaction between transducin and metarhodopsin II.

Transducin: Transducin α subunit is deactivated by hydrolysis of its bound GTP to GDP due to its slow intrinsic GTPase activity (Kühn, 1980; Kühn *et al.*, 1981). This slow GTPase activity is accelerated by the binding of PDE, specifically the γ subunit of PDE, to the transducin α subunit (Arshavsky and Bownds, 1992). Binding of cGMP to PDE at the non-catalytic cGMP-binding sites on PDE $\alpha\beta$ subunits partially suppresses this acceleration (Arshavsky and Bownds, 1992). Following nucleotide hydrolysis, the α subunit with bound GDP is able to reassociate with transducin $\beta\gamma$ subunits.

PDE: Deactivation of PDE has been widely believed to be coupled to the hydrolysis of GTP bound to the transducin α subunit. Dissociation of transducin α subunit from the inhibitory PDE γ subunit allows the PDE γ subunit to inhibit the catalytic activity of the PDE $\alpha\beta$ subunits. A recent report by Erickson *et al.* (1992), however, suggests that PDE is inhibited by an unknown soluble inhibitor before transducin α subunit is inactivated by GTP hydrolysis. PDE is inactivated within seconds following the initiation of visual excitation (Sitaramayya and Liebman, 1983).

Reopening of the cGMP-gated cation channel

In the dark, the ROS cytosolic Ca^{2+} concentration is maintained at approximately 0.3 uM (McNaughton *et al.*, 1986; Ratto *et al.*, 1988; Korenbrot and Miller, 1989) by a balanced Ca^{2+} extrusion and re-entry cycle described above in 1.4.1 (Dark state). It has been hypothesized that Ca^{2+} is involved in reopening the

cGMP-gated channel by modulating the activity of two calcium-binding proteins: recoverin (which promotes the resynthesis of hydrolyzed cGMP) and calmodulin (which facilitates the reopening of the cGMP-gated cation channel).

Cyclic GMP resynthesis

Cyclic GMP hydrolyzed by PDE upon light stimulation is resynthesized from 5'GMP by guanosine monophosphate kinase (synthesis of GDP from GMP), nucleoside diphosphate kinase (synthesis of GTP from GDP) and guanylate cyclase (synthesis of cGMP from GTP). Unlike guanosine monophosphate kinase and nucleoside diphosphate kinase which are constitutively active, guanylate cyclase has been proposed to be activated only upon light illumination by a 26 kDa soluble activator protein, recoverin, in a Ca^{2+} dependent manner (Koch and Stryer, 1988; Dizhoor *et al.*, 1991; Lambrecht and Koch, 1991). In dark, guanylate cyclase is inactive because Ca^{2+} binding to recoverin prevents guanylate cyclase activation by recoverin. In light, closure of the cGMP-gated cation channel prevents the re-entry of Ca^{2+} ions extruded by the light-insensitive Na^+/Ca^{2+}-K^+ exchanger, thus resulting in a decrease in the cytoplasmic Ca^{2+} concentration to below 70 nM. A low cytoplasmic Ca^{2+} concentration causes Ca^{2+} to dissociate from recoverin, allowing recoverin to activate guanylate cyclase. Restoration of the Ca^{2+} levels to that in the dark state will again result in the binding of Ca^{2+} to recoverin and the inactivation of guanylate cyclase. A direct interaction between recoverin and guanylate cyclase, however, has not been detected. At present it is still controversial whether recoverin is the soluble factor that regulates guanylate cyclase activity.

Facilitated channel reopening: Calmodulin has been postulated to participate in facilitating the reopening of the cGMP-gated cation channel through its interaction with the spectrin-like protein associated with the cation channel complex (Hsu and Molday, 1993). Following visual excitation, a low cytoplasmic

Ca^{2+} concentration due to cGMP-gated cation channel closure results in the dissociation of calmodulin from the channel/spectrin-like protein complex. Dissociation of calmodulin causes the channel complex to switch to a high affinity conformation for cGMP, allowing the channel to reopen at a lower free cGMP concentration than that required to keep the channel open in the dark. This facilitates the recovery of the photoreceptor cell after visual excitation. Reopening of the cation channel restores the cytoplasmic Ca^{2+} concentration to its dark state level, allowing calmodulin to bind to the channel/spectrin-like protein complex. Reassociation of calmodulin causes the channel to switch to its low affinity cGMP-binding conformation. The channel, in its low cGMP affinity form, will now again be sensitive to small decreases in free cGMP concentration.

Regeneration of rhodopsin: Upon photoactivation of rhodopsin, all-*trans*-retinal released from activated rhodopsin is reduced to all-*trans*-retinol by a NADPH-specific retinol dehydrogenase (Wald, 1968; Lion *et al.*, 1975; and Ishiguro *et al.*, 1991) and transported to the retinal pigment epithelial cells by an interphotoreceptor retinoid binding protein (Bok and Heller, 1976; Liou *et al.*, 1982; Pfeffer *et al.*, 1983). In the retinal pigment epithelial cell, all-*trans*-retinol is converted to 11-*cis*-retinal through a series of enzyme catalyzed reactions and transported back to the ROS by the interphotoreceptor retinoid binding protein (Bok, 1985; Saari and Bredberg, 1988, 1989; Deigner *et al.*, 1989).

Upon reduction of all-*trans*-retinal to all-*trans*-retinol, arrestin is released from opsin which is then dephosphorylated by a phosphatase (Fowles *et al.*, 1989; Palczewski *et al.*, 1989). The newly synthesized 11-*cis*-retinal is transported back from retinal pigment epithelial cells and interacts with dephosphorylated opsin to regenerate rhodopsin.

1.5. GLUCOSE TRANSPORT

Transport of glucose into eukaryotic cells is mediated by two classes of glucose transporters: the facilitative glucose transporters and the Na^+-glucose cotransporter (reviews: Gould and Bell, 1990; Bell *et al.*, 1990; Kasanicki and Pilch, 1990; Thorens *et al.*, 1990 and Silverman, 1991).

1.5.1. Facilitative glucose transporters

This family of glucose transporters consists of five isoforms designated as GLUT 1, GLUT 2, GLUT 3, GLUT 4 and GLUT 5. Some physical properties of these isoforms are listed in Table II.

Structure: The primary sequences of these isoforms have been determined and shown to range from 492 to 524 amino acids in length. In humans, the isoforms share 39-65% identity and 50-70% similarity among each other. Hydropathy analyses, in conjunction with protease cleavage, antibody tagging and spectroscopic studies of the GLUT 1 isoform, suggest that all isoforms have twelve transmembrane helices with their N- and C- termini located on the cytoplasmic side of the plasma membrane. There is a single N-glycosylation site at the exofacial loop between transmembrane helices 1 and 2 (Fig. 6).

Transport mechanism: All transporter isoforms prefer D-glucose in the chair conformation as their substrate. Kinetic properties of these transporter isoforms are listed in Table II. Presently, the molecular mechanism of glucose transport has only been studied in detail for the GLUT 1 isoform in human red blood cells (Vidaver, 1966; review: Baldwin and Lienhard, 1981; Walmsley, 1988 and Silverman, 1991). According to the alternating conformation model, the transporter oscillates between inward- and outward-facing conformations (Fig. 7). A transport cycle involves the binding of a glucose molecule to one conformation of the transporter through hydrogen bonding at helices seven to eleven, followed by

Table II
Characteristics of Mammalian Glucose Transporters

Type	Tissue distribution	Size (no. of amino acids)	Kinetic properties
A) Facilitative glucose transporters			
GLUT-1	ubiquitous; most abundant in fetal placenta	492	human erythrocyte: - asymmetric - Vmax: uptake < exchange - Km: 5-30 mM (depending on assay condition)
GLUT-2	liver, kidney, intestines, pancreatic β cells	524	liver: - symmetric - Km: 20-66 mM intestines: - asymmetric - Km: 23-48 mM
GLUT-3	ubiquitous; very abundant in brain	496	?
GLUT-4	cardiac and skeletal muscle; brown and white fat	509	adipocyte: - symmetric - Km: 2-10 mM
GLUT-5	small intestines	501	?
B) Na^+/glucose co-transporter			
SGLT1	small intestines	664	intestines: - Km: -high affinity: 0.35 mM -low affinity: 6 mM

This table summarizes some physical and biochemical properties of glucose transporters reviewed by Kasanicki and Pilch (1990), Mueckler (1990), and Silverman (1991).

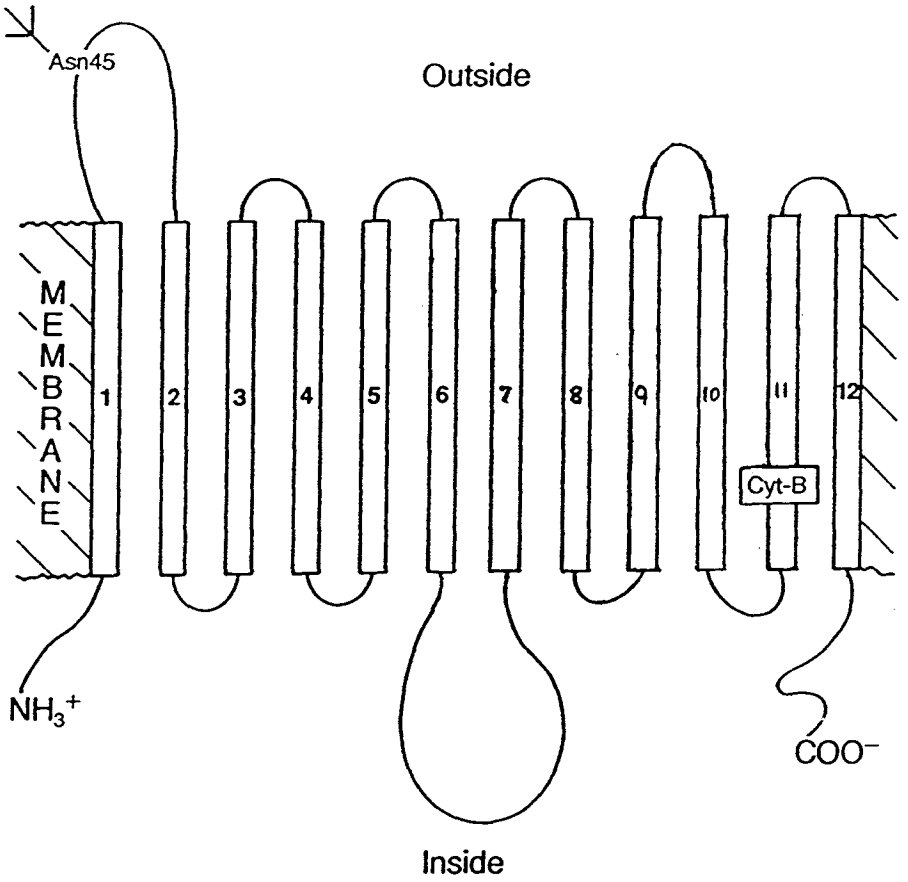

Fig. 6: **Structural model for facilitative glucose transporters.**

1-12 denotes eleven putative transmembrane α-helices in facilitative glucose transporters. **Asn 45** denotes the single asparagine-linked glycosylation site. **Cyt B** shows the proposed cytochalasin binding site. Cytochalasin B, an inhibitor of GLUT-1 type glucose transporter, binds to the cytoplasmic side of the transporter (diagram adapted from Walmsley, 1988).

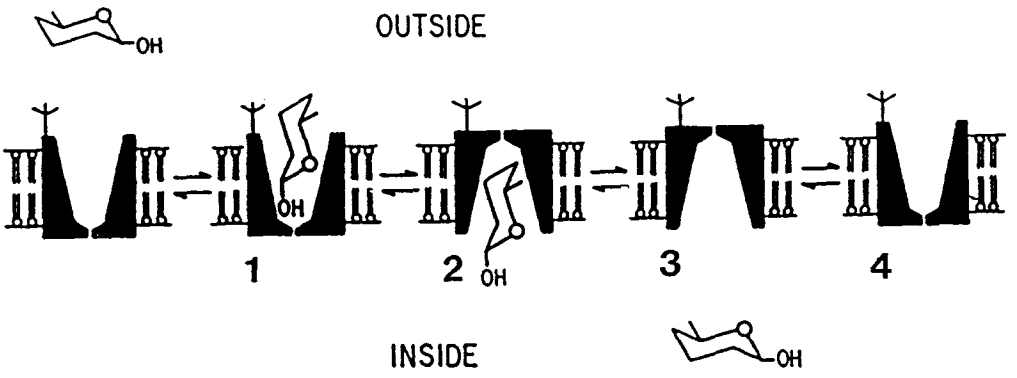

Fig. 7: **Schematic diagram illustrating the alternating conformation model for glucose transport by the GLUT-1 glucose transporter.**

According to the model, each glucose transport cycle starts with (**1**) the binding of glucose to one conformation of the transporter, follows by (**2**) the re-orientation of the transporter shuttling glucose to the other side of the membrane, and concludes with (**3**) the release of glucose from the transporter. The transporter (**4**) can return to the original conformation with or without bound glucose (diagram adapted from Baldwin and Lienhard, 1981).

reorientation of the transporter to the other conformation facing the opposite side of the membrane, and concludes with the release of glucose from the transporter. If there is a glucose concentration gradient across the membrane, the empty transporter will return to the opposite-facing conformation without glucose. This results in a net movement of glucose across the membrane until an equilibrium is achieved. Since transporter reorientation is the rate-limiting step and binding of glucose to the transporter facilitates this process, the rate of glucose transport across the membrane is faster under equilibrium exchange than under net transport conditions.

1.5.2. Na^+-glucose cotransporter

This type of transporter is detected only in specialized epithelial cells of small intestines and proximal tubules of kidney (Fig. 8).

Structure: The primary sequence of this type of transporter has been determined in humans and shown to contain 664 amino acids (Hediger *et al.*, 1987). Hydropathy analysis suggests that it contains 11 transmembrane helices with its N- and C- termini located at opposite sides of the membrane. There is a single N-glycosylation site at the exo-facial loop between helices 5 and 6. Presently it is not known if there is a family of Na^+-glucose cotransporters similar to that of facilitative glucose transporters.

Transport mechanism: Na^+-glucose transporter actively transports glucose against its concentration gradient by coupling with Na^+ uptake which is transported down its concentration gradient. The transport is electrogenic and does not involve co- or counter-transportation of other ions. It has been hypothesized that the transport mechanism involves the binding of Na^+ to the transporter, resulting in a conformational change in the transporter that increases its affinity for glucose.

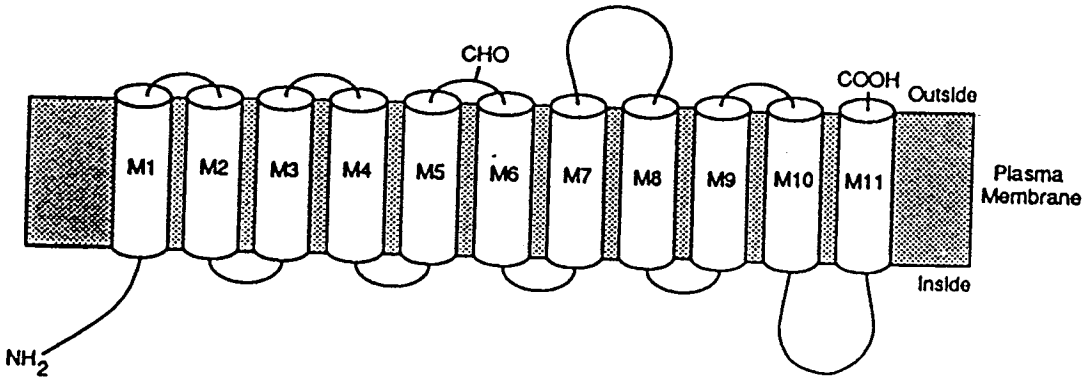

Fig. 8: **Structural model for Na^+-glucose co-transporter in plasma membrane.** **M1-M11** denotes eleven transmembrane helices in the transporter. **CHO** indicates the single glycosylation site (diagram adapted from Bell *et al.*, 1990).

Once a glucose molecule is bound, the transporter reorients to translocate both Na^+ and glucose to the other side of the membrane (Silverman, 1991).

1.6. GLUCOSE OXIDATION

Once glucose is inside the cell, it can be metabolized either by glycolysis and the citric acid cycle to produce energy in the form of ATP (via respiration in mitochondria) or by the hexose monophosphate pathway to produce reducing power in the form of NADPH (Fig. 9). Transaldolase and transketolase mediate the interconversion of sugar intermediates between glycolytic (fructose-6-phosphate and glyceraldehyde-3-phosphate) and hexose monophosphate pathways. This allows the channeling of sugar intermediates from the hexose monophosphate pathway back to the glycolytic pathway so that both NADPH (via the hexose monophosphate pathway) and ATP (via glycolysis) can be produced. Both glycolytic and hexose monophosphate pathways take place in the cytosol while the tricarboxylic acid cycle occurs within the mitochondrion.

1.7. PHOSPHOCREATINE SHUTTLE

In cells with immediate high energy requirements such as muscle, sperm and photoreceptor cells, a phosphocreatine shuttle has been hypothesized to mediate energy transport between mitochondria and the site of energy demand (Bessman and Geiger, 1981, Tombes and Shapiro, 1985 and Walliman *et al.*, 1986). According to this hypothesis, the phosphocreatine shuttle is driven by two isozymes of creatine kinase (Fig. 10). A mitochondrion-associated creatine kinase isozyme transfers the high energy phosphate group from respiration-derived ATP to creatine to produce phosphocreatine. Phosphocreatine diffuses to the target site where its high energy phosphate is transferred to ADP to produce ATP by a target site-specific creatine kinase isozyme. Creatine diffuses back to the mitochondrion and the cycle repeats.

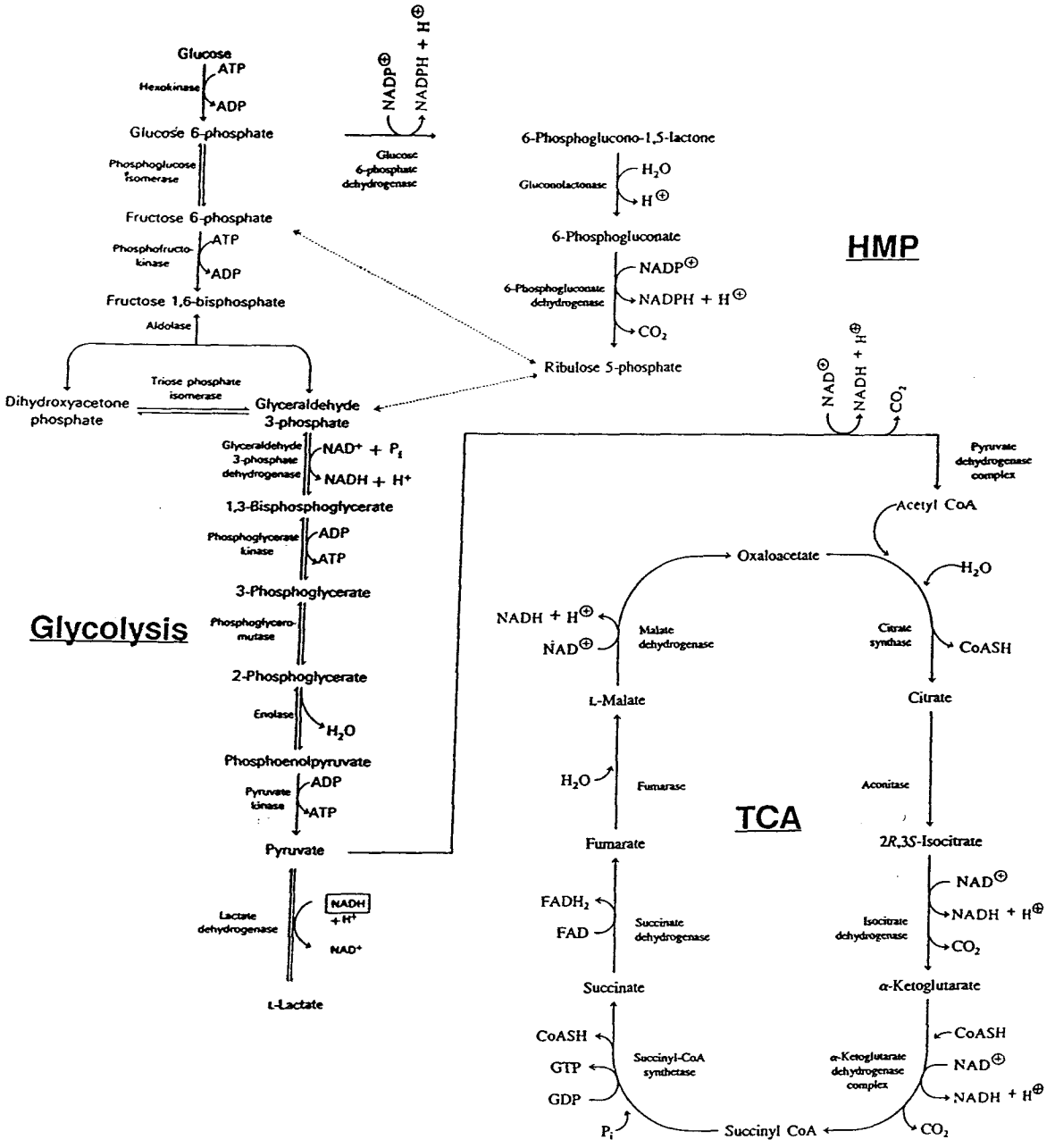

Fig. 9: **Glucose metabolism via glycolysis, the hexose monophosphate pathway and the tricarboxylic acid cycle.**

Glucose entering the glycolytic pathway can be oxidized via either the hexose monophosphate pathway (**HMP**) or the tricarboxylic acid cycle (**TCA**). Reversible reactions in the glycolytic pathway are indicated by double arrows. Dotted lines represent the interconversion of glycolytic and hexose monophosphate pathway intermediates by transaldolase and transketolase (diagram adapted from Stryer, 1988 and Rawn, 1989).

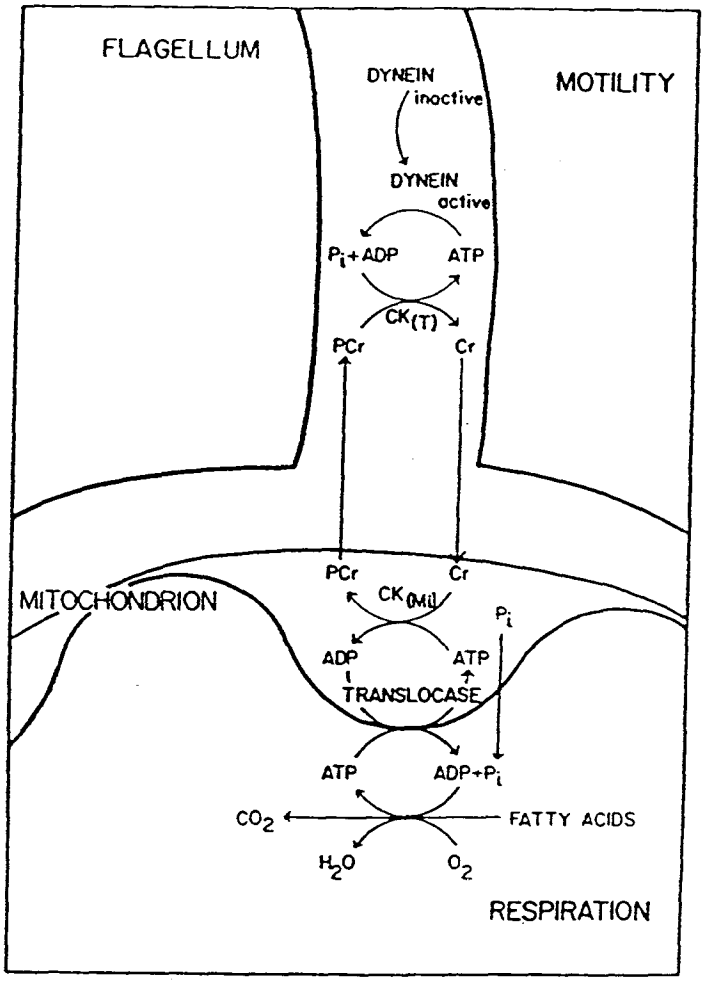

Fig. 10: **Phosphocreatine shuttle mediates high energy phosphate transport between sperm mitochondrion and flagellum.**

Phosphocreatine shuttle is driven by transphosphorylation reactions catalyzed by creatine kinase isozymes **CK(Mi)** in the mitochondrion and **CK(T)** in the sperm flagellum. In the mitochondrion, CK(Mi) transfers the high energy phosphate group from ATP produced during respiration to creatine (**Cr**). Phosphocreatine (**PCr**) produced by this reaction diffuses to the sperm flagellum where its high energy phosphate group is transferred to ADP by CK(T) to produce ATP required for flagellar motility. Creatine diffuses back to the mitochondrion and the cycle repeats again (diagram adapted from Tombes and Shapiro, 1985).

1.8. RETINAL GLUCOSE METABOLISM AND PHOTOTRANSDUCTION

The function of retina has been assessed either directly by measuring retinal electrical activities (ERG) or indirectly by quantitating retinal ATP content.

1.8.1. Electroretinogram

Electroretinogram or ERG was first recorded by Holmgren (1865) in studying retinal function by electrophysiology. It can be obtained either from transretinal recording of whole retina which measures the sum of electrical activities of all retinal cells or from intraretinal recording which selectively measures electrical activities of cells from a single layer of retina. The pattern of ERG recordings vary among different species and under different assay conditions (reviews: Brown, 1968 and Winkler, 1972, 1981b). ERG recorded *in vitro* and *in vivo*, however, has been shown to be essentially identical to each other in a number of animals and can therefore be used to evaluate retinal phototransduction in response to various metabolic stress *in vitro*. A typical ERG of neural retina begins with a hyperpolarizing *a*-wave followed by a depolarizing *b*-wave with superimposing oscillatory wavelets (Fig. 11). The *a*-wave or Fast PIII starts about 2.5 msec after light stimulation and reaches its peak amplitude after about 12 msec. It represents the hyperpolarization of photoreceptor cells due to a decrease in their membrane permeability to sodium ions (Brown, 1968). The *b*-wave or PII peaks approximately 50 msec after a light flash and and is believed to be due to the depolarization of bipolar or Müller cells (Miller and Dowling, 1970). The low amplitude oscillatory wavelets superimposed on the *b*-wave have been suggested to originate from bipolar and amacrine cells (Ogden, 1973). Postphotoreceptor potentials such as *b*-wave and oscillatory wavelets can be eliminated from ERG of rat retina by including sodium aspartate in the retina perfusion medium to block synaptic transmission from the photoreceptor cells to the postsynaptic neurons.

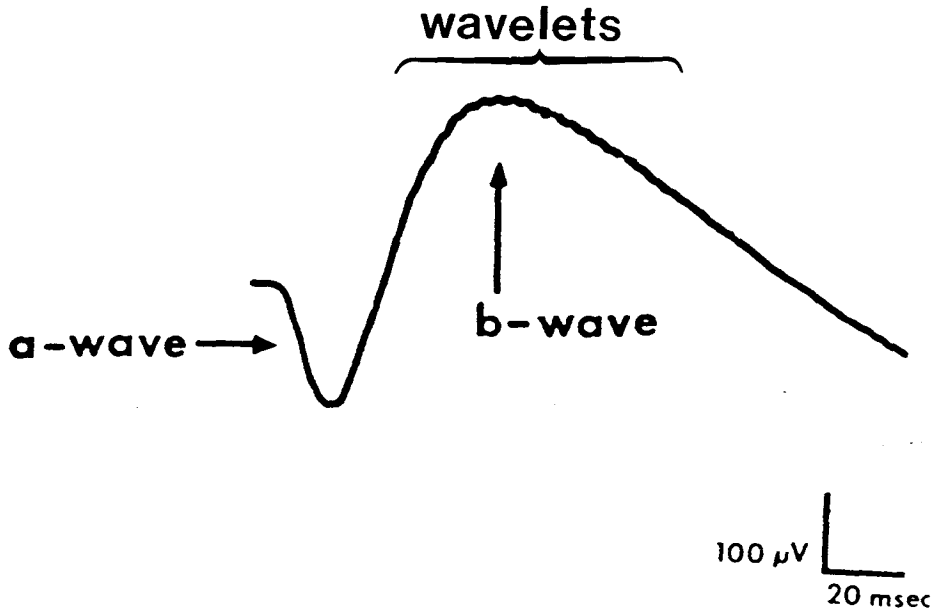

Fig. 11: **Electroretinogram illustrating the rat retinal response to light illumination.**

A typical electroretinogram in response to light consists of an *a*-wave and a *b*-wave with superimposing wavelets (diagram adapted from Winkler, 1981b).

Changes in the *a*-waves or the photoreceptor potential in response to various metabolic poisons can thus be utilized to assess the importance of glucose metabolism in supporting phototransduction.

1.8.2. Effects of glucose metabolism on retinal function

Parallel studies of ERG and retinal ATP content indicate that while the rate of retinal glucose metabolism is not stimulated by visual excitation, maintenance of the phototransduction process in photoreceptor cells is highly dependent on glucose metabolism (Cohen and Noell, 1960; and Winkler, 1981a,b). Inhibition of retinal glucose metabolism by removing the extracellular glucose or by adding the metabolic poison iodoacetate (which inhibits triose phosphate isomerase and glyceraldehyde-3-phosphate dehydrogenase in glycolysis) abolishes the photoreceptor potential. Glycolysis alone in the absence of aerobic glucose metabolism supports only 40 % of the optimal photoreceptor potential in the presence of physiological concentrations of glucose. Aerobic glucose metabolism alone in the presence of 5 mM pyruvate can maintain up to 95 % of retinal ATP content and photoreceptor potential in the presence of 5 mM pyruvate. Maintenance of a 100 % photoreceptor potential and retinal ATP content, however, requires the participation of both anaerobic (glycolysis) and aerobic (tricarboxylic acid cycle) glucose metabolism (Winkler, 1981b).

1.9. GLUCOSE METABOLISM OF RETINA

Glucose metabolism in the retina has been investigated *in vitro* using intact retinas and freeze-dried tangential retina sections. These studies showed that although vertebrate retinas are similar to each other in cellular organization, retinal glucose metabolism varies among different species. These differences may be

attributed to variations in the physical properties of the retinas such as cell density and thickness of various retinal layers, ratio of cones to rods, morphology of photoreceptor cells and blood (therefore nutrient and oxygen) supply to the retinas. In addition, the observed *in vitro* rate of retinal metabolism is approximately two fold higher than that expected *in vivo* and is affected by the concentration of ions such as bicarbonate, chloride, potassium, sodium, and calcium in the retina incubation media.

1.9.1. Intact retina

Studies with isolated whole retinas showed that retinal metabolism has three distinctive features compared to other tissues (Futterman and Kinoshita, 1959; Graymore, 1959, 1970; Cohen and Noell, 1960, 1965; Riley and Voaden, 1970 and Winkler, 1981a,b):

1. The retina has one of the highest respiratory rates compared to other tissues (average rate is approximately 1.5 *u*mol O_2/mg dry wt/hr). The respiratory rate of the brain cortex, for example, is only 50 % that of retina even though the retina is an extension of the central nervous system.

2. The retina has one of the highest glycolytic capacities compared to other tissues, converting glucose to lactate at a rate of 1.5 *u*mol lactate/mg dry wt. of retina/hr even in the presence of oxygen.

3. Glycolysis and respiration in retina are not as tightly coupled to each other, as demonstrated by comparatively small Pasteur and Crabtree effects in adult retinas. The Pasteur effect describes the stimulation of respiration and depression of glycolysis under aerobic conditions. In the retina, aerobic conditions depress the glycolytic lactate production by a maximum of only 50 %. The Crabtree effect is characterized by the depression of glycolysis and stimulation of respiration by the removal of glucose from the extracellular medium. Removal of glucose from the

retina incubation medium resulted in only a 10 % increase in retinal respiration. Both Pasteur and Crabtree effects are believed to be, in part, due to both competition for substrates and cofactors by aerobic and anaerobic glucose metabolic pathways and allosteric inhibition of glycolytic enzymes (especially phosphofructokinase) by intermediates and products from the citric acid cycle. A lack of these two effects suggests that aerobic and anaerobic glucose metabolic pathways may be separately compartmentalized in the retina.

The retina is also very rich in glucose-6-phosphate dehydrogenase, the first enzyme in the hexose monophosphate pathway (Shimke, 1959). Glucose taken up by the retina can be utilized by the hexose monophosphate pathway to produce NADPH required for retinal reduction and for protection of the retina against oxidative damage. When the retina is not under oxidative stress, the hexose monophosphate pathway produces approximately 23 % of the total carbon dioxide formed by the retina. This rate is increased at least three-fold when the retina is under oxidative stress. There is no appreciable recycling of glucose in the hexose monophosphate pathway (via the gluconeogenic pathway) under both aerobic and anaerobic conditions since only the first carbon of glucose is oxidized to CO_2 by the pathway when the citric acid cycle is inhibited (Futterman and Kinoshita, 1959; Cohen and Noell, 1960; Rahman and Kerly, 1961; Graymore and Towlson, 1965; review, Winkler, 1981b). Glycogen storage in the retina is very low and is primarily restricted to the Muller (glial) cells (Crane and Ball, 1951; Kuwabara and Cogan, 1961; Mizuno and Sata, 1975).

1.9.2. Photoreceptor cells

Glucose metabolism in photoreceptor cells was indirectly studied by comparing glucose metabolism in retinas lacking photoreceptor cells with that in normal retinas *in vitro* (Cohen and Noell, 1960; Graymore, 1959,1960; Graymore

and Tansley, 1959; Graymore, Tansley and Kerly, 1959). Retinas lacking fully developed photoreceptor cells can be obtained from either 7-day postnatal animals lacking fully developed photoreceptor cells, rats with degenerate visual cells due to retinitis pigmentosa or animals having resorbed photoreceptor cells due to intravenous iodoacetate administration.

The respiratory rate in retinas lacking photoreceptor cells is 12 to 60 % lower than that of normal retinas. Glucose oxidation accounts for 80 % of respiration in visual cells compared to only 55 % in non-visual cells indicating that glucose is the main substrate used by the photoreceptor cells for energy production. This may explain, in part, why photoreceptor cells are more sensitive to poisons which affect glucose metabolism (such as iodoacetate) than non-visual cells. A significant amount of energy (approximately 50 %) derived from glucose oxidation is used by the Na^+/K^+ ATPase in the photoreceptor inner segment for Na^+ and K^+ gradient maintenance (Winkler, 1981a). Glucose is not completely oxidized by the tricarboxylic acid cycle to CO_2. Approximately 20 % of carbon derived from glucose is used for the synthesis of glutamate, a neurotransmitter of the photoreceptor cells (Cohen and Noell, 1960; Morjaria and Voaden, 1979).

Glycolytic rates in retinas without visual cells was found to range from 50 - 100 % of values in normal retinas, depending on the species and conditions of tested animals. Assuming that the metabolism of other retinal cells is not affected by the absence of the photoreceptor cells from the retina, these observations suggest that the rate of respiration and glycolysis is higher, if not similar, in visual cells compared to other cells in the retina. The Pasteur and Crabtree effects are also more apparent in retinas lacking a photoreceptor cell layer, suggesting that there are very little or no Pasteur and Crabtree effects in the visual cells. These observations suggest that glycolysis and respiration are not tightly coupled to each other in the photoreceptor cells. Studies using retinas from postnatal animals

suggest that photoreceptor cells also have higher hexose monophosphate pathway activity than other non-visual cells in the retina.

1.9.3. Histochemistry of retina sections

Distribution of enzymes involved in glucose metabolism in retinas has been studied by quantitative histochemistry of freeze-dried retina sections. Activities of six glycolytic enzymes, hexokinase, phosphoglucoisomerase, phosphofructokinase, aldolase, glyceraldehyde-3-phosphate dehydrogenase, phosphoglyceromutase and lactate dehydrogenase, have been quantitated in the retina by Lowry *et al.* (1956, 1961, Fig. 12). Activity of the first glycolytic enzyme, hexokinase, was found to peak in the inner segments of photoreceptor cells near the choroidal blood supply. Activities of other glycolytic enzymes, however, were found to peak near the synaptic end of photoreceptor cells. This differential distribution of glycolytic enzymes may suggest that glycolysis is most active at the photoreceptor synaptic terminus. Alternatively, this may also reflect a mechanism by which glucose entering the inner segment from the blood supply can be drawn to the synaptic terminus located farther away from the blood supply by the formation of a glucose-6-phosphate gradient. Lowest glycolytic enzyme specific activities were found in photoreceptor outer segments and retinal pigmented epithelial cells. Activities of these enzymes in the outer segments were found to be 15 % or lower of that observed for brain.

Activities of tricarboxylic acid cycle enzymes malate and succinate dehydrogenases, as in the case of hexokinase, were found to peak at the ellipsoid region of the photoreceptor inner segment where all the mitochondria of the photoreceptor cell are located (Lowry, 1961; Wislocki and Sidman, 1954). Malate dehydrogenase showed a reciprocal retinal distribution pattern with respect to that of lactate dehydrogenase, an anaerobic glycolytic enzyme found in highest

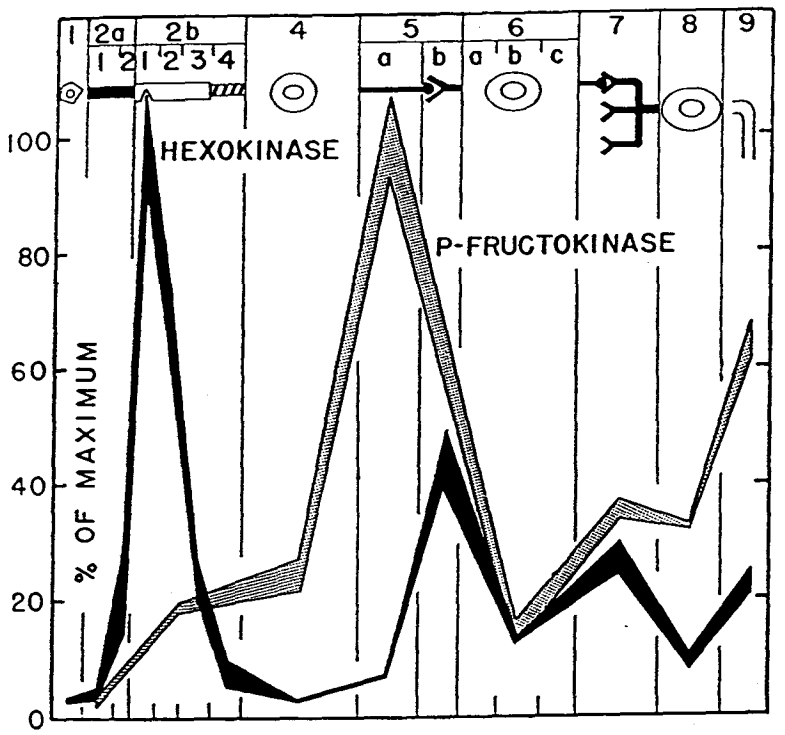

Fig. 12: **Localization of glycolytic enzymes in retina.**

Distribution profiles of hexokinase and phosphofructokinase activities show that while hexokinase is most abundant in photoreceptor inner segments, phosphofructokinase activity peak in photoreceptor synaptic termini. Enzymes involved in aerobic glucose metabolism such as succinate and malate dehydrogenases show retinal distribution patterns similar to that of hexokinase. Glycolytic enzymes (including lactate dehydrogenase) other than hexokinase exhibit retinal distribution patterns similar to that of phosphofructokinase. Glucose-6-phosphate dehydrogenase, the first enzyme in the hexose monophosphate pathway, is found in highest quantity in both photoreceptor inner segment and synaptic terminus. **1**, retinal pigment epithelial cells; **2a**, photoreceptor outer segments; **2b**, photoreceptor inner segments; **4**, outer nuclear layer; **5**, outer plexiform layer; **6**, inner nuclear layer; **7**, inner plexiform layer; **8**, ganglion cell body; and **9**, ganglion cell fibers (diagram adapted from Lowry *et al.*, 1961).

concentration near the synaptic terminus which is devoid of mitochondria. This is in agreement with intact retina studies suggesting that high rates of glycolysis under aerobic conditions in the retina may result from compartmentalization of enzymes involved in oxidative and anaerobic glucose metabolism in different parts of the retina.

Glucose-6-phosphate dehydrogenase and 6-phosphogluconate dehydrogenase, the first and third enzymes in the hexose monophosphate pathway, were found to be exceedingly rich in the photoreceptor inner segment and synaptic terminus (peak specific activity of glucose-6-phosphate dehydrogenase exceeds that of brain by a factor of 25). Activities of these two enzymes were found to be much lower in photoreceptor outer segment and other retinal cells.

Thus, results from both biochemical and histochemical studies suggest:

1. Photoreceptor cells have higher respiratory, glycolytic and hexose monophosphate pathway capacity than other non-visual cells in the retina.
2. Aerobic and anaerobic glucose metabolism in photoreceptor cells are not tightly coupled to each other due to differential compartmentalization of enzymes involved in the two pathways.

1.9.4. Photoreceptor outer segments

Although it is known that the maintenance of the phototransduction process in photoreceptor outer segments requires a large amount of energy and nucleotides such as GTP, ATP and NADPH, the source of its energy and nucleotide supply remains unclear.

Phosphocreatine shuttle: The inner segment contains all the mitochondria of the photoreceptor cell and exhibits much higher glycolytic enzyme activities than the outer segment (Lowry, 1956,1961; Lolley and Hess, 1969). This compartmentalization separating the phototransduction process in the outer

segment and glucose metabolism in the inner segment has led to a general view that energy required by the phototransduction process is supplied entirely by glucose metabolism in the inner segment. Localization of mitochondrial and brain-type creatine kinase isozymes in the inner and outer segments of photoreceptor cell, respectively, further suggests that a phosphocreatine shuttle analogous to that found in muscle, electric organ of *Torpedo marmorata* and sperm cells channels energy in the form of phosphocreatine from inner segment mitochondria to the outer segment (Wallimann, 1986). This hypothesis is supported by the detection of enzyme activities which rapidly transfer high-energy phosphate groups among adenine and guanine nucleotides and phosphocreatine (Dontsov *et al.*, 1978; Schnetkamp and Daemen, 1981).

Glucose metabolism in photoreceptor outer segments: McConnell *et al.* (1969), Futterman *et al.* (1970) and Schnetkamp (1981), on the other hand, have shown that isolated ROS contain glycolytic and hexose monophosphate pathway enzyme activities. Lactate and CO_2 production by isolated ROS in the presence of glucose indicate that both glycolytic and hexose monophosphate pathways are active in this organelle. Localization of a glycolytic enzyme, triose phosphate isomerase, in the outer segment layer of frozen bovine retina sections by enzyme histochemistry indicates that the observed enzyme activities are not likely due to contamination from other retinal cells (McConnell *et al.*, 1969). The detection of a phosphocreatine shuttle operating between the photoreceptor inner and outer segments and the presence of very low glycolytic enzyme activities in photoreceptor outer segments compared to other retinal layers, however, still favor the belief that phototransduction in the outer segment is maintained entirely by glucose metabolism in the inner segment.

1.10. THESIS INVESTIGATION

The principal objective of this thesis is to study the contribution of photoreceptor outer segment anaerobic glucose metabolism to the maintenance of the phototransduction process. In order to investigate the existence and function of photoreceptor outer segment glucose metabolism, glucose uptake and metabolic processes in this organelle were studied by activity assays, Western blot analyses and immunocytochemistry.

The first section of the thesis (Chapter 2) focuses on the identification and characterization of glyceraldehyde-3-phosphate dehydrogenase (G3PD), a glycolytic enzyme, in ROS. A major 38 kDa protein associated with ROS plasma, but not disk, membranes was identified to be G3PD by N-terminal sequence, specific activity and Western blotting analyses. Enzyme activity measurements indicate that G3PD makes up approximately 2 % of the total ROS protein and over 11 % of the ROS plasma membrane protein. Protease digestion and G3PD binding studies suggest that this enzyme reversibly interacts with a protease-sensitive plasma membrane-specific protein of ROS. The finding that G3PD is present in large quantities in ROS suggests that glycolysis may take place within this organelle.

Chapter 3 is devoted to the detection and characterization of glycolytic enzymes and a GLUT-1 type glucose transporter in photoreceptor outer segments. Enzyme activities of six glycolytic enzymes including the first and last enzymes in the glycolytic pathway were detected in purified ROS preparations. Localization of three glycolytic enzymes in the outer segment layer of both bovine and chicken retina sections indicate that glycolytic enzymes are present in both rod and cone photoreceptor outer segments and are not simply contaminants from the inner segments or other retinal cells. Glucose transport activity, Western blot and immunofluorescence microscopy analyses showed that both rod and cone outer

segment plasma membranes have a GLUT-1 type glucose transporter found in erythrocytes and brain cells.

Chapter 4 summarizes studies carried out to investigate the existence and function of glucose metabolism in rod photoreceptor outer segments. Glycolytic, hexose monophosphate and retinal reduction pathways were quantitated in purified ROS preparations. Glucose metabolism in ROS produces both ATP and NADPH required by phototransduction. A rate of 44 nmol ATP/min/mg ROS protein produced by glycolysis in ROS is sufficient to support cGMP regeneration, one of the major energy-consuming processes in phototransduction, under dark but not light conditions. The hexose monophosphate pathway in ROS can produce 40 nmol NADPH/min/mg ROS protein to support retinal reduction occurring at a rate of 1.2 nmol/min/mg ROS protein and the glutathione redox cycle to protect ROS from oxidative stress.

CHAPTER 2

IDENTIFICATION OF A MAJOR PROTEIN ASSOCIATED WITH THE PLASMA MEMBRANE OF RETINAL PHOTORECEPTOR OUTER SEGMENTS AS GLYCERALDEHYDE-3-PHOSPHATE DEHYDROGENASE

2.1. MATERIALS

2.1.1. Animal tissues: Fresh bovine eyes and blood were obtained from Intercontinental Packers (Vancouver, British Columbia).

2.1.2. Chemicals: NAD^+-C^6-hexane-agarose was purchased from Pharmacia LKB Biotechnology Inc. (Uppsala, Sweden), and Immobilon membranes were obtained from the Millipore Corp. (Bedford, MA). *Arthrobacter ureafaciens* neuraminidase was a product of Boehringer Mannheim Biochemicals (Indianapolis, IN). Bicinchoninic acid (BCA) protein assay reagents were purchased from Pierce (Rockford, IL). All other chemicals were from Sigma Chemical Co. (St. Louis, MO) or British Drug House Chemical Co. (Montreal, Quebec). Glyceraldehyde-3-phosphate was prepared from glyceraldehyde-3-phosphate diethylacetal monobarium salt (Sigma) using the Dowex-50 resin and stored at -70 °C.

2.1.3. Immunoreagents: Freund's complete adjuvant was purchased from Sigma Chemical Co.. Goat anti-mouse Ig antibodies were from Boehringer Mannheim Biochemicals. $Na^{125}I$ was obtained from New England Nuclear (Lachine, Quebec).

2.2. METHODS

2.2.1. Preparation of bovine ROS

ROS were prepared under dim red light from 100 freshly dissected bovine retinas as described by Molday and Molday (1987). Briefly, dissected retinas were gently agitated in a homogenization solution containing 20 % w/v sucrose, 10 mM β-D-glucose, 10 mM taurine, 0.25 mM $MgCl_2$ and 20 mM Tris-acetate, pH 7.4. The suspension was filtered through a Teflon 300 um mesh screen and approximately 5-8 ml filtrate was layered on a 28 - 60 % (w/v) sucrose gradient containing 10 mM taurine, 10 mM β-D-glucose, 0.25 mM $MgCl_2$ and 20 mM Tris-acetate, pH 7.4. After centrifugation in a SW 27 rotor (Beckman Instruments; Palo Alto, CA) at 25,000 rpm for 50 min at 4 °C, intact ROS were collected as a band near the top of the gradients. The collected ROS were washed once with 5-10 volumes of homogenization solution by centrifugation in a Sorvall SS-34 rotor (DuPont Co., Newton, CT) at 12,000 rpm for 10 min. The washed ROS were resuspended in the homogenization buffer at a protein concentration of 8-12 mg/ml and stored at -70 °C.

2.2.2. Isolation of ROS disk and plasma membranes

ROS plasma membrane was separated from disk membranes using a ricin-gold-dextran affinity density perturbation method previously described by Molday and Molday (1987). Briefly, ROS (20-80 mg) in 3-8 ml of homogenization solution were treated with 0.1 units of neuraminidase for 1 h, labeled with ricin-gold-dextran particles (approximate diameter, 15 nm), hypotonically lysed in 20 mM Tris-acetate buffer, pH 7.2, and treated with 0.4 ug/ml trypsin for 30 min to dissociate the disks from the plasma membrane. After trypsin digestion was stopped with excess soybean trypsin inhibitor, the disk membranes were separated from the ricin-gold-dextran-labeled plasma membrane by sucrose gradient centrifugation. The disk membrane band and the plasma membrane pellet were collected, resuspended in 10

% sucrose, 0.1 mM EDTA, 1 mM Na_2HPO_4, and 10 mM Tris-acetate, pH 7.2, and used immediately or stored at -70 °C until needed.

2.2.3. Preparation of bovine erythrocyte ghosts

Red blood cells and hemoglobin-free red blood cell ghosts were prepared according to the method of Fairbanks *et al.* (1971).

2.2.4. Purification of G3PD

All procedures were carried out at 4 °C, and all centrifugations were performed in a Sorvall SS-34 rotor at 15,000 rpm for 15 min. Bleached or unbleached ROS (90 mg) were lysed in 15 ml of 10 mM Tris-acetate buffer, pH 7.4, and washed twice by centrifugation with 15 ml of the same buffer containing 100 *u*M GTP to remove transducin and other peripheral proteins of ROS (Kühn, 1980). The ROS membranes were further extracted with 5 ml of NaCl extraction buffer (150 mM NaCl, 1 mM EDTA, 5 mM Na_2HPO_4, and 10 mM Tris-acetate at pH 7.4). After removal of the stripped ROS membranes by centrifugation, the NaCl extract containing G3PD was loaded onto a NAD^+-C^6-hexane-agarose column (0.5 mg -1.0 mg of NaCl extract per ml of beads) equilibrated with the NaCl extraction buffer. After the column was washed with 10 column volumes of 0.5 M NaCl, 1 mM EDTA, 5 mM Na_2HPO_4, and 10 mM Tris-acetate at pH 7.4, G3PD was eluted with the NaCl extraction buffer containing 10 mM NAD^+. A flow rate of 0.25 ml min^{-1} was used throughout the chromatography. Fractions containing the dehydrogenase activity were pooled and protein concentration was determined after dialysis against 0.1 mM EDTA and 5 mM Na_2HPO_4, pH 7.4, at 4 °C. G3PD was extracted from isolated ROS plasma membranes and purified by affinity chromatography by the same procedure. Bovine erythrocyte G3PD was also extracted by isotonic washes as described above for ROS membranes. The ROS membranes and purified ROS

plasma membranes after extraction were further washed with the NaCl extraction buffer by centrifugation until no significant G3PD activity (less than 1 % of the total G3PD activity associated with the membranes before NaCl extraction) was detected. These G3PD-stripped ROS membranes and purified plasma membrane were used in the G3PD binding assays.

2.2.5. Assay of G3PD activity

G3PD activity in ROS membranes, NaCl extracts of ROS membranes and purified G3PD preparations was monitored by following the reduction of NAD to NADH at 340 nm according to the method of Steck (1974). All assays were carried out in 30 mM sodium pyrophosphate buffer, pH 8.4, in a final volume of 0.5 ml, containing 12 mM sodium arsenate, 1 mM NAD, and 1.5 mM glyceraldehyde-3-phosphate. One unit of enzyme activity is defined as the production of 1 *u*mol of NADH at 25 °C/min/mg of protein using 6.22 x 10^3 M^{-1} cm^{-1} as the extinction coefficient for NADH.

2.2.6. Amino acid sequence analysis

The N-terminal sequence of NaCl-extracted 38 kDa protein from ROS plasma membrane and of the NAD^+-C^6-hexane-agarose column-purified G3PD was determined by the Protein Microchemistry Centre at the University of Victoria using an Applied Biosystems Gas-Phase Microsequenator. A protein search of the sequence was performed using a Swiss-Prot protein data base.

2.2.7. Generation of anti-G3PD monoclonal antibody

Hybridoma cell line gpd 2C11 was generated by fusion of NS-1 mouse myeloma cells with spleen cells from a BALB/c mouse immunized with NAD^+ affinity-purified bovine ROS G3PD as described by Lane *et al.*, 1986. Briefly, a

female Balb/c mouse was immunized with subcutaneous injections of 50 *u*g of G3PD emulsified in 0.1 ml of Freund's complete adjuvant at 3 week intervals. An intraperitoneal booster injection of 50 *u*g G3PD was given 14 days after the third immunization and cell fusion was carried out 5 days later. Approximately 1 x 10^8 spleen cells were fused with 5 x 10^7 mouse NS-1 cells in 1 ml 50 % polyethylene glycol 1500. Hybridoma cells secreting antibodies against G3PD were detected by solid phase ELISA 10-14 days following cell fusion. Culture supernatant from the cloned antibody secreting hybridoma cell line was used for Western blot analyses.

2.2.8. Conditions for extraction of G3PD from ROS membranes

The effect of salt, nucleotides and chelating agents on the extraction of G3PD from ROS membranes was studied as follows: 1 mg of ROS was lysed in 1 ml of 10 mM Tris-acetate buffer, pH 7.4, for 1 h at 4 °C. The ROS membranes were sedimented by centrifugation at 15,000 rpm for 15 min in a Sorvall SS-34 rotor. The ROS membrane pellet was resuspended in 50 *u*l of 10 mM Tris-acetate buffer, pH 7.4, containing 25-200 mM NaCl, 1 mM nucleotide, or 2 mM EDTA or EGTA. After incubation for 15 min at 4 °C, the supernatants were collected following centrifugation as above, and 25 *u*l was subjected to SDS-polyacrylamide gel electrophoresis. The relative quantity of extracted G3PD protein was determined by densitometry using a LKB Ultra Scan XL laser densitometer.

2.2.9. Binding of G3PD to ROS disk and plasma membranes

NAD^+ affinity-purified G3PD (75 *u*g) was added to a mixture of purified disk and plasma membranes prepared as described above (3 mg of ROS disk membranes and 0.15 mg G3PD-stripped ROS plasma membranes in a total volume of 500 *u*l) and dialyzed overnight against 0.1 mM EDTA, 5 % (w/v) sucrose, and 5 mM Na_2HPO_4, pH 7.4, at 4 °C. The unbound G3PD was separated from the membranes

by centrifugation in a Sorvall SS-34 rotor at 17,000 rpm for 30 min. The disk and plasma membranes were then separated on a 25 -60 % (w/v) sucrose gradient in 20 mM Tris-acetate, pH 7.4, by centrifugation at 45,000 rpm for 20 min in a TLS-55 rotor (Beckman Instruments). The association of G3PD with the membranes was assayed by both SDS-polyacrylamide gel electrophoresis and G3PD enzymatic activity.

2.2.10. Effect of trypsin and chymotrypsin on the G3PD binding sites on ROS membranes

All centrifugations were carried out in a SS-34 rotor at 15,000 rpm for 15 min and proteolytic digestion was carried out at 25 °C. Aliquots of 1 mg G3PD-stripped ROS membranes prepared as described above were treated with 10 *u*g/ml of either trypsin or chymotrypsin in 100 *u*l of 1 % sucrose, 0.1 mM EDTA and 5 mM Na_2HPO_4, pH 7.4 (buffer A). The digestion was stopped by transferring 25 *u*l aliqouts of digest to Eppendorf tubes containing appropriate protease inhibitors at 0 (before the addition of protease), 10 and 50 min intervals. Trypsin and chymotrypsin digestion were stopped with 20 *u*l of 1 mg/ml of soybean trypsin inhibitor and PMSF, respectively. The digested ROS membranes were then washed three times in 0.2 ml of buffer A before incubation for 30 min with 40 *u*l of 0.1 mg/ml NAD^+ affinity-purified G3PD previously dialyzed against 0.1 mM EDTA and 5 mM Na_2HPO_4, pH 7.4. The extent of G3PD binding to the membranes was monitored by measuring G3PD activity in both supernatants and membrane pellets following centrifugation.

2.2.11. Polyacrylamide gel electrophoresis

SDS-polyacrylamide slab gels were prepared and run as previously described (Molday and Molday, 1987), and gel slices were stained with Coomassie Blue or

electroblotted onto Immobilon membranes for Western blotting or N-terminal sequence analysis. Anti-G3PD monoclonal antibody gpd 2C11 and ^{125}I-labeled goat anti-mouse Ig (specific activity 1-2 x 10^6 dpm/*u*g) were used as primary and secondary antibodies, respectively, for Western blotting as previously described (Molday and Molday, 1987).

2.3. RESULTS

2.3.1. Identification of ROS 38 kDa protein as G3PD

N-terminal sequence analysis: Previous studies have indicated that the ROS plasma membrane isolated by the ricin-gold-dextran affinity density perturbation method under hypotonic conditions contains a major protein which migrates just above rhodopsin on SDS-polyacrylamide gels (Molday and Molday, 1987). This protein having an apparent molecular weight of 38,000 was absent in isolated ROS disk membranes (Fig. 13, *lanes a* and *b*). When the ROS plasma membrane was extracted with 0.15 M NaCl, the major M_r = 38,000 protein and minor proteins of M_r = 40,000 and 60,000 were released from the membrane (Fig. 13, *lane d*). The extracted ROS plasma membrane contained significantly reduced amounts of the 38-kDa protein (Fig. 13, *lane c*).

The N-terminal sequence of the extracted 38-kDa protein was determined after electrophoretic transfer onto Immobilon membranes. As shown in Fig. 14, the sequence of the N-terminal 22 amino acids is essentially identical to the N-terminal sequence of glyceraldehyde-3-phosphate dehydrogenase (G3PD) from bovine, porcine, rat, and human liver and muscle (Kulbe *et al.*, 1975; Nowak *et al.*, 1981; Arcari *et al.*, 1984; Fort *et al.*, 1985).

On the basis of this sequence identity, NAD^+-agarose affinity chromatography was used to further purify the 38-kDa protein from the NaCl

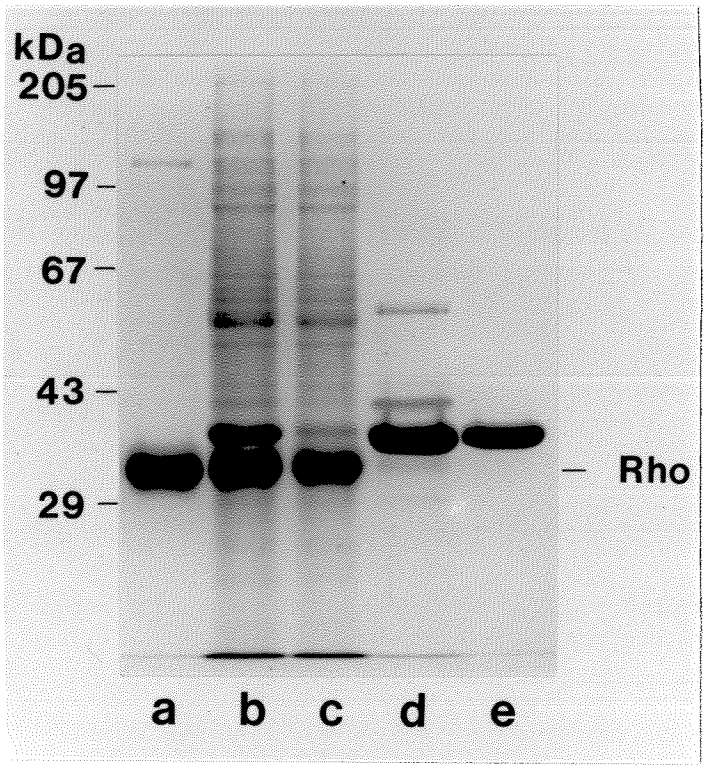

Fig. 13. **SDS-polyacrylamide gel electrophoresis of the 38 kDa protein isolated from ROS plasma membrane.**

Bovine ROS plasma membrane was separated from disk membranes by a ricin-gold-dextran affinity density perturbation method. The ROS plasma membrane was then extracted with 0.15 M NaCl and this extract was subjected to NAD^+-affinity chromatography. Samples (20-30 *u*g) were subjected to SDS-polyacrylamide gel electrophoresis on a 9% slab gel and stained with Coomassie Blue. *Lane a*, ROS disk membranes; *lane b*, ROS plasma membrane; *lane c*, ROS plasma membrane after extraction with 0.15 M NaCl; *lane d*, NaCl extract of the ROS plasma membrane; *lane e*, the 38 kDa protein purified from the NaCl extract by NAD^+-agarose affinity chromatography.

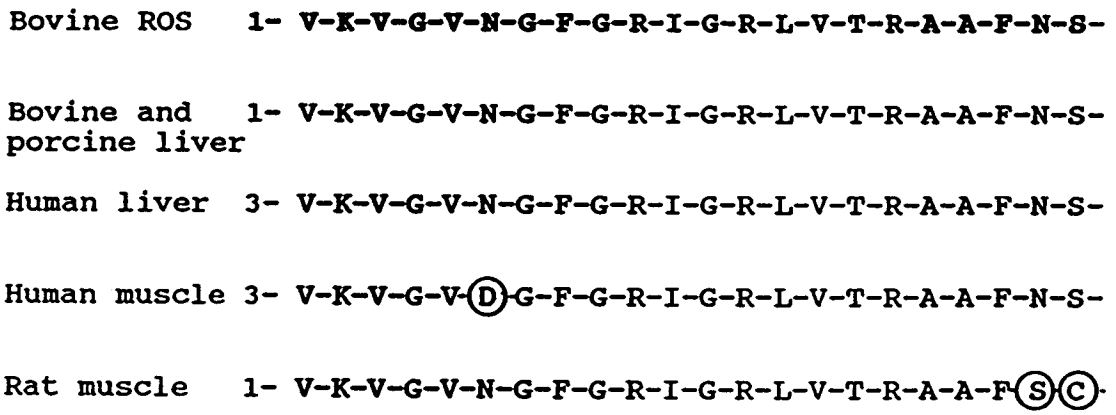

Fig. 14. **The N-terminal amino acid sequence of bovine ROS 38 kDa protein and homology to G3PD from other mammalian tissues.**

The sequence of the first 22 amino acid residues of bovine ROS 38 kDa protein isolated by NaCl extraction of ROS plasma membrane followed by NAD^+-affinity chromatography was determined by partial N-terminal amino acid sequencing. Sequences for other G3PD were obtained through the Swiss-Prot protein data base (Kulbe *et al.*, 1975; Nowak *et al.*, 1981; Arcari *et al.*, 1984; Fort *et al.*, 1985). Amino acid residues in the listed G3PD sequences which are different from ROS G3PD are circled. The position of the first amino acid residue of each displayed sequence in G3PD is indicated by the number preceding the sequence. A number "1" means the first amino acid residue of the sequence shown is the N-terminal amino acid residue of G3PD.

extract. As shown by SDS-polyacrylamide gel electrophoresis (Fig. 13, *lane e*), the 38 kDa protein was purified to homogeneity by this procedure.

Specific activity of G3PD purified from ROS and ROS plasma membranes: To further confirm the identity of the 38-kDa protein as G3PD and to obtain information on its abundance, the dehydrogenase activity was determined during purification of this protein from both ROS and isolated ROS plasma membranes. Tables III and IV show typical results obtained from the purification of G3PD from ROS and ROS plasma membranes.

Hypotonic lysis of ROS resulted in the recovery of 70-78 % of the G3PD activity in the ROS membrane fraction. Over 50 % of the lost G3PD activity was recovered in the supernatant fraction. Greater than 99 % of the G3PD activity associated with the ROS membrane fraction could be extracted from the membrane with 0.15 M NaCl. As shown in Table IV, the G3PD activity was associated with the plasma membrane fraction when the plasma membrane was separated from disk membranes by the ricin-gold-dextran affinity density perturbation method (Molday and Molday, 1987). The mild trypsin treatment of ROS membranes used to dissociate the plasma membrane from disk membranes did not result in significant loss in G3PD activity from the ROS membranes (Table IV). Approximately 60-75 % of the ROS membrane protein content was recovered in the disk and plasma membrane fractions, whereas approximately 30-40 % of the ROS membrane-associated G3PD activity was recovered in these fractions. It would appear that up to half of the G3PD is inactivated and/or released from the ROS plasma membranes during sucrose gradient centrifugation and subsequent washing procedures. Essentially all the membrane-bound G3PD activity is associated with the plasma membrane fraction (Table IV). In most isolated disk membrane preparations, no G3PD activity was detectable. In disk preparations which did contain G3PD activity (Table IV, for example), the specific activity was over 200-

Table III
Purification of Glyceraldehyde-3-phosphate Dehydrogenase From Bovine ROS

	Protein (mg)	Specific Activity (Units/mg)	Total Activity (units)	% Activity Recovered
Intact ROS	91	1.8	164	100
Lysed ROS	73	1.8	128	78
NaCl Extract	1.2	95	114	70
NAD^+-agarose	1.0	95	95	58

Table IV
Purification of Glyceraldehyde-3-phosphate Dehydrogenase From Purified Bovine ROS Plasma Membranes

	Protein (mg)	Specific Activity (Units/mg)	Total Activity (units)	% Activity Recovered
Ricin-gold ROS	19	1.9	37	100
Lysed ROS	16	1.6	26	70
Trypsinized ROS	16	1.5	24	65
Disk membranes[a]	12	0.04	0.5	1
Plasma membranes	0.67	11.0	7.4	20
NaCl Extract	0.08	92.5	7.4	20
NAD^+-agarose	0.07	91.4	6.4	17

[a] *Activity quoted in this table represents an upper limit in the amount of G3PD activity associated with the disk membranes; most preparations did not have detectable G3PD activity associated with the disk membranes.*

fold lower than that for the plasma membrane fraction. This residual activity present in some isolated disk preparations is most likely derived from contaminating plasma membrane fragments which are not completely dissociated from the disks during trypsin treatment (Molday and Molday, 1987).

The specific activity of G3PD isolated from total ROS membranes (Table III) or from plasma membranes (Table IV) by NaCl extraction and NAD^+-agarose affinity chromatography was 90-100 units/mg. This is within the range of specific activities reported for G3PD isolated from other mammalian systems (Heinz and Kulbe, 1970; Dagher and Deal, 1977; Kulbe *et al.*, 1982; Wang and Alaupovic, 1980). Comparison of the specific activities of G3PD in ROS and ROS plasma membranes with that of the purified enzyme indicates that G3PD constitutes about 2 % of the total ROS protein and over 11 % of the plasma membrane protein (Tables III and IV).

Purification of G3PD from ROS was also monitored by SDS-gel electrophoresis (Fig. 15). On 9 % SDS-polyacrylamide gels, G3PD co-migrates with the α and β subunits of ROS transducin. On gradient gels, however, these three components were resolved with G3PD migrating between the α- and β-transducin subunits (data not shown). After removal of transducin with GTP, G3PD was extracted with 150 mM NaCl and purified to homogeneity as a 38 kDa protein by NAD^+-agarose chromatography. As in the case of G3PD from other systems, bovine ROS G3PD was found to have a molecular weight of approximately 140,000 by gel filtration chromatography under non-denaturing conditions. Accordingly, ROS G3PD, like G3PD from various muscle sources (Harris and Perham, 1965 and Harrington and Karr, 1965), appears to be a tetrameric protein composed of identical subunits.

Monoclonal antibody to G3PD: Monoclonal antibody gpd 2C11 raised against NAD^+ affinity-purified ROS G3PD was found to bind to G3PD in both

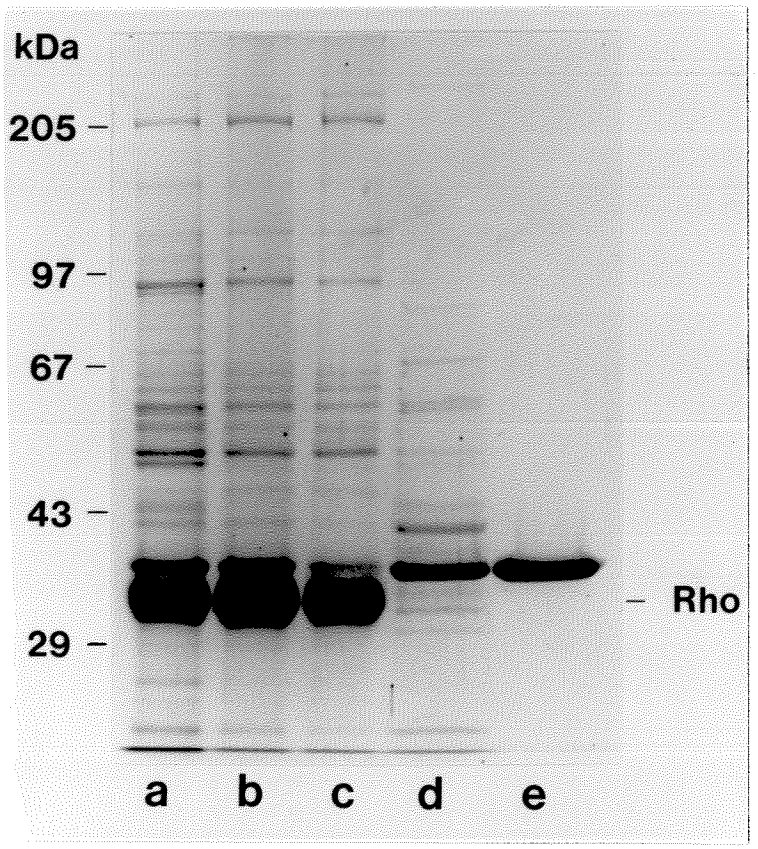

Fig. 15. **Purification of the 38 kDa protein from bovine ROS membranes.**
ROS which were hypotonically lysed and washed with GTP were further extracted with 0.15 M NaCl. The 38 kDa protein was isolated from this extract by NAD^+ affinity chromatography. Samples (20-30 *u*g) were subjected to SDS gel electrophoresis on a 9% polyacrylamide slab gel and stained with Coomassie Blue. *Lane a*, ROS isolated from a sucrose gradient; *lane b*, hypotonically lysed ROS membranes washed with 0.1 mM GTP; *lane c*, ROS membranes after extraction with 0.15 M NaCl; *lane d*, NaCl extract of ROS membranes; *lane e*, the 38 kDa protein purified from the NaCl extract by NAD^+-agarose affinity chromatography.

bovine ROS and bovine red blood cells by Western blotting (Fig. 16, *lanes a* and *b*). Extraction of erythrocyte ghosts with 150 mM NaCl resulted in a complete elution of G3PD from red blood cell ghosts (Fig. 16, *lanes d* and *f*). Two faint protein bands in the molecular mass range of 38-39 kDa were visible on the SDS-polyacrylamide gel following the NaCl extraction of ROS plasma membrane (Fig. 16, *lanes c*). The residual G3PD associated with the ROS plasma membrane was likely due to nonspecific adsorption of G3PD to ricin-gold-dextran particles since G3PD could be completely extracted from lysed ROS membranes. A small amount of G3PD was degraded by trypsin during the plasma membrane purification process, generating fragments of G3PD which still bind to the plasma membrane (Fig. 16, *lanes a*). Monoclonal antibody gpd 2C11 was found to cross-react with G3PD from human red blood cells and rabbit skeletal muscle (data not shown).

2.3.2. Nature of G3PD binding to ROS membranes

Conditions for G3PD elution from ROS membranes: The effect of NaCl concentration on the elution of G3PD from hypotonically lysed ROS membranes was studied. As shown in Fig. 17, a sigmoidal relation was apparent for the release of G3PD as a function of NaCl concentration. Half-maximum release was obtained at a concentration of 120 mM NaCl, and 95 % of maximum release was obtained at 150 mM NaCl. Other salts such as KCl and Na_2HPO_4 were also effective in releasing G3PD from ROS membranes indicating that ionic strength was the contributing factor. Extraction of G3PD was found to be independent of the state of bleaching of the ROS. In agreement with human erythrocyte G3PD (Kant and Steck, 1973; Shin and Carraway, 1973), 1 mM ATP and NADH partially released G3PD from ROS membranes (Table V). Other nucleotides including NAD, cGMP and cAMP, and chelating agents including EDTA and EGTA resulted in the release of less than 10 % of G3PD activity from ROS membranes. The basis for this

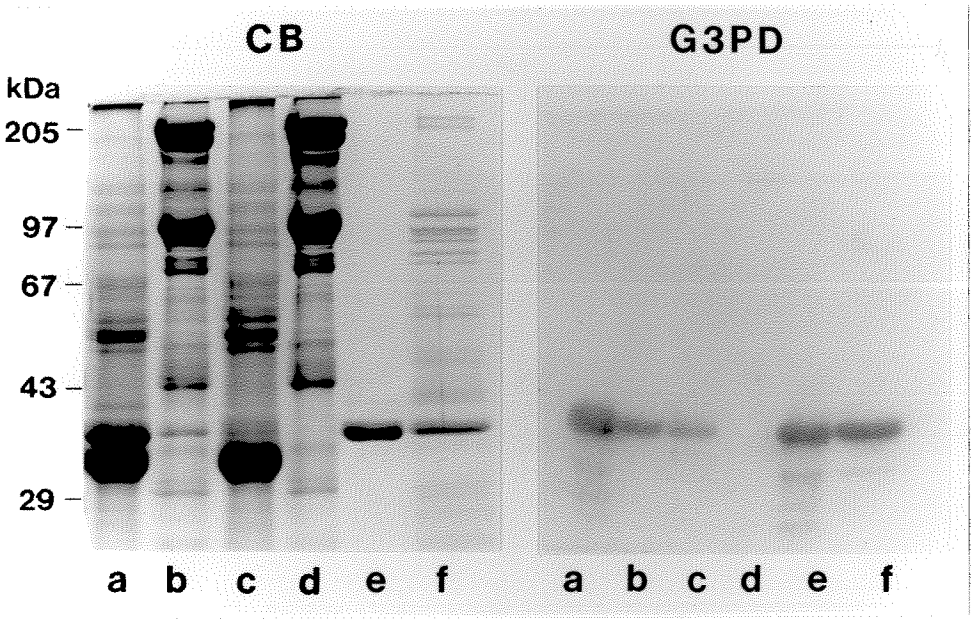

Fig. 16. **Anti-G3PD monoclonal antibody gpd 2C11 labelled Western blot of ROS plasma membrane and red blood cell ghosts and their NaCl extracts.**

Coomassie Blue-stained gel (CB) and immunoblot (G3PD) of the membranes and their NaCl extracts is shown for comparison. *Lanes a*, ROS plasma membrane; *lanes b*, red blood cell ghosts; *lanes c*, NaCl extracted ROS plasma membrane; *lanes d*, NaCl extracted red blood cell ghosts; *lanes e*, NaCl extract of ROS plasma membrane; *lanes f*, NaCl extract of red blood cell ghosts. Each lane contains 20-30 *u*g of membranes or 5 *u*g of NaCl extract.

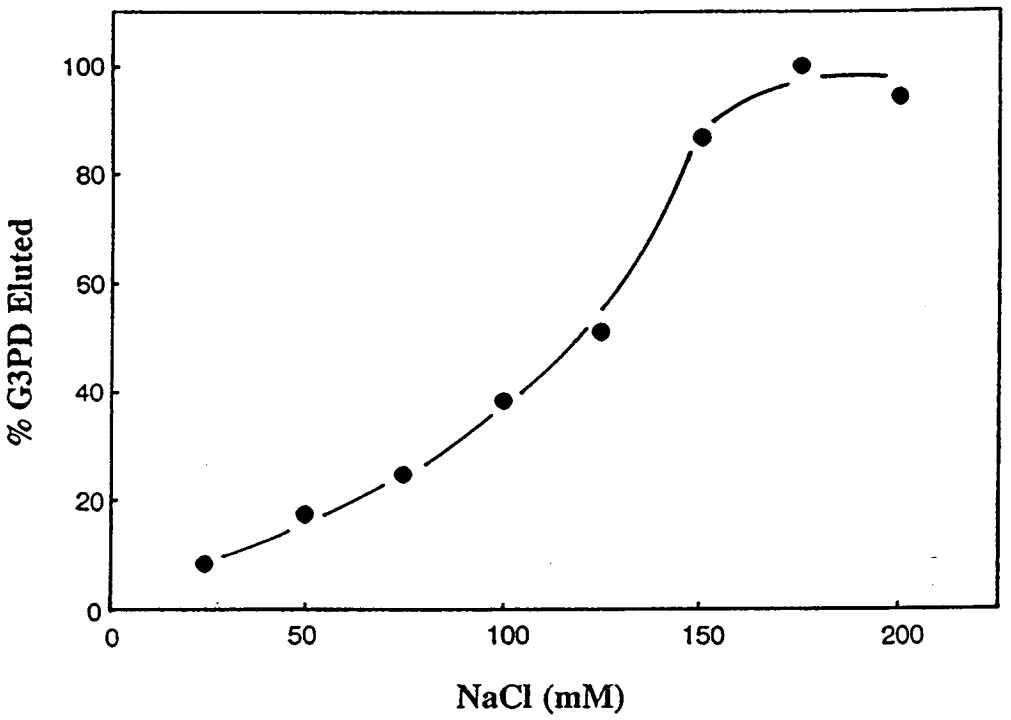

Fig. 17. **Effect of NaCl concentration on the extraction of the 38 kDa protein from ROS membranes.**

ROS membranes (1 mg protein) were incubated in 10 mM Tris buffer, pH 7.4, containing 20 - 200 mM NaCl for 15 min at 4 °C. The ROS membranes were sedimented by centrifugation and the supernatant extract was subjected to SDS-polyacrylamide gel electrophoresis. The amount of 38 kDa protein in the supernatant was quantified by scanning densitometry of Coomassie Blue stained gels. The assay was carried out in duplicate.

Table V

Effect of Nucleotides and Chelating Agents on the Binding of the 38 kDa Protein to ROS Membranes

Eluting Agent	% 38 kDa protein Eluted From ROS Membranes
150mM NaCl*	100
1mM ATP	49
1mM NAD	9
1mM NADH	34
1mM cGMP	4
1mM cAMP	6
2mM EDTA	9
2mM EGTA	9

* *The amount of 38 kDa protein eluted by each eluting agent was assessed by comparison with its elution from the ROS membranes by 150 mM NaCl. The assay was carried out in triplicate.*

nucleotide-specific elution of G3PD from ROS membranes and from erythrocyte membranes is not known. However, in the erythrocyte system, it has been postulated that ATP induces conformational changes in membrane proteins resulting in the dissociation of G3PD from the membrane (Shin and Carraway, 1973). The ionic strength of the buffer used to extract G3PD from ROS is similar to that used by Kühn to extract a 35-kDa protein from hypotonically lysed ROS (Kühn, 1980).

G3PD specifically binds to ROS plasma membrane: The binding of affinity-purified G3PD to ROS disk and G3PD-stripped ROS plasma membranes was studied by SDS-gel electrophoresis and enzyme activity measurements. As illustrated in Fig. 18, G3PD specifically bound to ROS plasma membranes, but not to disk membranes in low ionic strength buffer (0.1 mM EDTA and 5 mM Na_2HPO_4). No G3PD activity was detected in either disk membranes or in NaCl-extracted plasma membranes before the addition of exogenous G3PD. When purified G3PD was reassociated with disk membranes and G3PD-stripped ROS plasma membrane at a disk to plasma membrane protein ratio of 20:1, a G3PD specific activity of 5 units/mg of protein was measured for plasma membranes, but no activity was detected for disk membranes. When G3PD-stripped ROS membranes were treated with 10 *u*g/ml trypsin or chymotrypsin prior to reassociation with G3PD, binding of G3PD to these membranes was reduced by up to 75 % (Table VI). This indicates that G3PD preferentially binds to a protease-sensitive protein in ROS plasma membrane.

2.4. DISCUSSION

In this study, partial N-terminal sequence analysis and specific enzyme activity measurements have confirmed that the major 38-kDa protein associated

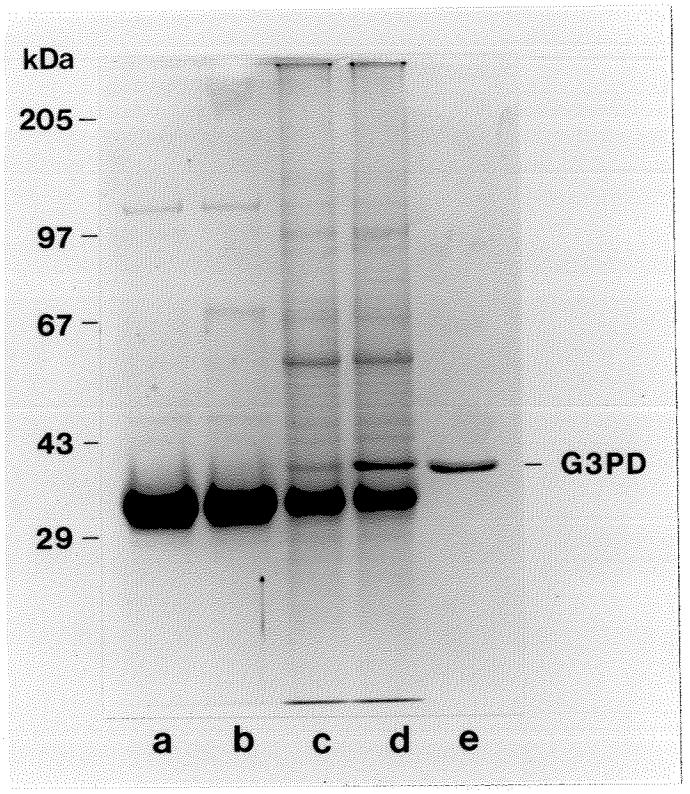

Fig. 18. **Specific binding of the 38 kDa protein to bovine ROS plasma membrane.** Purified ROS disk (3 mg) and NaCl extracted plasma membranes (0.15 mg) were mixed with NAD^+-agarose purified G3PD (75 *u*g) in a total volume of 0.5 ml. After dialysis against 0.1 mM EDTA, 5 % sucrose and 5 mM sodium phosphate buffer, pH 7.4, the membranes were separated from the unbound 38 kDa protein by centrifugation and subjected to SDS-polyacrylamide gel electrophoresis. *Lane a*, ROS disk membranes before the addition of 38 kDa protein; *lane b*, ROS disk membranes incubated with 38 kDa protein and washed by centrifugation; *lane c*, NaCl extracted ROS plasma membranes before the addition of 38 kDa protein; *lane d*, ROS plasma membrane incubated with 38 kDa protein and washed by centrifugation; *lane e*, NAD^+-agarose purified 38 kDa protein.

Table VI
Effect of Trypsin and Chymotrypsin on ROS G3PD Binding Sites

	G3PD activity*					
	Trypsin digest			Chymotrypsin digest		
Sample	control	10 min	50 min	control	10 min	50 min
ROS membrane pellet	280	60	55	280	105	50
Supernatant	34	200	220	34	150	190

* *Aliquots of G3PD-stripped ROS membranes were treated with trypsin or chymotrypsin at 25 °C for 0, 10 or 50 minutes before incubation with NAD^+-affinity purified G3PD. The extent of G3PD association with digested membranes was assessed by assaying G3PD activity associated with the membrane pellet and supernatant of each membrane aliquot. Activities are expressed as nanomoles of NADH produced per min for each membrane aliquot. The assay was carried out in triplicate.*

with purified ROS plasma membrane is G3PD. This enzyme makes up as much as 2 % of the total ROS protein and can be readily isolated from ROS membranes or purified ROS plasma membrane by extraction with 0.15 M NaCl and NAD^+-affinity chromatography. Activity measurements suggest that G3PD makes up at least 11 % of the protein in ROS plasma membrane prepared by hypotonic lysis of ROS and density gradient centrifugation in low ionic strength buffers. Coomassie Blue staining of ROS plasma membrane proteins separated by SDS-gel electrophoresis, however, indicates that up to 17 % is the 38 kDa protein (Molday and Molday, 1987). This difference may be explained, in part, by the presence of another protein(s) with similar mobility on the SDS-polyacrylamide gel. This protein may be the 39-kDa protein reported by Matesic and Liebman (1987) to have cGMP channel activity. Earlier, Kühn (1980) reported that a 35 kDa protein could be specifically eluted from ROS membranes with 100 mM Tris buffer. It appears likely that this protein is G3PD as reported here.

Glyceraldehyde-3-phosphate dehydrogenase binds to ROS plasma membranes but not disk membranes. Activity measurements and SDS-gel electrophoresis of ROS plasma and disk membranes isolated from trypsin-treated ROS membranes indicate that G3PD is only present in the plasma membrane fraction. The small amount of G3PD activity measured in the disk membrane fraction in some preparations is most likely due to contamination by plasma membrane fragments since G3PD specific activity of these disk fractions is at least two-hundredfold less than that of plasma membranes from the same preparation. Furthermore, G3PD reassociates with G3PD-stripped plasma membrane, but not disk membranes, even when disk membranes are present in significantly higher concentrations. Trypsin treatment used in the separation of disks from plasma membranes is not responsible for the absence of G3PD binding to disk membranes since it has been previously shown that disk membranes prepared in the absence of

trypsin do not contain the 38 kDa band characteristic of G3PD (Molday and Molday, 1987).

Like G3PD of red blood cell membranes, G3PD of ROS specifically and reversibly associates with the plasma membrane under conditions of low ionic strength. Although there has been some controversy concerning the physiological relevance of low ionic strength binding of G3PD to cell membranes (Keokitichai and Wrigglesworth, 1980; Kliman and Steck, 1980; Solti *et al.*, 1981; Rich *et al.*, 1984, 1985; Ballas *et al.* , 1985), recently Rogalski *et al.* (1989) have shown by immunofluorescence microscopy that G3PD is preferentially associated with the plasma membrane in intact and lysed human red blood cells. It is, therefore, possible that G3PD binding to ROS plasma membrane may also occur *in situ*. The release of 20-30 % of G3PD activity into the supernatant upon hypotonic lysis of ROS, however, may suggest that a portion of G3PD is not tightly associated with ROS membranes.

The site to which ROS G3PD binds is not yet known. Studies reported here indicate that G3PD binds to a protease-sensitive ROS plasma membrane-specific protein. In the case of red blood cell membranes, it has been shown that G3PD specifically binds to the negatively charged N-terminus of Band 3, the anion channel protein of red blood cell membranes (Yu and Steck, 1975). Since the binding of G3PD to ROS plasma membranes exhibits similar properties, it is likely that a negatively charged segment of a plasma membrane protein serves as the binding site for ROS G3PD.

Glyceraldehyde-3-phosphate dehydrogenase is an important enzyme in the glycolytic pathway. It is found in exceedingly large quantities in many cells and tissues. For example, G3PD constitutes about 5-7 % of the human red blood cell plasma membrane proteins (Kant and Steck, 1973), over 5 % of the total yeast protein (Krebs *et al.*, 1953), and up to 7 % of total rabbit skeletal muscle nonstromal

protein (Czok and Bücher, 1960). As yet, the need for such a large excess of G3PD (up to 3 orders of magnitude in human red blood cells) compared to some glycolytic enzymes such as hexokinase and pyruvate kinase is not known. Several functions outside its role in glycolysis, however, have been demonstrated for G3PD *in vitro*. These functions include ATP-modulated bundling of brain microtubules (Huitorel and Pantaloni, 1985), catalysis of triad junction formation from rabbit muscle transverse tubules and terminal cisternae (Caswell and Corbett, 1985) and ATP-dependent protein kinase activities in rabbit muscle (Kawamoto and Caswell, 1986). The role of G3PD in ROS is not known. The ROS, however, is a highly active organelle requiring large quantities of GTP, cGMP and ATP for the phototransduction process. If glycolysis does occur in ROS, other glycolytic enzymes should also be present in this organelle. The band at 40 kDa which elutes from ROS membranes with G3PD may in fact be aldolase. This enzyme is known to be associated with Band 3 of red blood cell membranes under conditions of low ionic strength and can be released with physiological buffer (Strapazon and Steck, 1976, 1977; and Murthy *et al.*, 1981). Detection of other glycolytic enzymes and of glucose transport activity in ROS is discussed in Chapter 3.

CHAPTER 3

DETECTION OF GLYCOLYTIC ENZYMES AND A GLUT-1 GLUCOSE TRANSPORTER IN THE OUTER SEGMENTS OF ROD AND CONE PHOTORECEPTOR CELLS

3.1. MATERIALS

3.1.1. Animal tissues: Fresh bovine eyes were obtained from Intercontinental Packers (Vancouver, British Columbia) or J & L Meats (Surrey, British Columbia). Fresh chicken eyes were from Hallmark Poultry Processors Ltd. (Vancouver, British Columbia). Fresh human blood was obtained from healthy donors.

3.1.2. Chemicals: 3-O-[^{14}C]methyl-glucose was a product of New England Nuclear (55 mCi/mmol) and the Ready Protein scintillation cocktail was from Beckman. Immobilon and nitrocellulose membranes were obtained from the Millipore Corp. and Schleicher & Schuell (Keene, NH), respectively and Sepharose 6B was from Pharmacia. All other chemicals were from Sigma or British Drug House Chemical Co. Glyceraldehyde-3-phosphate was prepared from glyceraldehyde-3-phosphate diethylacetal monobarium salt (Sigma) using the Dowex-50 resin and stored at -70 oC.

3.1.3. Immunoreagents: Reagents used here are described in Chapter 2.

3.2. METHODS

3.2.1. Preparation of bovine ROS, ROS membranes and ROS lysates

ROS were prepared under dim red light from freshly dissected bovine retina tissue by sucrose gradient centrifugation (Molday *et al.* 1987). ROS membranes and ROS lysates (soluble fraction) were prepared as follows: 15 mg (protein) of isolated

ROS in 20 mM Tris-acetate buffer, pH 7.4 containing 20% (w/v) sucrose and 0.2 mM $MgCl_2$ were centrifuged in a Sorvall SS-34 rotor at 10,000 rpm for 10 min. The ROS were resuspended in 1 ml of hypotonic extraction buffer (10 mM Tris-acetate buffer, pH 7.4) for 10 min at 4 °C to initiate lysis, and were then vigorously vortexed for 30 s. The ROS membranes and ROS lysate were separated by centrifugation in a Sorvall SS-34 rotor at 15,000 rpm for 15 minutes. The ROS membrane pellet was extracted two more times with 1 ml hypotonic extraction buffer. The ROS membrane pellet was resuspended in the same buffer at a final concentration of 15 mg protein/ml; the lysate from three hypotonic extractions were pooled for glycolytic enzyme assays. In some experiments, ROS membranes prepared by the hypotonic extraction of ROS were further extracted 3 times with 1 ml each of isotonic extraction buffer (10 mM Tris-acetate, pH 7.4 containing 150 mM NaCl) as described above. The isotonic extracts were pooled for enzyme assays.

ROS disk and plasma membranes were prepared using a ricin-gold dextran perturbation method in the presence of trypsin as previously described (Molday and Molday, 1987). Protein concentrations were determined by bicinchoninic acid method as described by the manufacturer, Pierce, Rockford, IL.

3.2.2. Preparation of red blood cells, red blood cell ghosts, and rat brain microsomes

Bovine and human red blood cells and hemoglobin-free red blood cell ghosts were prepared according to the method of Fairbanks *et al.* (1971). Rat brain microsomes were prepared as described by Wang (1987).

3.2.3. Glycolytic enzyme activity assays

Glycolytic enzyme activities in intact ROS, lysed ROS membranes and ROS lysates were monitored by following the consumption or production of NADH (or

NADPH in the case of hexokinase) at 340 nm either directly or through coupled enzyme reactions. Assay of hexokinase was carried out according to the method of Easterby and Qadri (1982); aldolase by the method of Yeltman and Harris (1982); glyceraldehyde-3-phosphate dehydrogenase (G3PD) by the method of Steck (1974); pyruvate kinase by the method of Kahn and Marie (1982) and lactate dehydrogenase (LDH) by the method of Lee *et al.* (1982). The phosphofructokinase assay was carried out according to the method of Harris *et al.*(1982) except 1 mM ATP was used. Phosphoglycerate kinase (PGK) activity was measured using the method of Kulbe and Bojanovski (1982) except 100 mM Tris-HCl buffer, instead of 100 mM triethanolamine buffer, was used. All assays were carried out in a final volume of 0.5 ml at 23 °C. One unit of enzyme activity is defined as the production of 1 *u*mol of NAD(P)H/min/mg of protein using 6.22 x 10^3 M^{-1} cm^{-1} as the extinction coefficient for NADH and NADPH. In all enzyme assays, the substrate for the enzyme to be measured was added to initiate the reaction. Negligible NADH production or consumption was detected before the addition of the substrate.

3.2.4. Determination of glucose transport activity in intact ROS

ROS were isolated by sucrose density centrifugation in the absence of glucose. The isolated ROS were washed once with transport assay buffer containing 150 mM NaCl, 1 mM $MgCl_2$ and 20 mM 4-(2-Hydroxyethyl)-1-piperazineethanesulfonic acid (HEPES), pH 7.2 (300 ml per 50 mg ROS), by centrifugation in a Sorvall SS-34 rotor at 9,000 rpm for 8 min. The ROS pellet was resuspended to a final concentration of 7 - 10 mg protein/ml in the assay buffer. A stock solution of 3-O-[^{14}C]methylglucose in ethanol was dried down under vacuum in Eppendorf tubes and rehydrated to the original volume in the assay buffer. Transport assay stop buffer containing 1 mM phloretin was prepared shortly before

use by dilution of a 100 mM phloretin/methanol stock solution with the assay buffer. All transport assays were carried out in triplicate.

Net influx assay: Net uptake of 3-O-[^{14}C]methylglucose by intact ROS was carried out at 23 °C based on modified methods of Toyoda *et al.* (1986) and Lowe and Walmsley (1985). One *u*l of assay buffer containing 3-O-[^{14}C]methylglucose (0.1 *u*Ci) was placed at the bottom of a round-bottom glass culture tube (13 x 100 mm) placed on an orbit shaker swirling at 150 rpm. The transporter assay was initiated by the addition of 40 *u*l of ROS suspension and terminated at the desired time by the addition of 1 ml of stop buffer containing 1 mM phloretin. The ROS suspension was immediately centrifuged in a Beckman Microfuge E for 20 s. The supernatant was carefully removed, and the ROS pellet was washed by resuspension in another 1 ml of stop buffer and centrifugation. The ROS pellet was directly dissolved in the Ready Protein scintillation cocktail and counted in a liquid scintillation counter. No detectable amount of ROS was lost during the two centrifugation steps. To study cytochalasin B inhibition of 3-O-[^{14}C]methylglucose uptake, the ROS suspension was pre-incubated with 0.1 mM cytochalasin B for at least 30 min prior to the addition of 3-O-[^{14}C]methylglucose to initiate the transport assay. Zero-time controls were carried out by adding the stop buffer to the ROS before initiating the transport assay. Counts obtained from zero-time controls accounted for less than 1 % of radioactivity observed at uptake equilibrium. Net uptake of 3-O-[^{14}C]methylglucose by red blood cells was carried out as described above except the washed red blood cell pellets were lysed in water and the RBC proteins were precipitated with 10 % trichloroacetic acid. The supernatants were collected and counted for radioactivity.

Equilibrium exchange assay: Equilibrium exchange uptake of 3-O-[^{14}C]methylglucose was also carried out using the same procedure described above except that ROS were pre-equilibrated for at least 30 min with the indicated

concentration of non-radioactive 3-O-methylglucose. Increases in osmotic pressure due to the inclusion of 3-O-methylglucose in the assay buffer was compensated by decreasing the concentration of NaCl in the buffer. Exchange velocity at each 3-O-methylglucose concentration was determined graphically from the initial rate of 3-O-[^{14}C]methylglucose tracer uptake into ROS.

Net efflux assay: The rate of 3-O-[^{14}C]methylglucose efflux from ROS was measured at 23 °C. The ROS suspension was first incubated with 0.1 mM 3-O-[^{14}C]methylglucose for at least 30 min and the efflux assay was initiated by the addition of 400 *u*l of 3-O-[^{14}C]methylglucose loaded ROS suspension into 4.6 ml of assay buffer with or without 1 mM phloretin in a glass culture tube swirling on an orbital shaker as described above. To terminate the assay, 0.5 ml aliquots of the ROS suspension were removed at pre-determined time intervals and added into 1 ml of stop buffer containing 1 mM phloretin. The ROS pellets were washed by centrifugation and counted for radioactivity as described for the net uptake assay.

3.2.5. Monoclonal and polyclonal antibodies

Monoclonal antibodies gpd 2F4, 3D4 and 3E11 and pgk 1C9 were obtained from the corresponding hybridoma cell lines generated by fusion of NS-1 mouse myeloma cells with spleen cells from BALB/c mice immunized with purified human red blood cell G3PD and Baker's yeast PGK, respectively as described in Chapter 2. Culture supernatants from gpd 3E11 and pgk 1C9 cell lines were used in Western blots and immunofluorescence labeling. Hybridoma cell culture fluid containing monoclonal antibody MAb65 against H-type lactate dehydrogenase (Pan *et al.*, 1989) was generously provided by Dr. P.G. Isaacson (University College, London). Monoclonal antibody 3D6 generated against bovine rhodopsin has been shown to cross-react with bovine and frog red- and green-sensitive cone opsin (Hicks and Molday, 1986). Chicken red-sensitive cone pigment, iodopsin, also contains the rho

3D6 binding site (Hodges *et al.*, 1988) on the basis of sequence analysis of chicken iodopsin by Kuwata *et al.* (1990).

Antisera against the C-terminus (synthetic peptide 480-492) of the rat brain glucose transporter (anti-GLUT-1) and against rat liver glucose transporter (anti-GLUT-2) were obtained from East-Acres Biologicals, Southbridge, MA; antiserum against insulin regulatable glucose transporter (anti-GLUT-4) was from Calbiochem, San Diego, CA. Goat anti-mouse Ig was coupled to Sepharose 6B by the cyanogen bromide method (March *et al.* 1974).

3.2.6. Radioimmune competitive inhibition assay

Solid-phase radioimmune competitive inhibition assays were carried out as previously described (Molday and MacKenzie, 1983). Briefly, ROS membranes or bovine or human red blood cell ghosts were solubilized in 1% Triton X-100 and diluted in PBS to obtain a Triton X-100 concentration of 0.1%. Fifty *u*l of serially-diluted samples in 0.1% Triton X-100/PBS were incubated with 25 *u*l of 1000 times diluted rabbit anti-GLUT-1 glucose transporter antiserum for 1 h at 23 °C. The unbound antibody was then determined by a solid phase radioimmune assay using Triton X-100 solubilized human red blood cell ghosts (7.5 *u*g per well) as immobilized antigen. ^{125}I-goat anti-rabbit Ig (specific activity 2 x 10^6 dpm/*u*g) was used as the secondary antibody and the level of ^{125}I was counted in a Beckman 8000 counter.

3.2.7. Immunofluorescence microscopy

Immunofluorescence microscopy was carried out according to the method of Johnson and Blanks (1984) with a few modifications. Bovine eyes for cryostat sectioning were enucleated and fixed by immersion in 3 % (w/v) paraformaldehyde-PBS, pH 7.3 at 23 °C for 3 h. Some eyes were fixed in the presence of 30% (w/v)

sucrose. The inclusion of sucrose in the fixation buffer did not affect subsequent labeling of retina sections by the antibodies. Paraformaldehyde fixed pieces of the eyecup were infiltrated with 8 % acrylamide for 8 to 12 h at 4 °C before initiating acrylamide polymerization with ammonium persulfate. The acrylamide embedded retina was frozen in Tissue Tek over the surface of liquid nitrogen. The embedded retinas were sectioned and used for immunolabeling within 72 h. Prolonged storage of Tissue Tek embedded retina or retina sections at -20 °C diminished the intensity of antibody labeling and increased the auto-fluorescence of retina sections. Six *u*m sections were first blocked with 5 % goat serum in PBS containing 0.1 % Triton X-100 for 30 min at 23 °C. The blocked sections were then incubated at 23 °C for 1-2 h with primary antibodies: anti-G3PD, anti-PGK and anti-LDH monoclonal antibody culture supernatants or anti-GLUT-1 antiserum diluted 2-50x in PBS containing 0.1 % Triton X-100 and 5 % goat serum. For controls, monoclonal antibody supernatants used in labeling were immunoprecipitated with goat anti-mouse Ig-Sepharose 6B. Anti-GLUT-1 rabbit polyclonal antiserum was pre-adsorbed with bovine red blood cell ghosts which exhibited very low glucose transport activity (Hoos *et al.*, 1972). For controls, the anti-GLUT-1 antiserum was pre-adsorbed with human red blood cell ghosts which contain relatively large amounts of the glucose transporter. The labeled sections were washed four times with PBS and incubated for 1 h at 23 °C with affinity-purified FITC conjugated goat anti-mouse Ig or goat anti-rabbit Ig (10 *u*g/ml) antibodies in blocking buffer. Sections were washed four times with PBS. Immunofluorescence microscopy was carried out with a Zeiss Axiophot photomicroscope equipped with a vertical illuminator for epifluorescence. Photographs were taken using Kodak Tri-X 400 film.

3.2.8. Polyacrylamide gel electrophoresis and Western blotting

SDS-polyacrylamide gel electrophoresis was carried out on slab gels using the buffer system of Laemmli (1970). Gel slices were either stained with Coomassie Blue or electroblotted onto Immobilon or nitrocellulose membranes for Western blots. Blots labelled with primary antibodies were detected with ^{125}I-goat anti-mouse Ig or ^{125}I-goat anti-rabbit Ig (1-2 X 10^6 dpm/μg) as previously described (Molday *et al.* 1987). Immunoblots were subjected to autoradiography overnight.

3.3. RESULTS

3.3.1. Glycolytic enzymes in photoreceptor rod outer segments

Glycolytic enzyme activities in bovine ROS preparations: Glyceraldehyde-3-phosphate dehydrogenase (G3PD), a key enzyme in glycolysis, has been shown to be a major protein associated with the plasma membrane of ROS (Hsu and Molday, 1990; see Chapter 2). To determine if other glycolytic enzymes are also present in isolated ROS preparations, established spectrophotometric methods were used to measure the activities of other glycolytic enzymes. As shown in Table VII, ROS preparations were found to contain significant activities of six other glycolytic enzymes including hexokinase and LDH, the first and last enzymes in the anaerobic glycolytic pathway. With the exception of G3PD, the enzyme activities were found to be present in the soluble fraction after extraction of ROS with hypotonic buffer (Table VII). Isotonic conditions were required to elute most of the G3PD activity as previously shown (Chapter 2); isotonic buffer was also required to extract the aldolase activity which had not been extracted by hypotonic buffer. Glycolytic enzyme activities have also been detected by McConnell *et al.* (1969) and Lopez-Escalera *et al.* (1991), but differ from values reported here by 3 to 140 fold (Table VIIB). Large discrepancies in these three sets of data are probably due to variation in the intactness of prepared ROS and the condition of enzyme assays. Lower glycolytic enzyme activities (2-140 fold lower compared to that found in the present

TABLE VII
Glycolytic Enzyme Activities in Bovine ROS

Enzyme	Specific Activities[a]	% Enzyme Activity in Extract[b] (Units/mg ROS)	
		Hypotonic	Isotonic
G3PD	1.8 ± 0.4	31.2 ± 9.3 %	68.7 ± 9.3 %
LDH	3.0 ± 0.4	94.4 ± 1.8 %	5.6 ± 1.8 %
PK	0.7 ± 0.1	92.5 ± 4.9 %	7.5 ± 4.9 %
PGK	0.6 ± 0.1	88.2 ± 6.0 %	11.8 ± 6.0 %
PFK	0.1 ± 0.01	93.0 ± 4.2 %	7.0 ± 4.2 %
ALD	0.08 ± 0.02	75.3 ± 9.3 %	24.6 ± 9.3 %
HK	0.02 ± 0.004	98.0 ± 2.8 %	2.0 ± 2.8 %

[a] *average data (units / mg ROS protein) from seven ROS preparations.*
[b] *determined by assigning the total activity of each enzyme detected in hypotonic and isotonic extracts as 100 %. No enzyme activity was detectable in ROS membranes after isotonic extraction.*

TABLE VIIb
Comparison of Bovine ROS Glycolytic Enzyme Activities with Values Reported in the Literature

Enzyme	Enzyme Activity (μmol/min/mg ROS protein)		
	Present Study	McConnell *et. al.* (1969)	Lopez-Escalera *et. al.* (1991)
G3PD	1.8	0.11	-
LDH	3.0	0.06	4.6[a]
PK	0.7	0.005	5.5[b]
PGK	0.6	0.14	-
PFK	0.1	-	-
ALD	0.08	0.02	-
HK	0.02	0.008	-

Activities were calculated from 12.6 mM/s[a] and 15.0 mM/s[b] respectively assuming that concentration of rhodopsin in ROS is 3 mM (Lopez-Escalera et al., 1991), rhodopsin constitutes 70 % of total ROS protein and rhodopsin has a molecular weight of 38,000 g/mol.

study) observed by McConnell *et al.* (1969) may be, in part, due to loss of glycolytic enzymes from ROS during a lengthy ROS isolation procedure which required repeated sedimentation and resuspension of ROS. Glycolytic enzyme activities have been found to slowly leak out from isolated ROS even when ROS were resuspended at high protein concentrations in 20 % sucrose and 5 % Ficoll (data not shown). For the present study, ROS were isolated from freshly dissected retinas by one sucrose density gradient centrifugation step within one and half hours after retina dissection. Glycolytic enzymes were immediately extracted from ROS by hypotonic and isotonic extraction after ROS isolation. Lopez-Escalera *et al.* (1991) also isolated ROS using a single sucrose gradient centrifugation procedure similar to that used in the present study. Higher glycolytic enzyme activities (1.5 to 8 fold higher compared to that found in present study) observed by Lopez-Escalera *et al.* (1991) could be due to differences in enzyme assay procedures. Nevertheless, despite differences in these three sets of data, they all suggest that ROS contain higher glycolytic enzyme activities than erythrocytes, muscle and liver cells.

The ratio of activity of each of the six measured glycolytic enzymes to the activity of G3PD was compared in ROS, human red blood cells (Maretski *et al.*, 1989) and rabbit muscle (Scopes and Stoter, 1982). As shown in Table VIII, the activity ratios are within the same order of magnitude suggesting that these glycolytic enzymes are present in similar proportions within these cells (Table VIII). A G3PD specific activity of 11 units per mg ROS plasma membrane protein is higher than the specific activity of G3PD of 1.83 units per mg red blood cell ghost membrane protein for human red blood cells (Kant and Steck, 1973), suggesting that glycolytic enzymes are present in higher quantities in ROS compared to erythrocytes. In this regard, the rate of glycolytic flux in ROS was found to be approximately three fold of that in human erythrocytes (section 4.4).

TABLE VIII
Glycolytic Enzyme Activity Ratios[a] in Bovine ROS and Other Tissues

Enzyme	ROS	Erythrocyte[b]	Muscle[c]
G3PD	1.0	1.0	1.0
LDH	1.5	1.0	1.0
PK	0.4	0.1	0.6
PGK	0.3	1.5	0.7/1.4
PFK	0.06	0.05	0.1
ALD	0.04	0.02	0.1
HK	0.009	0.007	-

[a] *ratios of each glycolytic enzyme activity to the activity of G3PD.*
[b] *calculated using data from Maretski et al., 1989.*
[c] *calculated using data from Scopes and Stoter, 1982.*

Localization of glycolytic enzymes by immunofluorescence microscopy: Two monoclonal antibodies, gpd 3E11 and pgk 1C9, were generated against human red blood cell G3PD and yeast phosphoglycerate kinase (PGK), respectively, for use as immunochemical probes. The reactivity and specificity of these two antibodies are shown by Western blot analysis in Figure 19. Monoclonal antibody gpd 3E11 labeled the G3PD protein (Mr = 38 K) in ROS (*lane a*) and G3PD purified from red blood cells (*lane b*), but not yeast PGK (*lane c*). Monoclonal antibody pgk 1C9 labeled the PGK protein (Mr 43 K) in ROS (*lane a*) and purified yeast PGK (*lane c*), but not purified G3PD (*lane b*).

In order to determine whether glycolytic enzymes found in ROS preparations are true ROS components or contaminants from other other retinal layers, the distribution of three glycolytic enzymes, PGK, G3PD and LDH, in retina cryosections was visualized by immunofluorescence microscopy. As shown in Fig. 20 (*a, d,* and *f*), monoclonal antibodies to these glycolytic enzymes labeled the bovine outer segment layer, as well as the inner segment and cell body layers. The labeling was most intense for G3PD, the most abundant glycolytic enzyme, and least intense for PGK. Labeling was essentially eliminated in controls in which the antibodies in the hybridoma cell culture fluid were removed by immunoprecipitation with goat anti-mouse Ig-Sepharose (*c, e* and *h*) . The specificity of the immunochemical reagents was also confirmed using anti-rhodopsin rho 1D4 monoclonal antibody which intensely labeled only the outer segment layer (*g*).

3.3.2. Glucose transport in photoreceptor rod outer segments

Detection of ROS glucose transport activity: Since glucose is required for glycolysis, glucose uptake activity was studied by measuring the uptake of 3-O-[^{14}C]methylglucose, a non-metabolizable analog of glucose, by isolated bovine ROS. Fig. 21 shows the time course for the uptake of 3-O-methylglucose by bovine ROS.

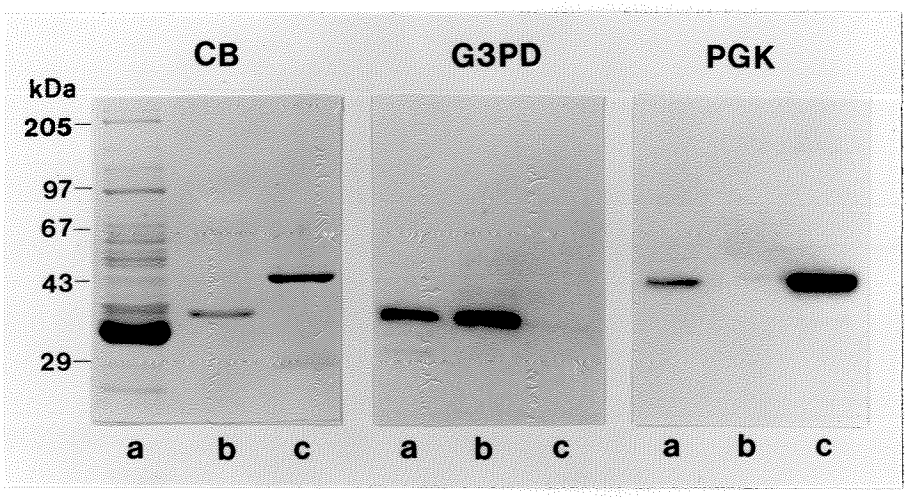

Fig. 19. **Western blots of ROS and purified G3PD and PGK labeled with monoclonal antibodies against G3PD and PGK.**

Bovine ROS (*lanes a*), G3PD purified from human red blood cells (*lanes b*), and PGK purified from yeast (*lanes c*) were subjected to SDS gel electrophoresis and either stained with Coomassie Blue (CB) or transferred to Immobilon membranes and labeled with anti-G3PD monoclonal antibody gpd 3E11 (G3PD) or anti-PGK monoclonal antibody pgk 1C9 (PGK) and ^{125}I-labeled goat anti-mouse Ig for autoradiography. Lanes contained either 20 *u*g of ROS or 5 *u*g of purified enzyme.

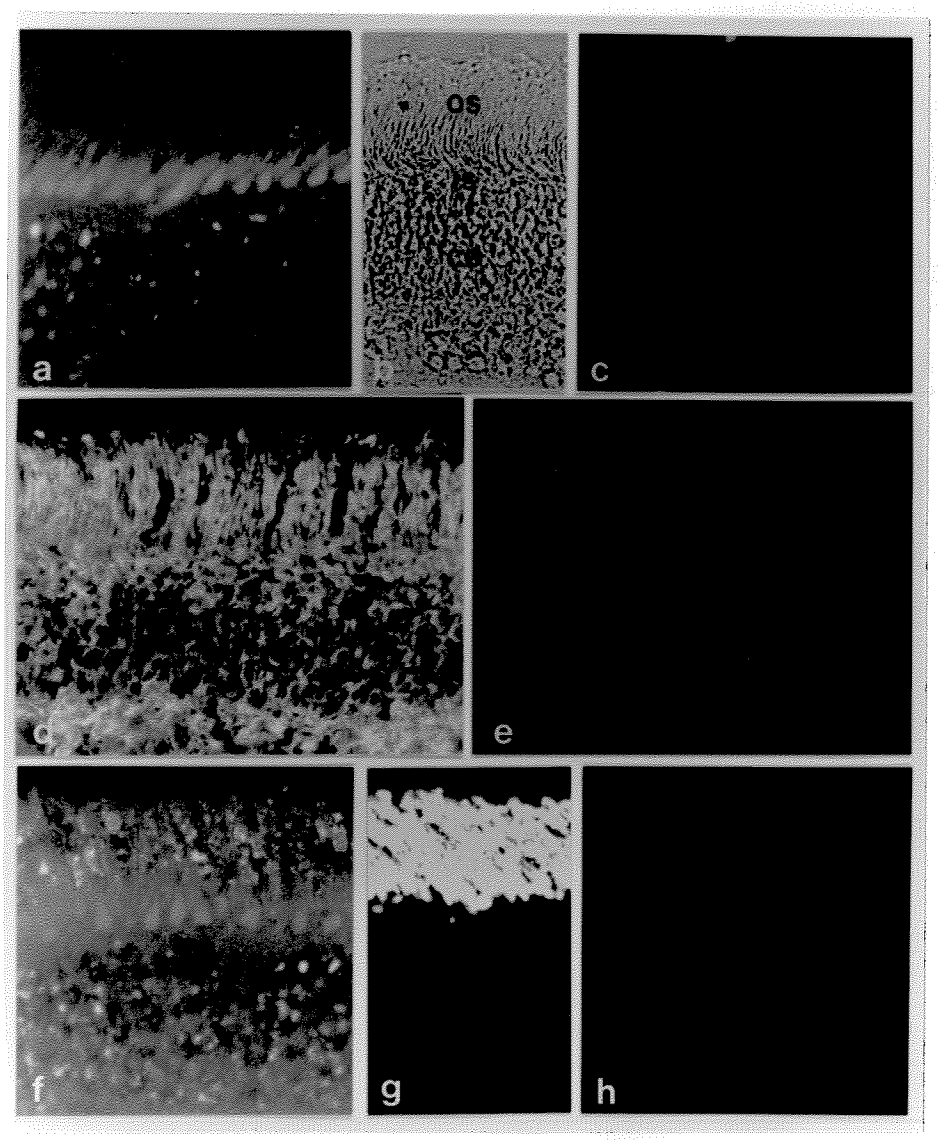

Fig. 20. **Localization of glycolytic enzymes in the photoreceptor layer of bovine retina by immunofluorescence microscopy.**

Cryosections of bovine retina were labeled with the indicated monoclonal antibodies and FITC-labeled goat anti-mouse Ig. Fluorescent micrographs of photoreceptors labeled with (*a*) pkg 1C9 hybridoma culture fluid containing anti-PGK monoclonal antibody; (*c*) the same culture fluid pre-adsorbed with goat anti-mouse Ig-Sepharose as a control; (*d*) gpd 3E11 hybridoma culture fluid containing anti-G3PD monoclonal antibody; (*e*) the same culture fluid pre-adsorbed with goat anti-mouse Ig-Sepharose as a control; (*f*) anti-LDH monoclonal antibody MAb65; (*h*) same antibody pre-adsorbed with goat anti-mouse Ig-Sepharose as a control. Phase contrast micrograph of photoreceptor layer showing the outer segment (os), the inner segment (is) and the cell body (cb) is shown in (*b*) and a fluorescent micrograph of the outer segment labeling with anti-rhodopsin monoclonal antibody rho 1D4 is shown in (*g*).

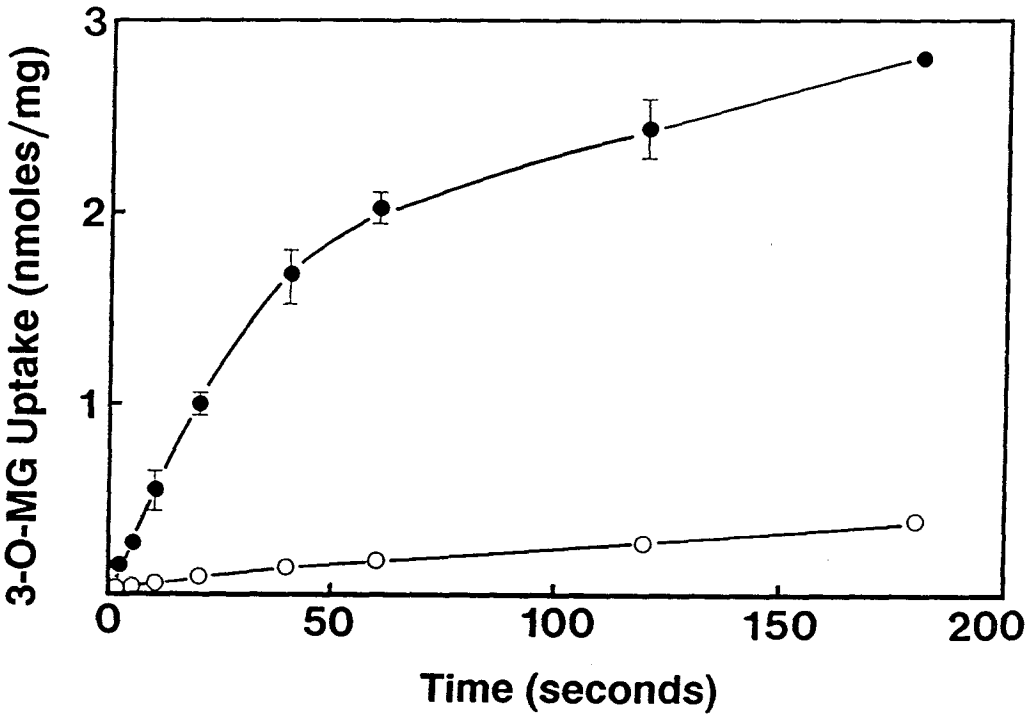

Fig. 21. **Effect of cytochalasin B on 3-O-methylglucose uptake by bovine ROS.**
The uptake 3-O-[^{14}C]methylglucose (45 uM) into isolated ROS was measured in the absence (●) and the presence (○) of 0.05 mM cytochalasin B. The assay was carried out in triplicate.

Uptake was inhibited by 0.05 mM cytochalasin B, a known inhibitor of glucose transport (Bloch, 1973). The rate of 3-O-methylglucose uptake was not affected by the state of bleaching of ROS and was not stimulated by insulin (data not shown).

The efflux of 3-O-[^{14}C]methylglucose from bovine ROS was also inhibited by phloretin (LeFevre and Marshall, 1959; Whitesell and Gliemann, 1979), another inhibitor of the glucose transporter (Fig. 22). Approximately 60 % of loaded 3-O-methylglucose was released from ROS into 3-O-methylglucose-free medium within 1 min in the absence of external phloretin. In the presence of 1 mM external phloretin, more than 70 % of loaded 3-O-methylglucose still remained within the ROS 10 min after the ROS were diluted in 3-O-methylglucose-free buffer. Loss of 3-O-methylglucose from the intracellular space of phloretin-treated ROS was approximately 3 % per minute. This is somewhat higher than a loss of 0 and 1 % per minute observed for phloretin-treated intact human red blood cells and rat adipocytes, respectively (Eilam and Stein, 1972; Whitesell and Gliemann, 1979), and is probably due to higher leakage from the ROS.

Chacterization of ROS glucose transport activity: The kinetic parameters of the ROS glucose transporter and the erythrocyte GLUT-1 type glucose transporter vary with the transport assay conditions (Table IX). Under net uptake (zero-*trans* entry) condition, the ROS glucose transport exhibited Michaelis-Menten kinetics with a K_m of 6.3 mM and a V_{max} of 0.15 nmol/s/mg ROS membrane protein (Fig. 23A). In a parallel study, human red blood cell glucose transport gave a similar K_m of 4.7 mM and a V_{max} of 17.4 nmol/s/mg ghost membrane protein. The K_m values of the ROS and red blood cell glucose transporter are within the range of K_m values of 1.6 and 6.6 mM previously reported for GLUT-1 type glucose transporters in human red blood cells by Stein (1986) and Lowe and Walmsley (1985), respectively.

Under the equilibrium exchange condition, ROS glucose transport had a higher K_m of 29 mM and a higher V_{max} of 1.06 nmol/s/mg ROS membrane protein

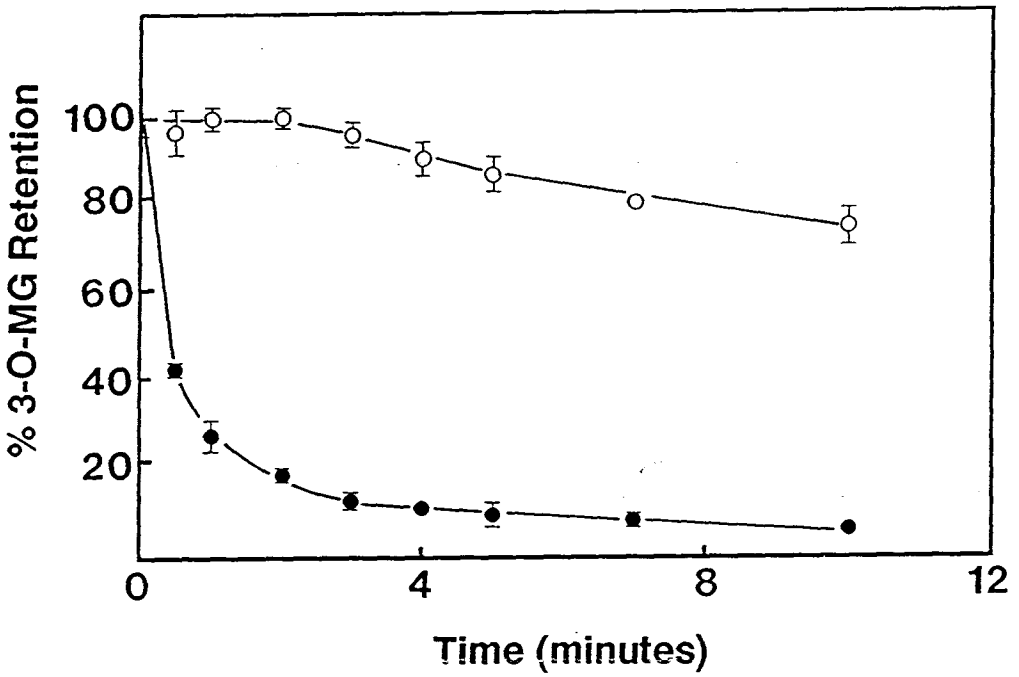

Fig. 22. **Inhibition of 3-O-methylglucose efflux from bovine ROS by phloretin.**
Isolated bovine ROS were loaded with 3-O-[^{14}C]methylglucose for 30 min. At time zero, ROS were diluted in 3-O-methylglucose-free buffer in the absence (●) or in the presence (○) of 1 mM phloretin. The assay was carried out in triplicate.

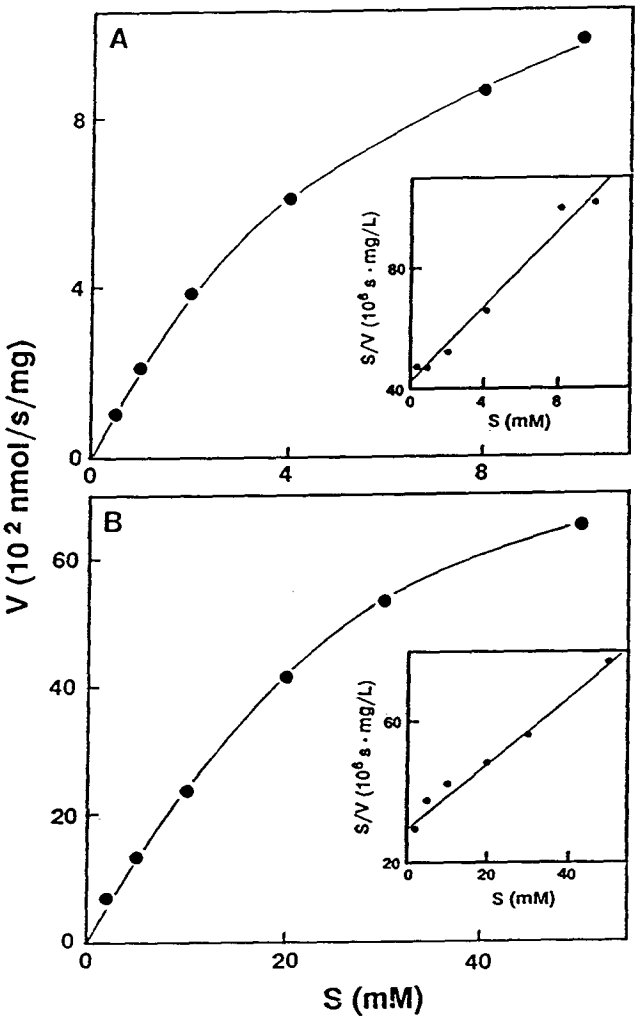

Fig. 23. **Concentration dependence of 3-O-methylglucose equilibrium exchange by bovine ROS.**

Isolated bovine ROS were allowed to equilibrate with indicated concentrations of unlabeled 3-O-methylglucose for 30 min. The exchange velocity of 3-O-methylglucose was measured by determining the initial uptake rate of externally added tracer amounts of 3-O-[^{14}C]methylglucose into ROS. Michaelis-Menten graph shows the equilibrium exchange velocity (V) as a function of 3-O-methylglucose concentrations (S). Insert shows Hane's plot analysis of the Michaelis-Menten graph.

TABLE IX
Kinetic Properties of ROS and Erythrocyte Glucose Transporter

	Net Uptake		Equilibrium Exchange	
	Km (mM)	Vmax (nmol/s/mg ROS)	Km (mM)	Vmax (nmol/s/mg ROS)
Bovine ROS[a]	6.3	0.15	29	1.06
Bovine ROS[b]	10	0.90	38	3.08
Human RBC[a]	4.7	17.4	26	144

[a] data obtained from present study; the assays were carried out in triplicate.
[b] data reported by Lopez-Escalera *et al.*, 1991.

(Fig. 23B). In a parallel study, human red blood cells also showed an increased K_m of 26 mM and a higher V_{max} of 144 nmol/s/mg ghost membrane protein. Similar increases in K_m and V_{max} under the equilibrium exchange condition have also been observed for the GLUT-1 type glucose transporter in human red blood cells with K_m ranging from 8.1 to 38 mM (Miller, 1968; Eilam and Stein, 1972; Edwards, 1974; Eilam, 1975; Brahm, 1983) and V_{max} from 130 to 217 nmol/s/mg ghost protein (Miller, 1968; Eilam and Stein, 1972; Wheeler and Hinkle, 1981). ROS glucose transport differs from the GLUT-2 type glucose tranport in liver which has a higher K_m of 18.1 mM for net uptake and a Km of 20.2 mM for equilibrium exchange (Craik and Elliot, 1979).

Lopez-Escalera *et al.* (1991) have also detected glucose transport activity in isolated ROS. Under the net uptake condition, ROS 3-O-methylglucose transport was found to have a K_m of 10 mM and a V_{max} of 0.038 mol/s/mol rhodopsin (or 0.90 nmol/s/mg ROS membrane protein assuming that rhodopsin constitutes 90 % of the total ROS membrane protein and has a molecular weight of 38,000 g/mol). Under the equilibrium exchange condition, 3-O-methylglucose transport also showed an increased K_m of 38 mM and V_{max} of 0.13 mol/s/mol rhodopsin (3.08 nmol/s/mg ROS membrane protein). Different values of 3-O-methylglucose transport K_m and V_{max} found by Lopez-Escalera *et al.* (1991) may reflect differences in conditions of transport assay. Nevertheless, both sets of data suggest that the ROS glucose transporter exhibits asymmetric transport kinetics (Km and Vmax of the transporter is dependent on the transport condition) similar to that observed in erythrocytes.

ROS plasma membrane contains a GLUT-1 type glucose transporter: Antibodies against several different types of glucose transporters were used with Western blotting to identify and localize the glucose transporter of ROS. As shown in Figure 24 (*lanes a-c*), anti-GLUT-1 antibodies labeled a diffuse protein band of

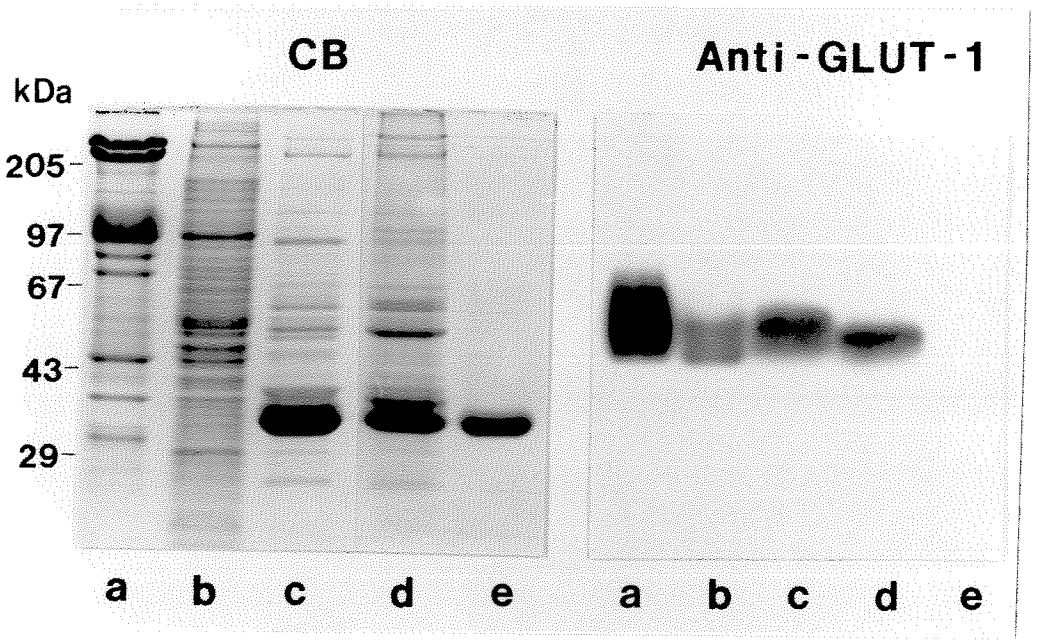

Fig. 24. **Western blots of red blood cell membranes, brain microsomes and ROS membranes labeled for the GLUT-1 type glucose transporter.**

Lanes a, human red blood cell ghosts; *lanes b*, rat brain microsomes; *lanes c*, bovine ROS; *lanes d*, purified bovine ROS plasma membrane; and *lanes e*, purified bovine ROS disk membranes were subjected to SDS gel electrophoresis and either stained with Coomassie Blue (CB) or transferred to nitrocellulose and labeled with polyclonal anti-GLUT-1 antiserum and ^{125}I-labeled goat anti-rabbit Ig for autoradiography. Coomassie Blue-stained gels contained 15-20 *u*g of membrane proteins; Western blots contained 3 *u*g of human red blood cell membrane protein and 30 *u*g of brain or ROS membrane protein.

45-50 kDa in human red blood cells, bovine brain microsomes, and isolated ROS membranes. Western blot analysis of isolated plasma and disk membranes further indicated that the GLUT-1 transporter is present in the ROS plasma membrane, and not in disk membranes (Figure 24, *lanes d* and *e*). An anti-GLUT-2 antiserum and anti-GLUT-4 antiserum which labeled glucose transporter in rat liver microsomes and adipocyte membranes respectively, did not label any protein in rat ROS membranes as analyzed by Western blot analyses (data not shown).

Quantitative comparison of the GLUT-1 type glucose transporter in ROS and red blood cell plasma membranes: The rate of 3-O-methylglucose uptake into ROS was compared with that into human and bovine red blood cells. At an external 3-O-methylglucose concentration of 45 *u*M, the rate of uptake was 738 pmol 3-O-methylglucose/s/mg membrane protein for human red blood cells; 12 pmol 3-O-methylglucose/s/mg membrane protein for bovine red blood cells; and 46 pmol 3-O-methylglucose/s/mg plasma membrane protein for ROS. The low glucose transport activity for bovine red blood cells compared to human red blood cells has been previously reported (Hoos *et al.*, 1972).

The quantity of GLUT-1 transporter in ROS and human red blood cell ghosts was also compared by solid-phase radioimmune competition assays. As shown in Figure 25, Triton X-100 solubilized red blood cell membranes and ROS membranes inhibited GLUT-1 antibody binding to immobilized glucose transporter. Half-maximum inhibition was obtained at a red blood cell membrane protein concentration of 1.2 *u*g/ml and at a ROS membrane protein concentration of 160 *u*g/ml. Since the ROS plasma membrane constitutes about 5% of the total ROS membrane, half maximum inhibition would be expected to be obtained at a 20 fold lower plasma membrane protein concentration or about 8 *u*g/ml. On this basis the ROS plasma membrane would contain about 15% the number of glucose transporters found in the human red blood cell plasma membrane. In agreement

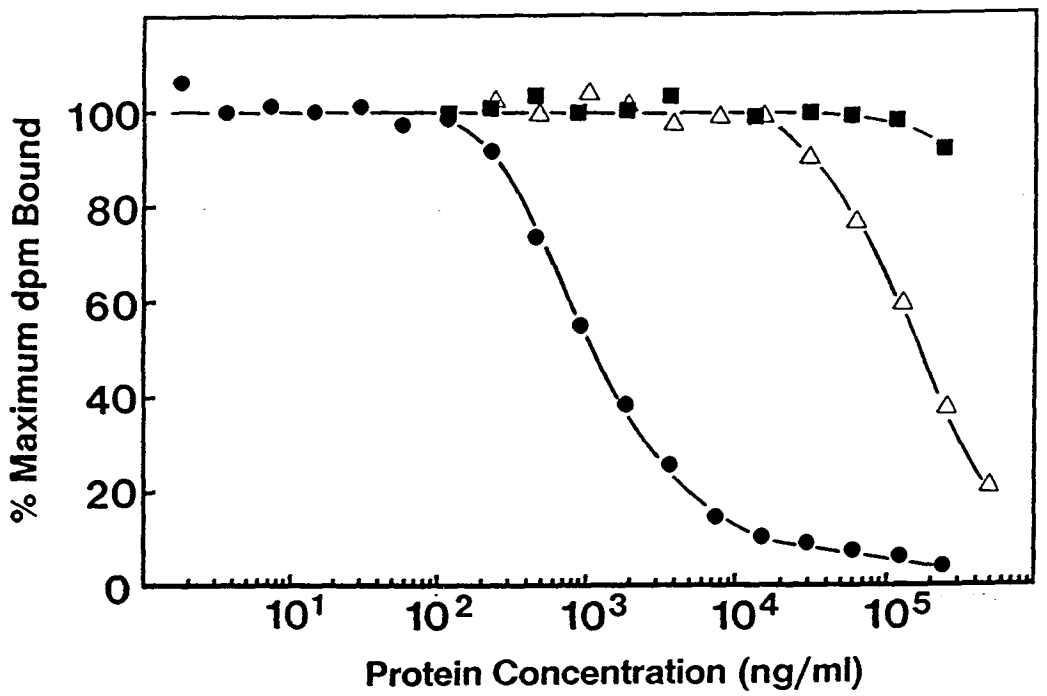

Figure 25. **Solid-phase radioimmune competitive inhibition assay of the GLUT-1 glucose transporter in ROS and in red blood cell ghosts.**

Anti-GLUT-1 glucose transporter antiserum was pre-incubated with serially-diluted Triton X-100 solubilized bovine ROS (△), human red blood cell ghosts (●) and bovine red blood cell ghosts (■) for 2 h. The unbound antibody was then quantified by solid phase radioimmune assay using human red blood cell ghosts as immobilized antigen and ^{125}I-labeled goat anti-rabbit Ig as secondary antibody. The assay was carried out in triplicate.

with the glucose uptake studies, bovine red blood cells contain much smaller amounts of transporter than either human red blood cells or bovine ROS.

Localization of the GLUT-1 type glucose transporter in bovine photoreceptor cells by immunofluorescence microscopy: Immunofluorescence microscopy of the photoreceptor layer of bovine retinal sections labeled with anti-GLUT-1 glucose transporter antiserum is shown in Figure 26. The ROS, as well as the rod inner segment and cell body, are labeled. Labeling pattern of the less numerous cone cells can not be readily seen against the fluorescently labeled rod cells. In control studies, adsorption of the anti-GLUT-1 antiserum with human red blood cell ghosts which contain large quantities of the GLUT-1 transporter abolished labeling of photoreceptor cells. Adsorption of the anti-GLUT-1 antiserum with bovine red blood cell membranes which contain very low amounts of transporter did not decrease the labeling of retina sections.

3.3.3. CONE OUTER SEGMENTS ALSO CONTAIN GLYCOLYTIC ENZYMES AND A GLUT-1 TYPE GLUCOSE TRANSPORTER

The presence of glycolytic enzymes and a GLUT-1 glucose transporter in cone cells was studied in chicken retinal sections which contain predominantly cone cells (Szél *et al.*, 1986). As shown in fluorescent micrographs in figure 27, the cone outer and inner segment of the photoreceptor layer were intensely labeled with the gpd 3E11 monoclonal antibody against G3PD, pgk 1C9 monoclonal antibody against PGK, MAb65 monoclonal antibody against LDH and anti-GLUT-1 antiserum against the GLUT-1 glucose transporter. Labeling was essentially abolished in controls in which antibodies in the hybridoma cell culture fluid and the antiserum were removed by immunoprecipitation with goat anti-mouse Ig-Sepharose and human red blood cell ghosts respectively (data not shown). These results indicate

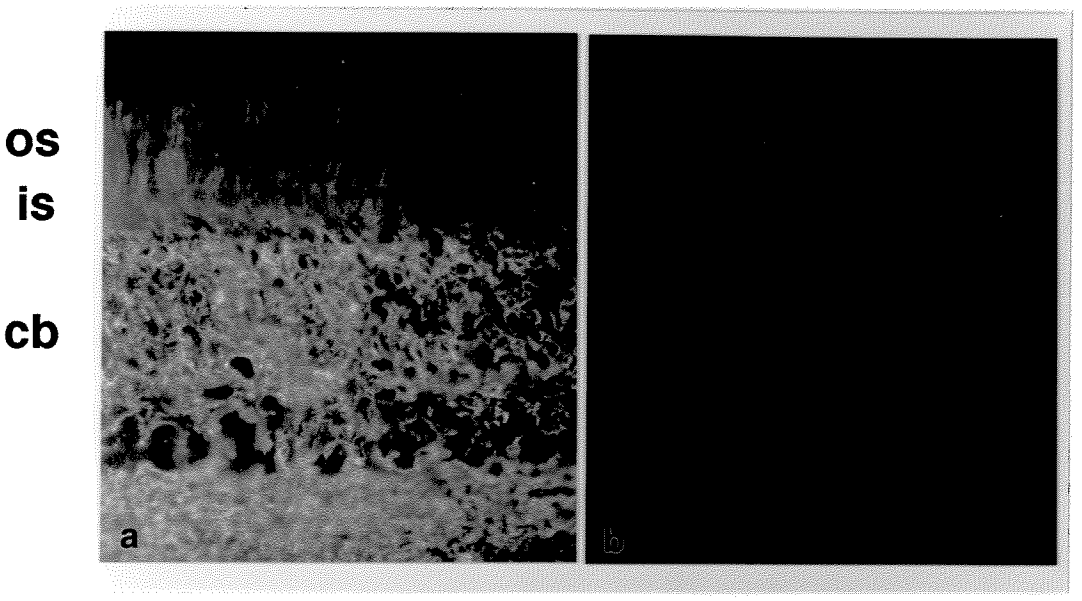

Figure 26. **Localization of the GLUT-1 glucose transporter in bovine photoreceptors by immunofluorescence microscopy.**

Cryosections of bovine retina were labeled with the anti-GLUT-1 type glucose transporter antiserum pre-adsorbed with (*a*) bovine red blood cell ghosts which contain very low levels of glucose transporter and (*b*) with human red blood cell ghosts which contain high levels of glucose transporter to serve as a control. Panel (a) shows the labeling of photoreceptor outer segments (os), inner segments (is) and cell bodies (cb) by the anti-GLUT-1 type glucose transporter antiserum.

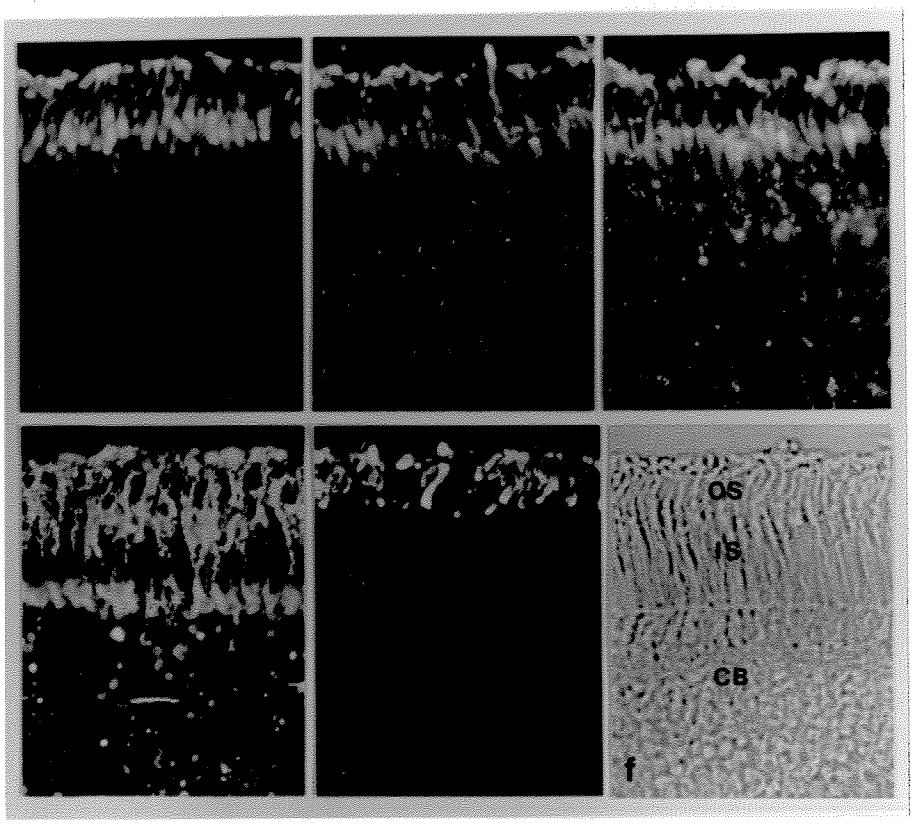

Figure 27. **Localization of glycolytic enzymes and a GLUT-1 glucose transporter in the photoreceptor cell layer of chicken retina by immunofluorescence microscopy.**

Cryosections of chicken retina were sequentially labeled with the indicated monoclonal antibody or antiserum and FITC-conjugated goat anti-mouse or goat anti-rabbit Ig. Fluorescent micrographs of photoreceptor layer labeled with (*a*) anti-G3PD monoclonal antibody gpd 3E11; (*b*) anti-PGK monoclonal antibody pgk 1C9; (*c*) anti-LDH monoclonal antibody MAb65; and (*d*) anti-GLUT 1 glucose transporter antiserum. Phase contrast micrograph of photoreceptor layer showing the outer segment (os), the inner segment (is) and the cell body (cb) is shown in (*f*) and a fluorescent micrograph of outer segment labeled with anti-rhodopsin antibody rho 3D6 which cross-reacts with cone opsin is shown in (*e*).

that cone outer segments, as well as rod outer segments, contain a glucose transporter and glycolytic enzymes for anaerobic glycolysis.

3.4. DISCUSSION

Glycolytic enzymes in photoreceptor outer segments: Enzyme activity measurements and glucose uptake studies indicate that isolated bovine ROS contain glycolytic enzymes and a glucose transporter required for anaerobic glycolysis. The possibility that these activities result from contaminants of the rod inner segment or from other retinal cells is excluded on the basis of immunofluorescence labeling studies. Monoclonal antibodies against G3PD, PGK and LDH and site-directed polyclonal antiserum against the GLUT-1 glucose transporter clearly label the outer segment layer, as well as the inner segment and cell body layer of bovine retinal sections. Immunofluorescent labeling of cone dominant chicken retina sections indicate that cone outer segments also contain glycolytic enzymes and the GLUT-1 glucose transporter. Although glycolytic enzyme activities in photoreceptor outer segments are low compared to other retinal layers (Lowry *et al.*, 1956 and 1961), they are comparable to that found in human red blood cells.

Glucose transport in photoreceptor outer segments: Biochemical and immunochemical studies carried out here indicate that rod and cone outer segments contain a GLUT-1 type glucose transporter (review, Gould and Bell, 1990) as found in human red blood cell membranes (Kasahara and Hinkle, 1977; Mueckler *et al.*, 1985; Allard and Lienhard, 1985) and in brain (Birnbaum *et al.*, 1986; Gerhart *et al.*, 1989). The transporter in ROS has a Km which is similar to that for GLUT-1 type transporters in other cells and is inhibited by both cytochalasin B and phloretin.

More importantly, a GLUT-1 specific antibody labels the 45 kDa protein in ROS which closely corresponds to the 45 kDa glucose transporter in human red blood cells and brain microsomal membranes (Figure 24). Small differences in the banding pattern of the glucose transporter from the different cell types is likely due to differences in glycosylation of this transporter (Gorga *et al.*, 1979; Wang, 1987). Western blotting of ROS plasma membrane and disk membrane fractions also indicate that the GLUT-1 transporter is only present in the plasma membrane of ROS. Thus, the glucose transporter, like the cGMP-gated channel (Cook *et al.* 1987) and the Na^+/Ca^{2+}-K^+ exchanger (Reid *et al.* 1990), must be selectively sorted to the plasma membrane and not to disk membranes during ROS morphogenesis. Two other types of glucose transporter, GLUT-2 found in liver (Fukumoto *et al.*, 1988; Thorens *et al.*, 1988) and GLUT-4 found in adipose cells (James *et al.*, 1988), are not present in outer segments.

An estimate of the amount of glucose transporter in ROS plasma membrane can be made by comparison with the amount reported in human red blood cell ghosts. On the basis of cytochalasin B binding studies, it has been estimated that the human red blood cell contains approximately 250,000-500,000 glucose transporters (Lin and Snyder, 1977; Zoccoli and Lienhard, 1977; Allard and Lienhard, 1985); using a value of 350,000 per red blood cell, this translates to a density of about 2600 transporters/um^2 for a red blood cell surface area of 135 um^2 (Evans and Fung, 1972). Solid phase competition assays indicate that ROS membranes contain about 0.75% of the transporter found in red blood cell ghost. If the plasma membrane constitutes 5% of the ROS membrane, then the amount of glucose transporter in the ROS plasma membrane is about 15% that of red blood cell ghosts. On this basis the density of the transporter in ROS plasma membrane is estimated to be on the order of 400/um^2. Glucose uptake studies indicate that ROS plasma membranes contains about 6% of transport activity of human red blood cell membranes. The

lower value relative to that observed by the radioimmune competition assay can be attributed to the presence of unsealed ROS in the preparations used for glucose uptake measurements.

The finding that glycolytic enzymes and a glucose transporter are present in outer segments further supports the view that outer segments have the capability of generating energy in the form of ATP by anaerobic glycolysis. Energy for outer segment function is also probably provided by a phosphocreatine shuttle between the inner and outer segments since it has been shown that outer segments contain significant amounts of creatine kinase (Walliman *et al.* 1986) and that rod outer segment preparations can efficiently transfer a phosphate from creatine phosphate to ADP and AMP (Dontsov *et al.*, 1978; Schnetkamp and Daemen, 1981). The relative contributions of glycolysis and the phosphocreatine shuttle system to the generation of ATP and GTP for outer segment function will be discussed in Chapter 4.

CHAPTER 4

GLUCOSE METABOLISM IN THE OUTER SEGMENTS OF RETINAL PHOTORECEPTOR CELLS: ITS INVOLVEMENT IN THE MAINTENANCE OF THE PHOTOTRANSDUCTION PROCESS

4.1. MATERIALS

4.1.1. Animal tissues: Fresh bovine eyes were obtained from J & L Meats (Surrey, British Columbia).

4.1.2. Chemicals: D-[^{14}C(U)]-glucose (11.5 mCi/mmol), Hyamine solution and Aquasol-2 scintillation cocktail were purchased from New England Nuclear (Boston, MA). Hydrazine was from Eastman Organic Chemicals (Rochester, NY). Bicinchoninic acid (BCA) protein assay reagents were purchased from Pierce (Rockford, IL). All other chemicals were from Sigma (St. Louis, MO) or British Drug House Chemical Co. (Vancouver, British Columbia).

4.2. METHODS

4.2.1. Preparation of bovine ROS

ROS were prepared under dim red light from freshly dissected bovine retinas by sucrose gradient centrifugation according to a modified method of Molday *et. al.*, 1987. Briefly, one hundred retinas were placed in 40 ml of homogenizing solution consisting of 20 % (w/v) sucrose, 0.25 mM $MgCl_2$, 10 mM taurine, and 20 mM KH_2PO_4, pH 7.0. After gently shaking the retinas for 1 min, the tissue suspension was filtered through a Teflon filter. The filtrate was layered onto six 22 ml 27 - 45 % (w/v) continuous sucrose gradients containing 10 mM taurine, 0.25 mM $MgCl_2$ and 20 mM KH_2PO_4, pH 7.0. After centrifugation in a SW-28 rotor (Beckman Instruments, Inc., Palo Alto, CA) at 25,000 rpm for 1 h at 4 °C, the pink ROS band

was collected and diluted to a final volume of 150 ml with a resuspension buffer consisting of 20 % (w/v) sucrose and 10 mM KH_2PO_4, pH 7.0. Following centrifugation in a Sorvall SS-34 rotor (E.I. DuPont de Nemours & Co., Inc., Sorvall Instruments Div., Newtown, CT), the ROS pellets were resupended at a protein concentration of 14 - 16 mg/ml in a lysis buffer containing 10 mM KH_2PO_4, pH 7.0. The isolated ROS membranes were stored in the dark at 4 °C and used for experimentation within 8 h. Protein concentration of the ROS preparation was determined using the Bicinchoninic acid protein assay (Pierce).

4.2.2. Quantitation of glycolysis, hexose monophosphate pathway and retinal reduction in bovine ROS preparation

Unbleached ROS resuspended in 10 mM KH_2PO_4, pH 7.0 at a protein concentration of 8 mg/ml were diluted with an equal volume of assay buffer consisting of 10 mM $MgSO_4$, 2 mM NaCl, 5 mM ATP, 2 mM ADP, 2 mM NAD, and 90 mM KH_2PO_4, pH 7.0. The mixture was incubated with shaking in a 37 °C water bath for 10 min at a distance of 1.8 m from two 34 watt fluorescent lights (light condition) or at at a distance of 1 m from a dim red light (dark condition) prior to assay initiation. All assays were carried out using three different ROS preparations.

Glycolysis: The rate of glycolytic flux was measured by monitoring the production of lactate using a modified method of Clegg and Jackson (1988). The assay was carried out at 37 °C. One *u*l of 0.5 M glucose in 10 mM KH_2PO_4, pH 7.0 was placed at the bottom of a 15 x 85 mm glass test tube shaking in a 37 °C water bath at 60 rev/min and the assay was initiated by the addition of 100 *u*l of ROS to the glucose solution. At the desired time, the assay was terminated by the addition of 100 *u*l of 12 % of perchloric acid. Zero-time controls were carried out by adding the perchloric acid to the ROS suspension before initiating the assay. The precipitated ROS suspension was transferred to an Eppendorf tube and pelleted by

centrifugation in an Eppendorf Centrifuge 5415C (Canlab; Mississauga, Ontario) at 14,000 rpm for 3 min. One hundred-and-fifty *u*l of supernatant was neutralized with 100 *u*l of 1.6 M NaOH and added to 250 *u*l of lactate detection reagent. Each ml of lactate detection reagent contained 25 units of lactate dehydrogenase, 4 mg of NAD, 37.6 mg glycine and 17.6 *u*l of 95 % hydrazine, pH 9.5. The mixture was incubated at 37 °C for 90 min. Absorbance at 340 nm due to the production of NADH from the oxidation of lactate to pyruvate was measured at the end of incubation. Lithium lactate was used as standard for lactate calibration. Only background absorbance at 340 nm similar to that observed for zero-time controls was detected if lactate dehydrogenase was omitted from the lactate detection reagent. This indicates that the observed absorbance at 340 nm was due to the presence of lactate, not NADH, produced by glycolysis during the assay period.

Hexose monophosphate pathway: The rate of glucose oxidation by the hexose monophosphate pathway was determined by monitoring the production of $^{14}CO_2$ from D-[^{14}C(U)]glucose using the method of Thomson and Richards (1977). D-[^{14}C(U)]glucose in 90 % methanol was dried down under vacuum and resuspended with unlabelled glucose in 10 mM KH_2PO_4, pH 7.0 to a final specific activity of 4.7 x 10^5 dpm per *u*mol glucose. One *u*l of resuspended glucose was placed at the bottom of a 15 x 85 mm test tube and the assay was initiated as described above. Two-hundred *u*l of Hyamine was added to the center well (Kontes; Owens-Kimble Unit 15, Scarborough, Ontario) 20 sec before the assay was terminated by the addition of 100 *u*l of 12 % perchloric acid to the ROS mixture. After 4 h incubation at 25 °C with constant shaking to allow the trapping of $^{14}CO_2$ by Hyamine, the center well was cut directly into 10 ml of Aquasol-2 scintillation cocktail and counted in a scintillation counter. $^{14}CO_2$ production was not detected if ROS were omitted from the assay mixture indicating that no spontaneous

breakdown of ^{14}C[U]-glucose to $^{14}CO_2$ occurred during the assay period. Zero-time controls were carried out as described for the glycolytic flux measurements.

Retinal reduction: The rate of retinal reduction was determined by monitoring the disappearance of retinal in a ROS suspension using a modified method of Futterman and Saslaw (1961). The assay was initiated as described for glycolytic flux measurements and was terminated by the addition of 0.4 ml of ethanol. Procedures below were carried out under dim light. Retinal in the ROS mixture was assayed by incubation with 0.14 ml of thiobarbiturate and 0.14 ml of thiourea reagents in an Eppendorf tube for 30 min at room temperature. At the end of incubation, the mixture was centrifuged at 14,000 rpm for 5 min in an Eppendorf Centrifuge 5415C and the supernatant was collected for absorbance measurement at 530 nm. Purified all-*trans*-retinal was used as standard for retinal calibration.

4.2.3. Glycolytic enzyme assays

The efficiency of pig ROS hexokinase, phosphofructokinase, phosphoglycerate kinase and pyruvate kinase to use guanine and adenine nucleotides as their substrates were assessed by comparing the K_m and V_{max} of these glycolytic enzymes in the presence of corresponding nucleotide substrates. Pig ROS instead of bovine ROS were used for this study because pig ROS contain much higher glycolytic enzyme activities than bovine ROS (maximally 5 fold for pyruvate kinase, unpublished data). Enzyme activities were monitored at 25 °C by following the consumption or production of NADH at 340 nm through coupled enzyme reactions as described previously (Hsu and Molday, 1991). The hexokinase assay was carried out according to the method of Bucher *et al.* (1953); the phosphofructokinase assay according to the method of Harris *et al.* (1982); the phosphoglycerate kinase assay according to the method of Kulbe and Bojanovski (1982) except 100 mM Tris instead of 100 mM triethanolamine was used as the

buffer; and the pyruvate kinase assay according to the method of Kahn and Marie (1982). Changes in absorbance at 340 nm were monitored using a SLM Aminco spectrophotometer. One unit of enzyme activity is defined as the production of 1 *u*mol of NADH at 25 °C/min/mg of ROS protein using 6.22 x 10^3 M^{-1} cm^{-1} as the extinction coefficient for NADH.

4.2.4. Assessment of ROS purity

The extent of bleaching and purity of ROS membrane preparations were assessed by measuring the ROS A_{400}/A_{500} and A_{280}/A_{500} ratios respectively. Hypotonically lysed unbleached ROS were solubilized in 1.1 % cetyltrimethyl ammonium bromide (CTAB) at a protein concentration of 0.5 -1.5 mg/ml in the dark. Absorbances were measured by an Ultrospec II spectrophotometer (LKB, Milwaukee, WI) in the dark. The rhodopsin concentration of prepared ROS was determined by the method of Wald and Brown (1953) with few exceptions. ROS solubilized in CTAB at a protein concentration of 0.5-1.5 mg/ml were incubated with a final concentration of 20 mM hydroxylamine for 2 min. Absorbance of unbleached and bleached hydroxylamine-treated ROS solution at 500 nm was measured. The rhodopsin content in ROS was calculated from the difference in A_{500} values of unbleached and bleached ROS solutions using a molar extinction coefficient of 40,600 for rhodopsin. ROS membrane preparations used in this study had A_{400}/A_{500} ratios of 0.20-0.22, A_{280}/A_{500} ratios of 2.1-2.3 and retinaldehyde content of 16-20 nmol/mg total ROS protein.

4.3. RESULTS

4.3.1. Glycolytic flux in ROS

Assay condition: Because isolated ROS are not as well sealed as intact cells, metabolic cofactors such as adenine and guanine nucleotides are slowly lost from

ROS during the isolation procedure (Robinson and Hagins, 1979). In order to initiate glycolysis in ROS preparations, ROS have to be lysed in a sucrose-free buffer supplemented with cofactors such as NAD, ATP and ADP required to support glycolysis. Glycolytic flux was measured in a potassium-rich, phosphate-buffered assay medium similar in ionic composition to the intracellular fluid of muscle cells (Gregersen, 1961) in an effort to mimic the intracellular environment of ROS. The concentrations of supplied cofactors such as ATP, ADP and NAD in the assay buffer were similar to their corresponding intracellular concentrations in ROS as previously reported by Matchinsky (1968) and Robinson and Hagins (1979).

Glycolytic rate: The rate of glycolysis was quantitated by measuring the rate of lactate production. Fig. 28 shows a typical time course of lactate production by isolated bovine ROS. After a four minute lag period, lactate accumulation proceeded at a steady rate of 44.0 $\pm$ 6.4 nmol/min/mg ROS protein for at least eight minutes (three ROS preparations). This rate is higher than that of 27 nmol lactate/hr/mg ROS protein (0.45 nmol lactate/min/mg ROS protein) observed by McConnell *et al.* (1969) or 1.4 umol/10 mg dry wt./hr (4.7 nmol lactate/min/mg ROS protein) observed by Futterman *et al.* (1970), assuming that proteins constitute 50 % of the total ROS dry weight (Nielsen *et al.*, 1970). A higher lactate production rate observed here may be due to the omission of sucrose and Triton X-100 in the assay buffer and the measurement of the initial, rather than the overall, lactate production rate. Triton X-100 and high concentrations of sucrose inhibit glycolytic enzyme activities and decrease the overall glycolytic rate (unpublished observation). The overall rate of lactate production may be lower than the initial lactate production rate due to inactivation or end product inhibition of enzymes during a one-hour assay period.

The rate of lactate production was decreased by 20 % to 35.0 $\pm$ 4.9 nmol/min/mg ROS protein when 0.2 mM NADP was included in the assay buffer to

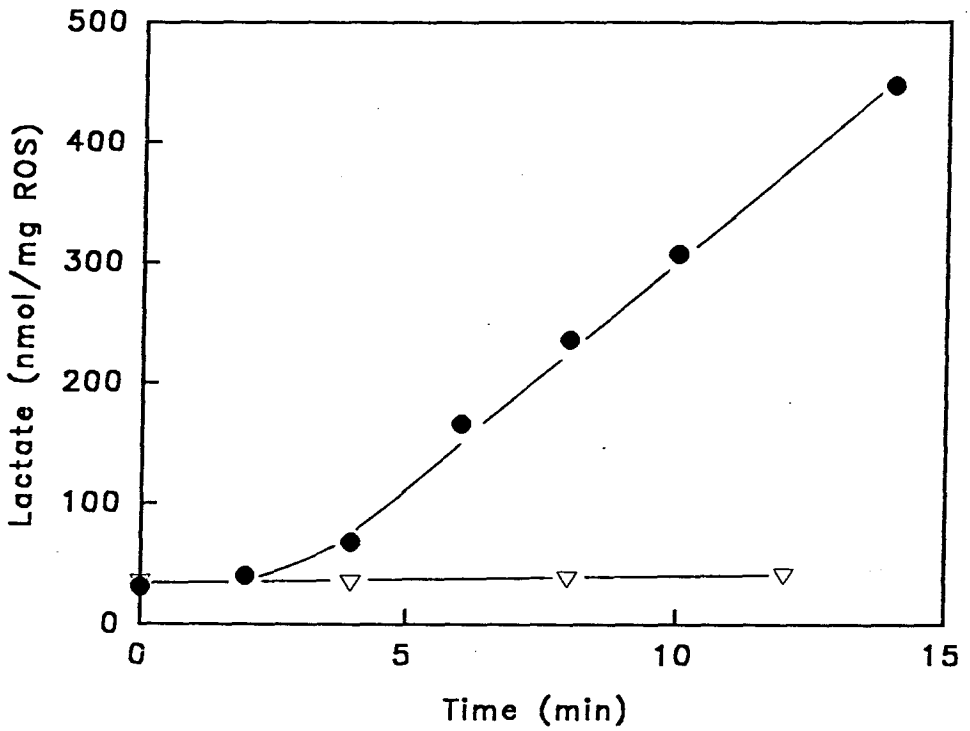

Fig. 28. **Glycolytic flux in isolated bovine ROS.**
A typical time course of glycolytic lactate production by isolated bovine ROS in the presence (●) and the absence (▽) of 5 mM glucose.

stimulate the hexose monophosphate pathway (three ROS preparations). This decrease in glycolytic rate is most likely due to channeling of glucose-6-phosphate from the glycolytic pathway to the hexose monophosphate pathway. The rate of glycolysis in ROS was not significantly affected by light. The lactate production rate was only maximally 10 % higher in light than in dark. This small increase in the glycolytic rate under light condition was probably due to the stimulation of glycolysis by ATP consumption during visual excitation. Lactate production was abolished when glucose was omitted from the assay buffer (Fig. 28). The presence of iodoacetate, an inhibitor of glycolytic enzymes triose phosphate isomerase and glyceraldehyde-3-phosphate dehydrogenase, in the assay buffer also inhibited glycolytic flux (data not shown).

GTP production by glycolysis: Because guanosine phosphates are present in similar concentrations as adenosine phosphates in ROS (Robinson and Hagins, 1979), the possibility of a direct GTP production by glycolysis to regenerate cGMP hydrolyzed by the cGMP-phosphodiesterase was investigated (Table X). Glycolysis has two energy-requiring steps catalyzed by hexokinase (HK) and phosphofructokinase (PFK) and two energy-generating steps carried out by phosphoglycerate kinase (PGK) and pyruvate kinase (PK, Fig. 9). GTP was used by phosphofructokinase but not by hexokinase for glucose phosphorylation. Figure 29 illustrates the dependence of phosphofructokinase activity on GTP and ATP concentrations. Both phosphoglycerate kinase and pyruvate kinase, however, were capable of using GDP for the production of GTP. All three glycolytic enzymes exhibited greater preference for ADP(ATP) over GDP(GTP) as their substrates. Since guanine and adenine nucleotides are present in similar concentrations in ROS, it may be estimated that GTP could be produced from 36 % and 29 % of total phosphorylation reactions catalyzed by phosphoglycerate kinase and pyruvate kinase respectively. The specificity of phosphoglycerate kinase and pyruvate kinase for

TABLE X

Specificity of Glycolytic Enzymes for Guanine and Adenine Nucleotides[a]

Enzyme	Nucleotide substrate	Km (uM)	Vmax (U/mg ROS)	Enzyme Specificity $\frac{kcat^{(GTP)}/Km^{(GTP)}}{kcat^{(ATP)}/Km^{(ATP)}}$ [b]
HK	ATP	150	0.023	0
	GTP	0[c]	0[c]	
PFK	ATP	35	0.088	0.26
	GTP	55	0.056	
PGK[d]	ATP	110	0.524	0.57
	GTP	155	0.596	
PK	ADP	350	3.76	0.41
	GDP	530	3.53	

[a] *Average values from two pig ROS preparations.*

[b] *This indicates the ratio of*

$$\frac{\text{specificity of enzyme using GDP or GTP as the substrate}}{\text{specificity of enzyme using ADP or ATP as the substrate.}}$$

[c] *Hexokinase activity was not detectable.*

[d] *PGK activity was assayed in a backward direction using ATP and GTP as its substrates.*

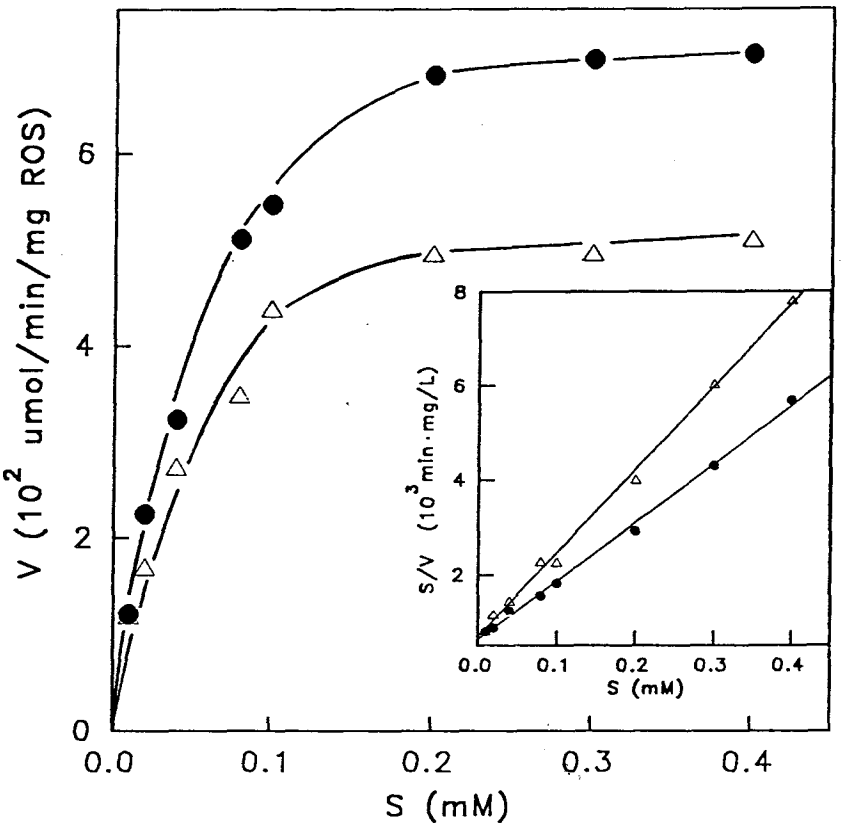

Fig. 29. **Specificity of phosphofructokinase for ATP and GTP.**
The activity of phosphofructokinase in isolated pig ROS was determined by measuring the initial rate of NADH production in coupled enzyme reactions (Harris *et al.*, 1982) initiated by the addition of of ATP or GTP. Michaelis-Menten graph shows the phosphofructokinase activity (V) as a function of ATP (●) or GTP (△) concentrations (S). Insert shows Hane's plot analysis of the Michaelis-Menten graph.

guanine over adenine nucleotides, as determined by the k_{cat}/K_m ratios shown in Table X, were 0.57 and 0.41, respectively. Thus approximately 11 % and 89 % of nucleoside triphosphates produced by glycolysis (specifically by reactions catalyzed by phosphoglycerate and pyruvate kinases) are GTP and ATP respectively. This would translate to a GTP production rate of 4.8 nmol/min/mg ROS protein by glycolysis since 22 nmol glucose/min/mg ROS protein was consumed by glycolysis.

4.3.2. Hexose monophosphate pathway

The rate of the hexose monophosphate pathway (HMP) in isolated bovine ROS was determined from CO_2 production by ROS. In the absence of added NADP, HMP proceeded at a rate of 2.9 $\pm$ 0.2 nmol CO_2/min/mg ROS protein or 6 nmol NADPH/min/mg ROS protein (three ROS preparations; Fig. 30). The detected CO_2 production was likely due to the presence of endogenous NADP in ROS (Schnetkamp *et al.*, 1979) rather than the presence of contaminating pyruvate dehydrogenase and tricarboxylic acid cycle enzymes isocitrate and *a*-ketoglutarate dehydrogenases from rod inner segments because the addition of unlabelled pyruvate, a substrate for the citric acid cycle, did not inhibit $^{14}CO_2$ production (see Fig. 9 for tricarboxylic acid cycle). In the presence of 2 mM iodoacetate which inhibited over 90 % of glycolysis, inclusion of 5 mM unlabelled pyruvate in the assay buffer actually increased the $^{14}CO_2$ production by 14 % (data not shown). This increase in CO_2 production was probably due to the consumption of NADPH formed by the HMP by lactate dehydrogenase in the presence of excess pyruvate (Cohen and Noell, 1960). Futterman (1963) had also detected CO_2 production by isolated bovine ROS in the absence of added NADP. A lower CO_2 production rate of 26 nmol/5mg dry wt./30min or 0.35 nmol/mg ROS protein/min observed by Futterman may be in part due to his measurement of an overall rather than the initial rate of CO_2 production for reasons discussed above in 4.3.1.

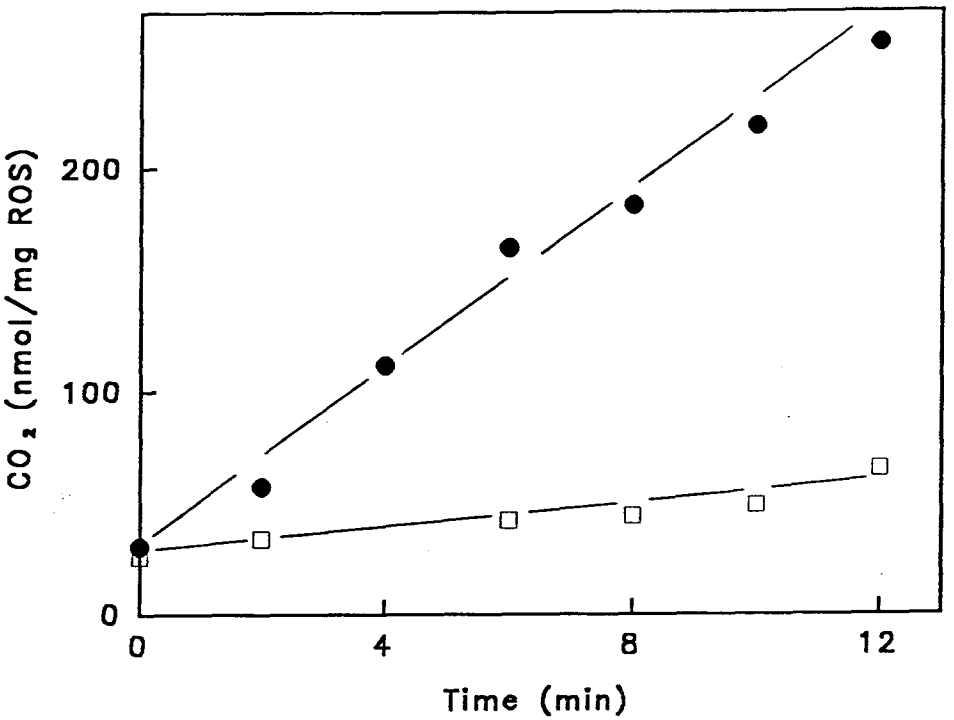

Fig. 30. **Hexose monophosphate pathway in isolated bovine ROS.**

The rate of glucose oxidation to CO_2 via the hexose monophosphate pathway in ROS was quantitated by measuring the rate of $^{14}CO_2$ production by isolated bovine ROS supplied with tracer amount of D-[^{14}C(U)]-glucose in the presence (●) and the absence (□) of 0.2 mM NADP.

The addition of 0.2 mM NADP in the assay buffer resulted in a 6-7 fold increase in CO_2 production by HMP to 19.8 $\pm$ 1.1 nmol CO_2 produced/min/mg ROS protein or about 40 nmol NADPH produced/min/mg ROS protein (three ROS preparations; Fig. 30). This increase in the HMP rate could be due to either an increase in glucose consumption by ROS or a rapid channeling of glucose intermediates through both the HMP and glycolysis so that both NADPH and lactate can be produced from each molecule of glucose. However, since lactate production using an HMP intermediate ribose-5-phosphate at 5 mM concentration was only 10 % of that using 5 mM glucose as the substrate, it is likely that the observed increase in the HMP rate was due to an increase in both the glucose consumption by ROS and the proportion of glucose-6-phosphate entering the HMP (Table XI). In the presence of a low concentration of NADP, approximately 24.9 nmol glucose/min/mg ROS protein was phosphorylated by hexokinase, and 12 % of phosphorylated glucose (2.9 nmol/min/mg ROS protein) was channeled to the HMP. In the presence of excess NADP, the rate of glucose phosphorylation was increased by 50 % to 37.5 nmol/min/mg ROS protein and 54 % of phosphorylated glucose (20 nmol/min/mg ROS protein) was used by the HMP. The extent of bleaching of ROS did not have a detectable effect on the rate of CO_2 production by the HMP.

4.3.3. RETINAL REDUCTION

ROS retinal content: To assess the potential of HMP in ROS to support retinal reduction, the rate of reduction of endogenous retinal to retinol in ROS was monitored using a thiobarbiturate assay previously described by Futterman and Saslaw, 1961 (Fig. 31). According to this assay, bovine ROS preparations used in this study contained approximately 18-19 nmol retinal/mg total ROS protein (three ROS preparations), in agreement with that of 16-20 nmol rhodopsin/mg total ROS

TABLE XI
Glucose Utilization by Bovine ROS

Condition	Glycolysis	HMP[a]	ROS glucose consumption
	(nmol/min/mg ROS protein)		
-NADP	22.0	2.9	24.9
+NADP (0.2mM)	17.5	20.0	37.5

[a] Hexose monophosphate pathway.

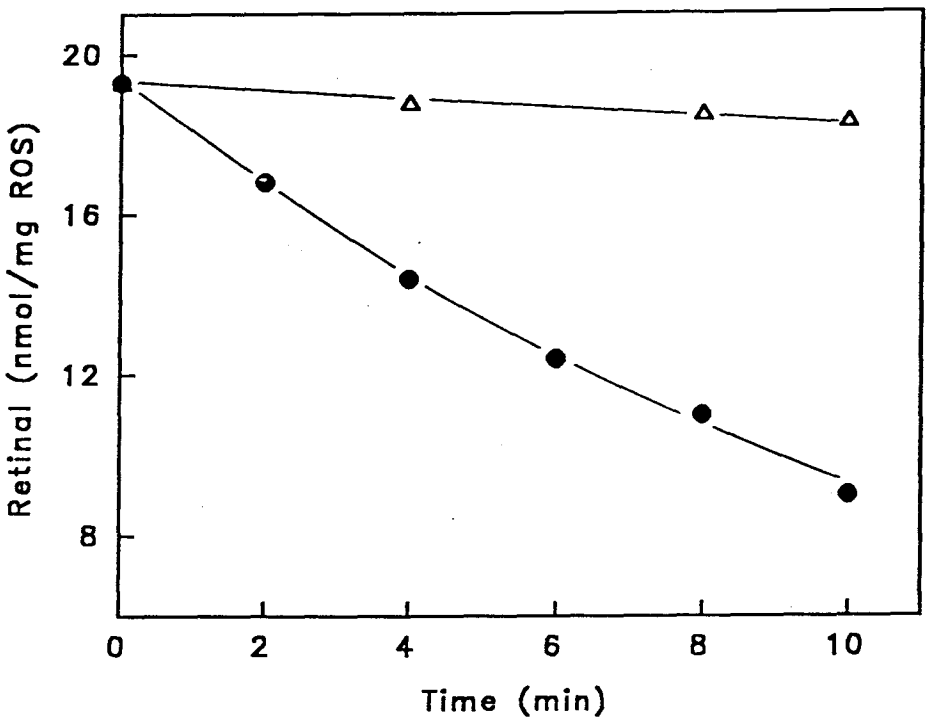

Fig. 31. **Retinal reduction in isolated bovine ROS.**

The rate retinal reduction to retinol in ROS was quantitated by measuring the disappearance of retinal in isolated bovine ROS in the presence (●) and absence (△) of 5 mM glucose.

protein quantitated using the spectrophotometric method described above in 4.2.4 assuming that each rhodopsin molecule has one molecule of bound retinal. Assuming that rhodopsin has a molecular weight of 38,000 g/mol and comprises 70 % of the total ROS protein, isolated bovine ROS should contain about 20 nmol rhodopsin or retinal/mg total ROS protein. Thus isolated bovine ROS used in this study contained approximately 85-100 % unbleached rhodopsin.

ROS retinal reduction: Figure 31 shows a typical time course of retinal reduction in bovine ROS. Very little retinal (0.09 $\pm$ 0.02 nmol retinal/min/mg ROS protein) was reduced when glucose was omitted from the assay buffer or when ROS were unbleached. In dark, it is likely that 11-*cis*-retinal bound to rhodopsin is unavailable for reduction. In addition, retinol dehydrogenase has been shown to reduce free all-*trans*-retinal 10 times more rapidly than it does free 11-*cis*-retinal (ref. Lion *et al.*, 1975). Under the light condition, an initial retinal reduction rate of 1.2 $\pm$ 0.2 nmol retinal/min/mg ROS protein was observed when bleached ROS were supplemented with 5 mM glucose and 0.2 mM NADP (three ROS preparations). Nicotra and Livrea (1982) have reported a retinal reduction rate of 5.8 nmol retinal reduced/min/mg ROS protein when retinal reduction was carried out in the presence of 0.5 mM NADPH. This higher rate is likely an overestimate of retinal reduction rate in ROS because the intracellular ratio of NAPDH to NADP in monkey and rabbit ROS is approximately 1:4 (Matschinsky, 1968) and NADP is a competitive inhibitor of retinal reduction process (Nicotra and Livrea, 1982). Substitution of glucose by fructose-1,6-bisphosphate did not support retinal reduction, suggesting that very little or no gluconeogenesis takes place in ROS.

4.4. DISCUSSION

The existence of glycolytic and hexose monophosphate pathways in isolated bovine ROS preparation suggests that glycolysis in ROS supplies both NADPH and

energy in the form of ATP and GTP for the maintenance of the phototransduction process. Energy-requiring processes in phototransduction include phosphorylation of photoactivated rhodopsin, replenishment of GTP hydrolyzed by transducin and regeneration of cGMP hydrolyzed by cGMP-phosphodiesterase (described in more detail in Chapter 1, 1.4). The rate of cGMP regeneration, one of the most energy-consuming processes in phototransduction, has been determined in intact rabbit retina by Ames *et al.* (1986). In dark, cGMP hydrolysis occurs at a basal intracellular rate of 1.7 mM cGMP/min. This translates to an ATP consumption of 3.4 mM/min since 2 ATP molecules are required to regenerate 1 molecule cGMP from 5'GMP in reactions catalyzed by guanosine monophosphate kinase, nucleoside diphosphate kinase and guanylate cyclase (Chapter 1, Fig. 5). Upon photoexcitation, the rate of cGMP hydrolysis increases by a maximal 4.5 fold to an ATP consumption of 15.3 mM/min. Glycolysis in ROS produces about 44 nmol lactate/min/mg ROS protein or 5.7 mM ATP/min, assuming that rhodopsin constitutes 70 % of the total ROS protein, has a molecular weight of 38,000 g/mol, and is present at an intracellular concentration of 2.4 mM in ROS (Ames *et al.*, 1986). This value is slightly higher compared to the human erythrocyte intracellular glycolytic flux rate of 6.76 *u*mol/10 min/100 mg hemoglobin (Harrison *et al.*, 1991) or 1.7 mM ATP/min assuming that each red blood cell has a volume of 116 $u m^3$ (Evans and Fung, 1972), that there are 15 g hemoglobin/dl blood and that there are 5.1×10^6 red blood cells/*u*l blood (Berne and Levy, 1988). Thus, glycolysis in ROS has the capacity to maintain cGMP regeneration in dark but not in light. A direct GTP production by glycolysis at a rate of 4.8 nmol/min/mg ROS protein or 0.6 mM/min alone is not sufficient to support cGMP regeneration in dark. It is likely that most cGMP is synthesized from GTP derived from ATP produced by glycolysis. In this regard, enzyme activities which rapidly transfer high-energy phosphate

groups between adenine and guanine nucleotides have been detected in ROS (Dontsov *et al.*, 1978).

NADPH produced by the HMP is required to support retinal reduction and the glutathione redox cycle in ROS. In the absence of exogenous NADP, about 12 % of the total glucose utilized by ROS is oxidized by the HMP. This ratio is the same as that calculated from Futterman's data for bovine ROS (1963, 1970) and is similar to the ratio of 10-11 % observed in human erythrocytes (Brin and Yonemoto, 1958; Murphy, 1960). This basal level of NADPH production by the HMP (5.8 nmol NADPH/min/mg ROS protein) is more than sufficient to support retinal reduction (1.2 nmol retinal/min/mg ROS protein) in ROS. The necessity of ROS glucose metabolism to support retinal reduction is reflected in the observation that the substitution of glucose by pyruvate, a substrate that supports the aerobic Krebs cycle in rod inner segment but not anaerobic glycolysis in ROS, cannot maintain the photoreceptor electrical activity at the optimal level (Winkler, 1981a). Upon stimulation by excess exogenous NADP, as much as 54 % of glucose consumed by ROS can be oxidized by the HMP. This large excess of NADPH produced by the HMP may be used to protect ROS against oxidative damage via the glutathione redox cycle (Winkler *et al.*, 1986; and Winkler, 1987).

Thus, glucose metabolism in both inner and outer segments of photoreceptor cells are required for the maintenance of the phototransduction process. Glucose metabolism in the outer segment has the capacity to maintain the basal rate of phototransduction in the dark, to buffer against sudden changes in ROS ATP concentration upon visual excitation and to support rhodopsin regeneration during visual recovery. Additional energy demand beyond the capacity of ROS glycolysis under light condition is satisfied by the phosphocreatine shuttle channeling energy from inner segment mitochondria to the outer segment.

SUMMARY

Photoreceptor cells are highly specialized neurons involved in mediating vision. Each photoreceptor cell is elongated in shape and is divided into four compartments: the outer segment, the inner segment, the cell body and the synaptic terminus. The process of phototransduction takes place in the outer segment while most anaerobic and all aerobic glucose metabolism in the photoreceptor cell occur in the inner segment. This compartmentalization of the photoreceptor cell has led to a general view that all the energy and nucleotides required by the phototransduction process are supplied by the inner segment. This belief is supported by three findings: Firstly, activities of enzymes involved in glycolysis and the hexose monophosphate pathway in the outer segment are less than 15 % of those in the inner segment in photoreceptor cells of both mammals and amphibians (Lowry *et al.*, 1956, 1961; Lolley and Hess, 1969). Secondly, mitochondrion- and brain-type creatine kinase isozymes have been detected in both cone and rod photoreceptor cells. The mitochondrion-type isozyme is found only in the inner segment where all the mitochondria of the photoreceptor cell are located. The brain-type isozyme, on the other hand, is distributed in both inner and outer segments. This differential localization of creatine kinase isozymes suggests that there is a phosphocreatine shuttle analogous to that found in muscle, spermatozoa and electric organ of *Torpedo marmorata* (Wallimann *et al.*, 1986) channeling energy derived from mitochondrial respiration to sites of energy-requiring processes in both inner and outer segments. In sea urchin spermatozoa, the phosphocreatine shuttle has been shown to provide all the energy required for sperm tail motility (Tombes and Shapiro, 1985). Thirdly, inhibition of aerobic glucose metabolism in intact retina by KCN resulted in a 60 % decrease in the photoreceptor current (Winkler, 1981) in the presence of physiological concentrations of glucose. This observation

suggests that anaerobic glucose metabolism in the photoreceptor outer segment alone is not sufficient to maintain phototransduction.

The results in this thesis suggest that there is glucose metabolism taking place in the outer segments of photoreceptor cells and that some energy and nucleotides required by the phototransduction process can be supplied by glucose metabolism in the outer segment. Activities of glycolytic enzymes, including the first and last enzymes in the glycolytic pathway have been detected in isolated photoreceptor rod outer segments (ROS). Although the specific activities of these glycolytic enzymes in ROS are much lower than that found in the photoreceptor inner segments, they are higher than that found in red blood cells. In fact, one glycolytic enzyme, glyceraldehyde-3-phosphate dehydrogenase (G3PD), was found to be a major protein associated with the ROS plasma membrane constituting up to 11-17 % of the total ROS plasma membrane protein. The binding site for this enzyme on the ROS plasma membrane is not known although it has been shown to be a trypsin- and chymotrypsin-sensitive protein that associates with G3PD in an electrostatic manner similar to that observed between G3PD and an anion channel Band 3 in human erythrocytes (Yu and Steck, 1975). Binding of G3PD to Band 3 has been shown to inhibit G3PD activity (Tsai *et al.*, 1982) and dissociation of G3PD due to tyrosine phosphorylation of Band 3 was found to be accompanied by a concomitant elevation in the erythrocyte glycolytic rate (Harrison *et al.*, 1991). It is possible that such enzyme release/activation mechanism could also play a role in regulating the glycolytic rate in the photoreceptor outer segment.

Immunohistochemical localization of glycolytic enzymes and detection of a GLUT-1 type glucose transporter in photoreceptor outer segments suggest that the measured glycolytic enzyme activities were not due to contaminating enzymes from

inner segments or other retinal cells. Three glycolytic enzymes, glyceraldehyde-3-phosphate dehydrogenase, phosphoglycerate kinase and lactate dehydrogenase have been localized in the outer segment layer of frozen retina sections by immunofluorescence microscopy. The presence of a glucose transporter on the plasma membrane of photoreceptor outer segments was investigated by the glucose transport assay, Western blot analyses and immunofluorescence microscopy. Both transport kinetics and Western blot analyses indicated that the outer segment glucose transporter is of the GLUT-1 type similar to that found in erythrocytes and brain cells. No GLUT-2 (liver-type) or GLUT-4 (adipocyte-type) glucose transporters were detected in photoreceptor outer segments by Western blotting analyses. Concurrently, Lopez-Escalera *et al.* (1991) have also detected glucose transport activity in rod outer segments exhibiting similar transport kinetics. It is possible that the photoreceptor outer segment also contains a GLUT-3 or a novel type glucose transporter in addition to the GLUT-1 isoform. Nevertheless, the presence of at least a GLUT-1 type glucose transporter in the photoreceptor outer segment suggests that this organelle can potentially obtain glucose from the blood supply to maintain its glucose metabolism.

The existence of a GLUT-1 type glucose transporter as well as enzymes involved in glucose metabolism in the photoreceptor outer segment raises questions of whether glucose metabolic pathways are active in the outer segment and how they may contribute to the maintenance of the phototransduction process. Three hypotheses have been put forward to define the function of glucose metabolism in ROS. First, ROS glucose metabolism may be required to produce NADPH for a partial maintenance of the retinal reduction process during the visual recovery phase of phototransduction (Futterman *et al.*, 1970). Second, glycolysis in ROS may specialize in phosphosphorylating GDP to form GTP via pyruvate kinase to

regenerate cGMP hydrolyzed by PDE (Lopez-Escalera *et al.*, 1991). Third, glucose metabolism in ROS may be involved in supplying energy to maintain housekeeping but not a phototransduction function in ROS (McConnell *et al.*, 1969). Present studies showed that glucose metabolism in ROS produces both the ATP and NADPH required by phototransduction. Glycolysis in ROS has the capacity to support cGMP regeneration, one of the most energy-consuming processes in phototransduction, under dark but not light conditions. Although ROS glycolysis can produce both ATP and GTP, only ATP is produced in sufficient quantity to maintain cGMP regeneration in the dark. GTP required for cGMP synthesis can therefore be produced from glycolysis-derived ATP since enzyme activities which rapidly transfer high-energy phosphate groups between adenine and guanine nucleotides have been detected in ROS (Dontsov *et al.*, 1978). The hexose monophosphate pathway in ROS produces sufficient NADPH to support retinal reduction during visual recovery. Excess NADPH produced by the hexose monophosphate pathway may be used to maintain the glutathione redox cycle to protect ROS from oxidative damage.

Thus glucose metabolism in both inner and outer segments of photoreceptor cells participate in the maintenance of phototransduction (Fig. 32). Glucose metabolism in the outer segment supplies NADPH and some energy in the form of ATP required by the phototransduction process. The hexose monophosphate pathway in the outer segment provides all the NADPH required for retinal reduction during visual recovery. Glycolysis, on the other hand, supplies energy in the form of ATP to maintain the basal level of cGMP regeneration in the dark and to buffer against sudden changes in ATP concentration upon illumination. During visual excitation, additional energy required for processes such as rhodopsin phosphorylation, transducin activation and a higher rate of cGMP regeneration can

be channeled from the inner segment to the outer segment by the phosphocreatine shuttle.

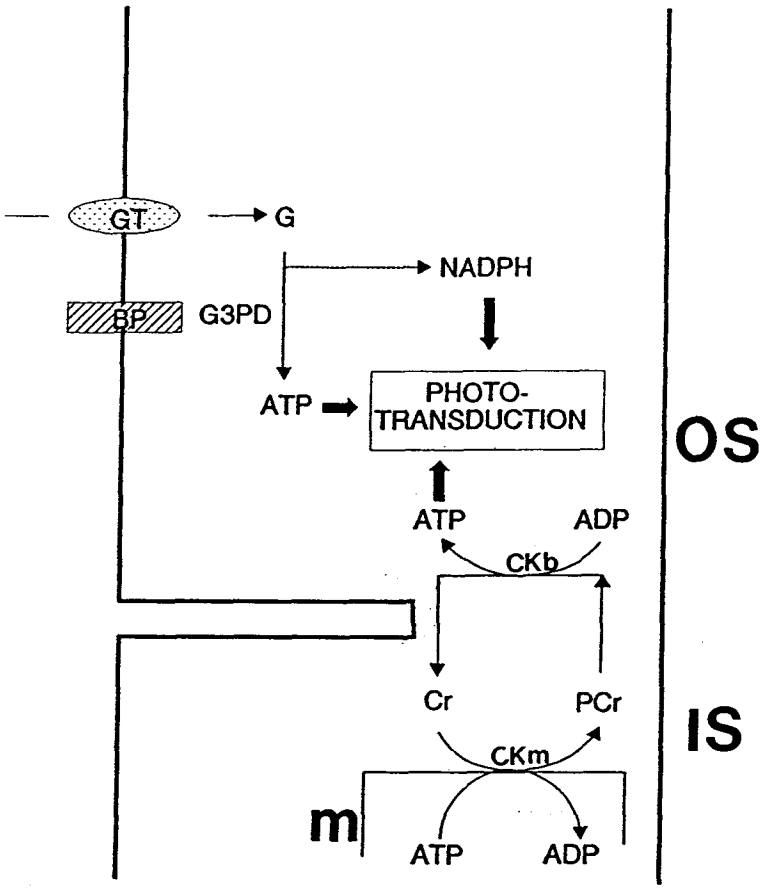

Fig. 32. **Maintenance of phototransduction by glucose metabolism in photoreceptor inner and outer segments.**

In the photoreceptor outer segment (OS), glucose metabolism is supported by glucose obtained from the blood supply through a GLUT-1 type glucose transporter (GT) located on the outer segment plasma membrane. The hexose monophosphate pathway (⇢) in this organelle provides NADPH required for retinal reduction to retinol (for rhodopsin regeneration) during visual recovery. The glycolytic pathway (→) in this organelle, on the other hand, supplies energy in the form of ATP to maintain phototransduction in the dark and to buffer against sudden changes in ATP concentration upon light illumination. One glycolytic enzyme, glyceraldehyde-3-phosphate dehydrogenase (G3PD) associates reversibly with an outer segment plasma membrane specific protein (BP). The function of this association is not known.

Additional energy required by the phototransduction process during visual excitation is provided by aerobic glucose metabolism in the photoreceptor inner segment (IS) via a phosphocreatine shuttle. ATP produced by aerobic glucose metabolism in the mitochondrion (M) is transphosphorylated to creatine (Cr) by a mitochondrion-type creatine kinase (CK_m) to produce phosphocreatine (PCr). Phosphocreatine diffuses to the outer segment where it is used to phosphorylate ADP by a brain-type creatine kinase (CK_b) to produce ATP required to support phototransduction during visual excitation. Creatine diffuses back to the inner segment and the shuttle repeats again.

REFERENCES

Allard, W.J., and Lienhard, G.E. (1985) Monoclonal Antibodies to the Glucose Transporter from Human Erythrocytes. *J. Biol. Chem.* **260**, 8668-8675.

Ames, A. III, Walseth, T.F., Heyman, R.A., Barad, M., Graeff, R.M. and Goldberg, N.D. (1986) Light-induced Increases in cGMP Metabolic Flux Correspond with Electrical Responses of Photoreceptors. *J. Biol. Chem.* **261**, 13034-13042.

Arcari, P., Martinelli, R., and Salvatore, F. (1984) The Complete Sequence of a Full Length cDNA for Human Liver Glyceraldehyde-3-phosphate Dehydrogenase: Evidence for Multiple mRNA Species. *Nucleic Acids Res.* **12**, 9179-9189.

Arshavsky, V.Y. and Bownds, M.D. (1992) Regulation of Deactivation of Photoreceptor G Protein by Its Target Enzyme and cGMP. *Nature* **357**, 416-417.

Baldwin, S.A. and Lienhard, G.E. (1981) Glucose Transport Across Plasma Membranes: Facilitated Diffusion Systems. *TIBS* **6**, 208-211.

Ballas, S.K., Kliman, H.J., and Smith, E.D. (1985) Glyceraldehyde-3-phosphate Dehydrogenase of Rat Erythrocytes Has No Membrane Component. *Biochim. Biophys. Acta* **831**, 142-149.

Bascom, R.A., Manara, S., Collins, L., Molday, R.S., Kalnins, V.I., and McInnes, R.R. (1992) Cloning of the cDNA for a Novel Photoreceptor Membrane Protein (rom-1) Identifies a Disk Rim Protein Family Implicated in Human Retinopathies. *Neuron* **8**, 1171-1184

Baylor, D.A., Lamb, T.D. and Yau, K.-W. (1979a) The Membrane Current of Single Rod Outer Segments. *J. Physiol.* **288**, 589-611.

Baylor, D.A., Lamb, T.D. and Yau, K.-W. (1979b) Responses of Retinal Rods to Single Photons. *J. Physiol.* **288**, 613-634.

Bell, G.I., Kayano, T., Buse, J.B., Burant, C.F., Takeda, J., Lin, D., Fukumoto, H. and Seino, S. (1990) Molecular Biology of Glucose Transporters. Diabetes Care 13, 198-208.

Bennett, N., Michel-Villaz, M., Kuhn, H. (1982) Light-induced Interaction Between Rhodopsin and the GTP-Binding Protein. Eur. J. Biochem. 127, 97-103.

Berger, S.J., DeVries, G.W., Carter, J.G., Schulz, D.W., Passonneau, P.N., Lowry, O.H., and Ferrendelli, J.A. (1980) The Distribution of the Components of the Cyclic GMP Cycle in Retina. *J. Biol. Chem.* **255**, 3128-3133.

Berne, R.M., and Levy, M.N. (1988) *Physiology*, 2nd ed., p. 361, The C.R. Mosby Company, St. Louis.

Bessman, S.P. and Geiger, P.J. (1981) Transport of Energy in Muscle: The Phosphorylcreatine Shuttle. *Science* **211**, 448-452.

Birnbaum, M.J., Haspel, H.C., and Rosen, O.M. (1986) Cloning and Characterization of a cDNA Encoding the Rat Brain Glucose-transporter Protein. *Proc. Natl. Acad. Sci. U.S.A.* **83**, 5784-5788.

Bloch, R. (1973) Inhibition of Glucose Transport in the Human Erythrocyte by Cytochalasin B. *Biochemistry* **12**, 4799-4801.

Bok, D. (1985) Retinal Photoreceptor-Pigment Epithelium Interactions. *Invest. Ophthalmol. Vis. Res.* **26**, 1659-1694.

Bok, D. and Heller, J. (1976) Transport of Retinol from the Blood to the Retina: Autoradiographic Study of the Pigment Epithelial Cell Surface Receptor for Plasma Retinol-binding Protein. *Exp. Eye Res.* **22**, 395-402.

Bownds, D., Dawes, J., Miller, J., and Stahlman, M. (1972) Phosphorylation of Frog Photoreceptor Membranes Induced by Light. *Nature New Biol.* **237**, 125-127.

Brahm, J. (1983) Kinetics of Glucose Transport in Human Erythrocytes. *J. Physiol.* **339**, 339-354.

Brin, M., and Yonemoto, R.H. (1958) Stimulation of the Glucose Oxidative Pathway in Human Erythrocyte by Methylene Blue. *J. Biol. Chem.* **230**, 307-317.

Brown, K.T. (1968) The Electroretinogram: Its Components and Their Origins. *Vision* **8**, 633-677.

Bücher *et al.* (1953) *Z. Naturforsch* from protocol supplied by ICN Biomedicals Canada Ltd., St. Laurent, Quebec.

Caswell, A.H., and Corbett, A.M. (1985) Interaction of Glyceraldehyde-3-phosphate Dehydrogenase with Isolated Microsomal Subfractions of Skeletal Muscle. *J. Biol. Chem.* **260**, 6892-6898.

Charbonneau, H., Prusti, R.K., LeTrong, H., Sonnenburg, W.K., Mullaney, P.J., Walsh, K.A., and Beavo, J.A. (1990) Identification of a Noncatalytic cGMP-binding Domain Conserved in Both the cGMP-stimulated and Photoreceptor Cyclic Nucleotide Phosphodiesterases. *Proc. Natl. Acad. Sci. U.S.A.* **87**, 288-292.

Cervetto, L., Lagnado, L., Perry, R.J., Robinson, D.W. and McNaughton, P.A. (1989) Extrusion of Calcium from Rod Outer Segments Is Driven by Both Sodium and Potassium Gradients. *Nature (London)* **337**, 740-743.

Clegg, J.S. and Jackson, S.A. (1988) Glycolysis in Permeabilized Cells. *Biochem. J.* **255**, 335-344.

Cohen, L.H. and Noell, W.K. (1960) Glucose Catabolism of Rabbit Retina Before and After Development of Visual Function. *J. Neurochem.* **5**, 253-276.

Cohen, L.H. and Noell, W.K. (1965) Relationships between Visual Function and Metabolism. In *Biochemistry of the Retina.* C. Graymore (ed.) Academic Press, London, 36-50.

Connell, G.J. and Molday, R.S. (1990) Molecular Cloning, Primary Structure, and Orientation of the Vertebrate Photoreceptor Cell Protein Peripherin in the Rod Outer Segment Disk Membrane. *Biochemistry* **29**, 4691-4698.

Cook, N.J., Hanke, W. and Kaupp, U.B. (1987) Identification, Purification, and Functional Reconstitution of the Cyclic GMP-dependent Channel from Rod Photoreceptors. *Proc. Natl. Acad. Sci. U.S.A.* **84**, 584-589.

Cook, N.J. and Kaupp, U.B. (1988) Solubilization, Purification, and Reconstitution of the Sodium-Calcium Exchanger from Bovine Retinal Rod Outer Segments. *J. Biol. Chem.* **263**, 11382-11388.

Cook, N.J., Molday, L.L., Reid, D., Kaupp., U.B. and Molday, R.S. (1989) The cGMP-gated Channel of Bovine Rod Photoreceptors Is Localized Exclusively in the Plasma Membrane. *J. Biol. Chem.* **264**, 6996-6999.

Craik, J.D. and Elliott, K.R.F. (1979) Kinetics of 3-O-Methyl-D-Glucose Transport in Isolated Rat Hepatocytes. *Biochem. J.* **182**, 503-508.

Crane, K. and Ball, E.G. (1951) Relationship of $^{14}CO_2$ Fixation to Carbohydrate metabolism in Retina. *J. Biol. Chem.* **189**, 269.

Czok, R., and Bücher, Th. (1960) Crystallized Enzymes from the Myogen of Rabbit Skeletal Muscle. *Adv. Protein Chem.* **15**, 315-415.

Dagher, S.M., and Deal., W.C., Jr. (1977) Pig Liver Glyceraldehyde-3-P Dehydrogenase: Purification, Crystallization, and Characterization. *Arch. Biochem. Biophys.* **179**, 643-653.

Deigner, P.S., Law, W.C., Canada, F.J. and Randon, R.R. (1989) Membranes as the Energy Source in the endergonic Transformation of Vitamin A to 11-*cis*-retinol. *Science* **244**, 968-971.

Dizhoor, A.M., Ray, S., Kumar, S., Niemi, G., Spencer, M., Brolley, D., Walsh, K.A., Philipov, P.P., Hurley, J.B., and Stryer, L. (1991) Recoverin: A Calcium Sensitive Activator of Retinal Rod Guanylate Cyclase. *Science* **251**, 915-918.

Dontsov, A.E., Zak, P.P. and Ostrovskii, M.A. (1978) Regeneration of ATP in Outer Segments of Frog Photoreceptors. *Biochemistry U.S.S.R.* **43**, 471-474.

Easterby, J.S. and Qadri, S.S. (1982) Hexokinase Type II from Rat Skeletal Muscle. *Methods Enzymol.* **90**, 11-15.

Edwards, P.A.W. (1974) A Test for Non-specific Diffusion Steps in Transport Across Cell Membranes, and Its Application to Red Cell Glucose Transport. *Biochim. Biophys. Acta* **345**, 373-386.

Eilam, Y. (1975) Two-carrier Models for Mediated Transport. II. Glucose and Galactose Equilibrium Exchange Experiments in Human Erythrocytes as a Test for Several Two-Carrier Models. *Biochim. Biophys. Acta* **401**, 364-369.

Eilam, Y. and Stein, W.D. (1972) A simple Resolution of the Kinetic Anomaly in the Exchange of Different Sugars Across the Membrane of the Human Red Blood Cell. *Biochim. Biophys. Acta* **266**, 161-173.

Emeis, D., Kuhn, H., Reichert, J., Hofmann, K.P. (1982) Complex Formation Between Metarhodopsin II and GTP-binding Protein in Bovine Photoreceptor Membranes Leads to a Shift of the Photoproduct Equilibrium. *FEBS Lett.* **143**, 29-34.

Erickson, M.A., Robinson, P., and Lisman, J. (1992) Deactivation of visual Transduction Without Guanosine Triphosphate Hydrolysis by G Protein. *Science* **257**, 1255-1258.

Evans, E. and Fung, Y.-C. (1972) Improved Measurements of the Erythrocyte Geometry. *Microvascular Res.* **4**, 335-347.

Fairbanks, G., Steck, T.L., and Wallach, D.F.H. (1971) Electrophoretic Analysis of the Major Polypeptides of the Human Erythrocyte Membranes. *Biochemistry* **10**, 2606-2617.

Fesenko, E.E., Kolesnikov, S.S. and Lyubarsky, A.L. (1985) Induction by Cyclic GMP of Cationic Conductance in Plasma Membrane of Retinal Rod Outer Segment. *Nature* **313**, 310-313.

Fort, P., Marty, L., Piechaczyk, M., El Sabrouty, S., Dani, C., Jeanteur, P., and Blanchard, J.M. (1985) Various Rat Adult Tissues Express Only One Major mRNA Species from the Glyceraldehyde-3-phosphate Dehydrogenase Multigenic Family. *Nucleic Acids Res.* **13**, 1431-1442.

Fowles, C., Akhtar, M. and Cohen, P. (1989) Interplay of Phosphorylation and Dephosphorylation in Vision: Protein Phosphatases of Bovine Rod Outer Segments. *Biochemistry* **28**, 9385-9391.

Fukumoto, H., Seino, S., Imura, H., Seino, Y., Eddy, R.L., Fukushima, Y., Byers, M.G., Shows, T.B., and Bell, G.I. (1988) Sequence, Tissue Distribution, and Chromosomal Localization of mRNA Encoding a Human Glucose Transporter-like Protein. *Proc. Natl. Acad. Sci. U.S.A.* **85**, 5434-5438.

Fung, B.K.-K. (1983) Characterization of Transducin from Bovine Retinal Rod Outer Segments. Separation and Reconstitution of the Subunits. *J. Biol. Chem.* **258**, 10495-10502.

Fung, B.K. and Griswold-Prenner, I. (1989) G Protein-Effector Coupling: Binding of Rod Phosphodiesterase Inhibitory Subunit to Transducin. *Biochemistry* **28**, 3133-3137.

Fung, B.K.-K., Hurley, J.B., Stryer, L. (1981) Flow of Information in the Light-triggered Cyclic Nucleotide Cascade of Vision. *Proc. Natl. Acad. Sci. USA* **78**, 152-156.

Fung, B.K.-K. and Stryer, L. (1980) Photolyzed Rhodopsin Catalyzes the Exchange of GTP for GDP in Retinal Rod outer Segment Membranes. *Proc. Natl. Acad. Sci. U.S.A.* **77**, 2500-2504.

Futterman, S. (1963) Metabolism of the Retina: III. The Role of Reduced Triphosphopyridine Nucleotide in the Visual Cycle. *J. Biol. Chem.* **238**, 1145-1150.

Futterman, S. and Kinoshita, J. (1959) Metabolism of the Retina. I. Respiration of Cattle Retina. *J. Biol. Chem.* **234**, 723-726.

Futterman, S., Hendrickson, A., Bishop, P.E., Rollins, M.H., and Vacano, E. (1970) Metabolism of Glucose and Reduction of Retinaldehyde in Retinal Photoreceptors. *J. Neurochem.* **17**, 149-156.

Futterman, S., and Saslaw, L.D. (1961) The Estimation of Vitamin A Aldehyde with Thiobarbituric Acid. *J. Biol. Chem.* **236**, 1652-1657.

Gerhart, D.Z., LeVasseur, R.J., Broderius, M.A., and Drewes, L.R. (1989) Glucose Transporter Localization in Brain Using Light and Electron Immunocytochemistry. *J. Neuroscience Res.* **22**, 464-472.

Gorga, F.R., Baldwin, S.A., and Lienhard, G.E. (1979) The Monosaccharide Transporter from Human Erythrocytes is Heterogeneously Glycosylated. *Biochem. Biophys. Res. Commun.* **91**, 955-961.

Gould, G.W. and Bell, G.I. (1990) Facilitative Glucose Transporters: an Expanding Family. *TIBS* **15**, 18-23.

Graymore, C. (1959) Metabolism of the Developing Retina. I. Aerobic and Anaerobic Glycolysis in the Developing Rat Retina. *Br. J. Opthalmol.* **43**, 34-39.

Graymore, C. (1970) Biochemistry of the Retina in *Biochemistry of the Eye.* C. Graymore (ed.) Academic Press, London, 645-735.

Graymore, C.N. and Towlson, M.J. (1965) The Metabolism of the Retina of the Normal and Alloxan Diabetic Rat. *Vis. Res.* **5**, 379-389.

Gregersen, M.I. (1961) Total Body Water and Fluid Compartment in *Medical Physiology* (Philip Bard, ed), 11*th* ed., p. 307, The C.V. Mosby Co., St. Louis.

Hagins, W.A., Pen, R.D. and Yoshikami, S. (1970) Dark Current and Photocurrent in Retinal Rods. *Biophys. J.* **10**, 380-412.

Harrington, W.F., and Karr, G.M. (1965) Subunit Structure of Glyceraldehyde-3-phosphate dehydrogenase. *J. Mol. Biol.* **13**, 885-893.

Harris, J.I., and Perham, R.N. (1965) Glyceraldehyde-3-Phosphate Dehydrogenases: I. The Protein Chains in Glyceraldehyde-3-phosphate Dehydrogenase from Pig Muscle. *J. Mol. Biol.* **13**, 876-884.

Harris, B.G., Starling, J.A., and Hofer, H.W. (1982) Phosphofructokinase from *Ascaris suum* Muscle. *Methods Enzymol.* **90**, 45-49.

Harrison, M.L., Rathnavelu, P., Arese, P., Geahlen, R.L. and Low, P.S. (1991) Role of Band 3 Tyrosine Phosphorylation in the Regulation of Erythrocyte Glycolysis. *J. Biol. Chem.* **266**, 4106-4111.

Hediger, M.A., Coady, M.J., Ideda, T.S. and Wright, E.M. (1987) Expression Cloning and cDNA Sequencing of the Na^+-glucose Co-transporter. *Nature* **330**, 379-381.

Heinz, F., and Kulbe, K.D. (1970) Glyceraldehydephosphate Dehydrogenase from Liver, I. Isolation and Characterization of the Bovine Liver Enzyme. *Hoppe-Seyler's Z. Physiol. Chem.* **351**, 249-262.

Hicks, D. and Molday, R.S. (1986) Differential Immunogold-Dextran Labeling of Bovine and Frog Rod and Cone Cells Using Monoclonal Antibodies Against Bovine Rhodopsin. *Exp. Eye Res.* **42**, 55-71.

Hodges, R.S., Heaton, R.J., Parker, J.M.R., Molday, L., and Molday, R.S. (1988) *J. Biol. Chem.* **263**, 11768-11775.

Hodgkin, A.L., McNaughton, P.A. and Nunn, B.J. (1985) The Ionic Selectivity and Calcium Dependence of the Light-Sensitive Pathway in Toad Rods. *J. Physiol. (London)* **358**, 447-468.

Holmgren, F. (1865-6) Method Att Objectivera Effecten av Ljusintryck pa Retina. *Upsala Lakaref* **1**, 177-191.

Hoos, R.T., Tarpley, H.L., and Regen, D.M. (1972) Sugar Transport in Beef Erythrocytes. *Biochim. Biophys. Acta* **266**, 174-181.

Hsu, S.-C. and Molday, R.S. (1990) Glyceraldehyde-3-phosphate Dehydrogenase Is a Major Portein Associated with the Plasma Membrane of Retinal Photoreceptor Outer Segments. *J. Biol. Chem.* **265**, 13308-13313.

Hsu, S.-C. and Molday, R.S. (1991) Glycolytic Enzymes and a GLUT-1 Glucose Transporter in the Outer Segments of Rod and Cone Photoreceptor Cells. *J. Biol. Chem.* **266**, 21745-21752.

Hsu, Y.-T. and Molday, R.S. (1993) Modulation of the CGMP-gated Channel of Rod Photoreceptor Cells by Calmodulin. *Nature* **361**, 76-79.

Huitorel, P., and Pantaloni, P. (1985) Bundling of Microtubules by Glyceraldehyde-3-phosphate Dehydrogenase and Its Modulation by ATP. *Eur. J. Biochem.* **150**, 265-269.

Ishiguro, S.-I., Suzuki, Y., Tamai, M. and Mizuno, K. (1991) Purification of Retinol Dehydrogenase from Bovine Retinal Rod Outer Segments. *J. Biol. Chem.* **266**, 15520-15524.

James, D.E., Brown, R., Navarro, J., Pilch, P.F. (1988) Insulin-regulatable Tissues Express a Unique Insulin-Sensitive Glucose Transport Protein. *Nature* **333**, 183-185.

Johnson, L.V. and Blanks, J.C. (1984) Application of Acrylamide as an Embedding Medium in Studies of Lectin and Antibody Binding in the Vertebrate Retina. *Current Eye Res.* **3**, 969-973.

Kamps, K.M.P., DeGrip, W.J., and Daemen, F.J.M. (1982) Use of a Density Modification Technique for Isolation of the Plasma Membrane of Rod Outer Segments. *Biochim. Biophys. Acta* **687**, 296-302.

Kahn, A., and Marie, J. (1982) Pyruvate Kinases from Human Erythrocytes and Liver. *Methods Enzymol.* **90**, 131-140.

Kant, J.A., and Steck, T.L. (1973) Specificity in the Association of Glyceraldehyde-3-phosphate Dehydrogenase with Isolated Human Erythrocyte Membranes. *J. Biol. Chem.* **248**, 8457-8464.

Kasahara, M. and Hinkle, P.C. (1977) Reconstitution and Purification of the D-Glucose Transporter from Human Erythrocytes. *J. Biol. Chem.* **252**, 7384-7390.

Kasanicki, M.A. and Pilch, P.F. (1990) Regulation of Glucose-Transporter Function. *Diabetes Care* **13**, 219-227.

Kaupp, U.B. and Koch, K.-W. (1986) Mechanism of Photoreception in Vertebrate Vision. *TIBS* **11**, 43-47.

Kawamoto, R.M., and Caswell, A.H. (1986) Autophosphorylation of Glyceraldehydephosphate Dehydrogenase and Phosphorylation fo Protein from Skeletal Muscle Microsomes. *Biochemistry* **25**, 656-661.

Keokitichai, S., and Wrigglesworth, J.M. (1980) Association of Glyceraldehyde-3-phosphate Dehydrogenase with the Membrane of the Intact Human Erythrocyte. *Biochem. J.* **187**, 837-841.

Kliman, H.J. and Steck, T.L. (1980) Association of Glyceraldehyde-3-phosphate Dehydrogenase with the Human Red Cell Membrane. *J. Biol. Chem.* **255**, 6314-6321.

Koch, K.-W. and Kaupp, U.B. (1985) Cyclic GMP Directly Regulates a Cation Conductance in Membranes of Bovine rods by a Cooperative Mechanism. *J. Biol. Chem.* **260**, 6788-6800.

Koch, K.-W. and Stryer, L. (1988) Highly Cooperative Feedback Control of Retinal Rod Guanylate Cyclase by Calcium Ions. *Nature* **334**, 64-66.

Kokame, K., Fukada, Y., Yoshizawa, T., Takao, T., and Shimonishi, Y. (1992) Lipid Modification at the N Terminus of Photoreceptor G-protein *a*-Subunit. *Nature* **359**, 749-752.

Korenbrot, J.I. and Miller , D.L. (1989) Cytoplasmic Free Calcium Concentration in Dark-adapted Reinal Rod Outer Segments. *Vis. Res.* **29**, 939-948.

Krebs, E.G., Rafter, G.W., and Junge, J.M. (1953) Yeast Glyceraldehyde-3-phosphate Dehydrogenase: Yeast Protein II. *J. Biol. Chem.* **200**, 479-492.

Kühn, H. (1980) Light- and GTP-regulated Interaction of GTPase and Other Proteins With Bovine Photoreceptor Membranes. *Nature* **283**, 587-589.

Kühn, H., Bennett, N., Michel-Villaz, M., Chabre, M. (1981) Interactions Between Photoexcited Rhodopsin and GTP-binding Protein: Kinetics and Stoichiometric Analyses from Light-Scattering Changes. *Proc. Natl. Acad. Sci. USA* **78**, 6873-6877.

Kühn, H. and Dreyer, W.J. (1972) Light Dependent Phosphorylation of Rhodopsin by ATP. *FEBS Lett.* **20**, 1-6.

Kühn, H., Hall, S.W. and Wilden, U. (1984) Light-induced Binding of 48-kDa Protein to Photoreceptor Membranes Is Highly Enhanced by Phosphorylation of Rhodopsin. *FEBS Lett.* **176**, 473-478.

Kulbe, K.D., and Bojanovski, M. (1982) 3-Phosphoglycerate Kinase from Bovine Liver and Yeast. *Methods Enzymol.* **90**, 115-120.

Kulbe, K.D., Foellmer, H., and Fuchs, J. (1982) Simultaneous Purification of Glyceraldehyde-3-phosphate Dehydrogenase, 3-Phosphoglycerate Kinase, and Phosphoglycerate Mutase from Pig Liver and Muscle. *Methods Enzymol.* **90**, 498-511.

Kulbe, K.D., Jackson, K.W., and Tang, J. (1975) Structural Evidence for a Liver-specific Glyceraldehyde-3-phosphate Dehydrogenase. *Biochim. Biophys. Res. Commun.* **67**, 35-42.

Kuwabara, T. and Cogan, D.G. (1961) Retinal Glycogen. *Am. J. Ophthalmol.* **66**, 680-688.

Kuwata, O., Imamoto, Y., Okano, T., Kokame, K. Kojima, D., Matsumoto, H., Morodome, A., Fukada, Y., Shichida, Y., Yasuda, K., Shimura, Y., and Yoshizawa, T. (1990) The Primary Structure of Iodopsin, a Chicken Red-sensitive Cone Pigment. *FEBS Lett.* **272**, 128-132.

Laemmli, U.K. (1970) Cleavage of Structural Proteins During the Assembly of the Head of Bacteriophage T4. *Nature* **227**, 680-685.

Lamb, T.D., McNaughton, P.A. and Yau, K.-W. (1981) Spatial Spread of Activation and Background Desensitization in Toad Rod Outer Segments. *J. Physiol.* **319**, 463-496.

Lambrecht, H.-G. and Koch, K.-W. (1991) A 26 kd Calcium Binding Protein from Bovine Rod Outer Segments as Modulator of Photoreceptor Guanylate Cyclase. *EMBO* **10**, 793-798.

Lane, R.D., Crissman, R.S. and Ginn, S. (1986) High Efficiency Fusion Procedure for Producing Monoclonal Antibodies Against Weak Immunogens. *Methods Enzymol.* **121**, 183-192.

Lee, C.-Y., Yuan, J.H., and Goldberg, E. (1982) Lactate Dehydrogenase Isozymes from Mouse. *Methods Enzymol.* **89**, 351-358.

LeFevre, P.G. and Marshall, J.K. (1959) The attachment of Phloretin and Analogues to Human Erythrocytes in Connection with Inhibition of Sugar Transport. *J. Biol. Chem.* **234**, 3022-3026.

Liebman, P.A. and Pugh, E.N.Jr. (1980) Phosphodiesterase Activation in Visual Receptor Membranes. *Nature* **287**, 734-736.

Lin, S. and Snyder, C.E.Jr. (1977) High Affinity Cytochalasin B Binding to Red Cell Membrane Proteins Which Are Unrelated to Sugar Transport. *J. Biol. Chem.* **252**, 5464-5471.

Lion, F., Rotmans, J.P., Daemen, F.J.M. and Bonting, S.L. (1975) Biochemical Aspects of the Visual Process: XXVII. Stereospecificity of Ocular Retinol Dehydrogenases and the Visual Cycle. *Biochim. Biophys. Acta* **384**, 283-292.

Liou, G.I., Bridges, C.C.B., Fong, S.-L., Alvarez, R.A. and Gonzalez-Fernandez, F. (1982) Vitamin A Transport between Retina and Pigment Epithelium - An Interstitial Protein Carrying Endogenous Retinol (Interstitial Retinol-binding Protein). *Vision Res.* **22**, 1457-1467.

Lolley, R.N. and Hess, H.H. (1969) The Retinal Rod Outer Segment of the Frog: Detachment, Isolation, Phosphorus Fraction and Enzyme Activity. *J. Cellular Physiol.* **73**, 9-24.

Lolley, R.N. and Lee, R.H. (1990) Cyclic GMP and Photoreceptor Function. *FASEB J.* **4**, 3001-3008.

Lopez-Escalera, R., Li, X.-B., Szerencsei, R.T., and Schnetkamp, P.P.M. (1991) Glycolysis and Glucose Uptake in Intact Outer Segments Isolated from Bovine Retinal Rods. *Biochemistry* **30**, 8970-8976.

Lowe, A.G. and Walmsley, A.R. (1985) A Quenched-flow Technique for the Measurement of Glucose Influx into Human Red Blood Cells. *Anal. Biochem.* **144**, 385-389.

Lowry, O.H., Roberts, N.R., and Lewis, C. (1956) The Quantitative Histochemistry of the Retina. *J. Biol. Chem.* **220**, 879-892.

Lowry, O.H., Roberts, N.R., Schulz, D.W., Clow, J.E., and Clark, J.R. (1961) Quantitative Histochemistry of Retina: II. Enzymes of Glucose Metabolism. *J. Biol. Chem.* **236**, 2813-2820.

MacKenzie, D., and Molday, R.S. (1982) Organization of Rhodopsin and a High Molecular Weight Glycoprotein in Rod Photoreceptor Disc Membranes Using Monoclonal Antibodies. *J. Biol. Chem.* **257**, 7100-7105.

March, S.C., Parikh, I., and Cuatrecasas, P. (1974) A simplified Method for Cyanogen Bromide Activation of Agarose for Affinity Chromatography. *Anal. Biochem.* **60**, 149-152,

Maretzki, D., Reimann, B., and Rapoport, S.M. (1989) A Reappraisal of the Binding of Cytosolic Enzymes to Erythrocyte Membranes. *TIBS* **14**, 93-96.

Matchinsky, F.M. (1968) Quantitative Histochemistry of Nicotinamide Adenine Nucleotides in Retina of Monkey and Rabbit. *J. Neurochem.* **15**, 663-657.

Matesic, D., and Liebman, P.A. (1987) CGMP-Dependent Cation Channel of Retinal Rod Outer Segments. *Nature* **326**, 600-603.

McConnell, D.G. (1965) The Isolation of Retinal Outer Segment Fragments. *J. Cell Biol.* **27**, 459.

McConnell, D.G., Ozga, G.W. adn Solze, D.A. (1969) Evidence for Glycolysis in Bovine Retinal Microsomes and Photoreceptor Outer Segments. *Biochim. Biophys. Acta* **184**, 11-28.

McNaughton, P.A., Cervetto, L. and Nunn, B.J. (1986) Measurement of the Intracellular Free Calcium Concentration in Salamander Rods. *Nature* **322**, 261-263.

Miller, D.M. (1968) The Kinetics of Selective Biological Transport. *Biophys J.* **8**, 1329-1338.

Miller, J.L., Fox, D.A. and Litman, B.J. (1986) Amplification of Phosphodiesterase Activation is Greatly Reduced by Rhodopsin Phosphorylation. *Biochemistry* **25**, 4983-4988.

Miller, R.F. and Dowling I.E. (1970) Intracellular Responses of the Muller (Glial) Cells of Mudpuppy Retina. Their Relation to *b*-Wave of the Electroretinogram. *J. Neurophysiol.* **33**, 323-341.

Mizuno, K. and Sato, K. (1975) Reassessment of Histochemistry of Retinal Glycogen. *Exp. Eye Res.* **21**, 489-497.

Molday, L.L., Cook, N.J., Kaupp, U.B. and Molday, R.S. (1990) The cGMP-gated Cation Channel of Bovine Rod Photoreceptor Cells Is Associated with a 240-kDa Protein Exhibiting Immunochemical Cross-reactivity with Sepctrin. *J. Biol. Chem.* **265**, 18690-18695.

Molday, R.S., Hicks, D., and Molday, L. (1987) Peripherin, A Rim-specific Membrane Protein of Rod Outer Segment Discs. *Invest. Ophthalmol. Vis. Sci.* **28**, 50-61.

Molday, R.S. and MacKenzie, D. (1983) Monoclonal Antibodies to Rhodopsin: Characterization Cross-reactivity, and Application as Structural Probes. *Biochemistry* **22**, 653-660.

Molday, R.S. and Molday, L.L. (1987) Differences in the Protein Composition of Bovine Retinal Rod Outer Segment Disk and Plasma membranes Isolated by a Ricin-Gold-Dextran Density Perturbation Method. *J. Cell Biol.* **105**, 2589-2601.

Morjaria, B. and Voaden, M.J. (1979) The Formation of Glutamate, Aspartate and GABA in the Rat Retina; Glucose and Glutamine as Precursors. *Exp. Eye. Res.* **21**, 489-497.

Mueckler, M. (1990) Family of Glucose-Transporter Genes: Implications for Glucose Homeostasis and Diabetes. *Diabetes* **39**, 6-11.

Mueckler, M., Caruso, C., Baldwin, S.A., Panico, M., Blench, I., Morris, H.R., Allard, W.J., Lienhard, G.E., Lodish, H.F. (1985) Sequence of Structure of a Human Glucose Transporter. *Science* **229**, 941-945.

Murphy, J.R. (1960) Erythrocyte Metabolism: II Glucose Metabolism and Pathways. *J. Lab. Clin. Med.* **55**, 286-302.

Murthy, S.N.P., Liu, T., Kaul, R.K., Kohler, H., and Steck, T.L. (1981) The Aldolase-binding Site of the Human Erythrocyte Membrane Is at the NH_2 Terminus of Band 3. *J. Biol. Chem.* **256**, 11203-11208.

Nataki, K. and Yau, K.-W. (1988a) Calcium and Magnesium Fluxes Across the Plasma Membrane of the Toad Rod Outer Segment. *J. Physiol.* **395**, 695-792.

Nataki, K. and Yau, K.-W. (1988b) Guanosine 3'-5'-Cyclic Monophosphate-activated Conductance Studied in a Truncated Rod Outer Segment of the Toad. *J. Physiol. (London)* **395**, 731-753.

Neubert, T.A., Johnson, R.S., Hurley, J.B. and Walsh, K. (1992) *J. Biol. Chem.* **267**, 18274-18277.

Nicotra, C., and Livrea, M.A. (1982) Retinol Dehydrogenase from Bovine Retinal Rod Outer Segments. *J. Biol. Chem.* **257**, 11836-11841.

Nielsen, N.C., Fleischer, S., and McConnell, D.G. (1970) Lipid Composition of Bovine Retinal Outer Segment Fragments. *Biochim. Biophys. Acta* **211**, 10-19.

Nowak, K., Wolny, M., and Banas, T. (1981) The Complete Amino Acid Sequence of Human Muscle Glyceraldehyde-3-phosphate Dehydrogenase. *FEBS Lett.* **134**, 143-146.

Ogden, T.E. (1973) The Oscillatory Waves of the Primate Electroretinogram. *Vision Res.* **13**, 1059-1074.

Palczewski, K., Hargrave, P.A., McDowell, J.H. and Ingebritsen, T.S. (1989) The Catalytic Subunit of Phosphatase 2A Dephosphorylates Phosphoopsin. *Biochemistry* **28**, 415-419.

Pan, L., Beverley, P.C.L., Bobrow, L.G., Swallow, D.M., and Isaacson, P.G. (1989) Production of Monoclonal Antibodies to Lactate Dehydrogenase (LDH) Isoenzymes for Immunohistochemical Study on Fixed Tissue Section. *Histochem. J.* **21**, 638-644.

Papermaster, D.S. and Dreyer, W.J. (1974) Rhodopsin Content in the Outer Segment Membranes of Bovine and Frog Retinal Rods. *Biochemistry* **13**, 2438-2444.

Penn, R.D. and Hagins, W.A. (1972) Kinetics of the Photocurrent of Retinal Rods. *Biophys. J.* **12**, 1073-1094.

Pfeffer, B., Wiggert, B., Lee, L., Zonnenberg, B., Newsome, D. and Chader, G. (1983) The Presence of a Soluble Interphotoreceptor Retinol-binding Protein (IRBP) in the Retinal Interphotoreceptor Space. *J. Cell Physiol.* **117**, 333-341

Pugh, E.N.Jr. and Lamb, T.D. (1990) Cyclic GMP and Calcium: The Internal Messengers of Excitation and Adaptation in Vertebrate Photoreceptors. *Vision Res.* **30**, 1923-1948.

Rahman, M.A. and Kerly, M. (1961) pathways of Glucose Metabolism of Ox Retina In Vitro. *Biochem. J.* **78**, 536-540.

Ratto, G.M., Payne, R., Owen, W.G., and Tsien, R.Y. (1988) The Concentration of Cytosolic Free Calcium in Vertebrate Rod Outer Segments Measured with Fura-2. *J. Neurosci.* **8**, 3240-3246.

Rawn, J.D. (1989) in *Biochemistry*. Neil Patterson Publishers, North Carolina.

Reid, D.M., Friedel, U., Molday, R.S., and Cook, N.J. (1990) Identification of the Sodium-calcium Exchanger as the Major Ricin-binding Glycoprotein of Bovine Rod Outer Segments and Its Localization to the Plasma Membrane. *Biochemistry* **29**, 1601-1607.

Rich, G.T., Dawson, A.P., and Pryor, J.S. (1984) Lack of Binding of Glyceraldehyde-3-phosphate Dehydrogenase to Erythrocyte Membranes Under In Vivo Conditions. *Biochem. J.* **221**, 197-202.

Rich, G.T., Pryor, J.S., and Dawson, A.P. (1985) Glyceraldehyde-3-phosphate Dehydrogenase Release from Erythrocytes During Haemolysis. *Biochim. Biophys. Acta* **817**, 61-66.

Riley, M.V. and Voaden, M.J. (1970) The Metabolism of the Isolated Retina. *Ophthalmic Res.* **1**, 58-64.

Robinson, W.E., and Hagins, W.A. (1979) GTP Hydrolysis in Intact Rod Outer Segments and the Transmitter Cycle in Visual Excitation. *Nature* **280**, 398-400.

Rogalski, A.A., Steck, T.L., and Waseem, A. (1989) Association of Glyceraldehyde-3-phosphate Dehydrogenase with the Plasma Membrane of the Intact Human Red Blood Cell. *J. Biol. Chem.* **264**, 6438-6446.

Saari, J.C. and Bredberg, L. (1988) CoA- and Non-CoA-dependent Retinol Esterification in Retinal Pigment Epithelium. *J. Biol. Chem.* **263**, 8084-8090.

Saari, J.C. and Bredberg, L. (1989) Lecithin:Retinol Acyltransferase in Retinal Pigment Epthelial Micromomes. *J. Biol. Chem.* **264**, 8636-8640.

Schnetkamp, P.P.M. (1986) Sodium-calcium Exchange in the Outer Segments of Bovine Rod Photoreceptors. *J. Physiol. (London)* **373**, 25-45.

Schnetkamp, P.P.M., and Daemen, F.J.M. (1981) Transfer of High energy Phosphate in Bovine Rod Outer Segments: A Nucleotide Buffer System. *Biochim. Biophys. Acta* **672**, 307-312.

Schnetkamp, P.P.M., Klompmakers, A.A., and Daemen, F.J.M. (1979) The Isolation of Stable Cattle Rod Outer Segments With An Intact Plasma Membrane. *Biochim. Biophys. Acta* **552**, 379-389.

Schroder, W.H. and Fain, G.L. (1984) Light-dependent Calcium Release from Photoreceptors Measured by Laser Micro-mass Analysis. *Nature* **309**, 268-270.

Scopes, R.K. and Stoter, A. (1982) Purification of All Glycolytic Enzymes from One Muscle Extract. *Methods Enzymol.* **90**, 479-490.

Shichi, H. (1983) in *Biochemistry of Vision*. Academic Press, New York.

Shimke, R.T. (1959) Effects of Prolonged Light Deprivation on the Development of Retinal Enzymes in the Rabbit. *J. Biol. Chem.* **234**, 700-703.

Shin, B.C., and Carraway, K.L. (1973) Association of Glyceraldehyde-3-phosphate Dehydrogenase with the Human Erythrocyte Membrane. *J. Biol. Chem.* **248**, 1436-1444.

Sillman, A.J., Ito, H. and Tomita, T. (1969) Studies on the Mass Receptor Potential of the Isolated Frog Retina: On the Basis of the Ionic Mechanism. *Vision Res.* **9**, 1443-1451.

Silverman, M. (1991) Structure and Function of Hexose Transporters. *Annu. Rev. Biochem.* **60**, 757-794.

Sitaramayya, A. and Liebman, P.A. (1983) Mechanism of ATP Quench of Phosphodiesterase Activation in Rod Disk Membranes. *J. Biol. Chem.* **258**, 1205-1209.

Solti, M., Bartha, F., Halasz, N., Toth, G., Sirokman, F., and Friedrich, P. (1981) Localization of Glyceraldehyde-3-phosphate Dehydrogenase in Intact Human Erythrocytes. *J. Biol. Chem.* **256**, 9260-9265.

Steck, T.L. (1974) Preparation of Impermeable Inside-out and Right-side-out Vesicles from Erythrocyte Membranes. *Methods Membr. Bio.* **2**, 245-281.

Stein, W.D. (1986) in *Facilitated Diffusion Across Cell Membranes*, p. 231-306, Academic Press, New York.

Steinberg, R.H., Fisher, S.K. and Anderson, D.H.(1980) Disc Morphogenesis in Vertebrate Photoreceptors. *J. Comp. Neurol.* **190**, 501-518.

Stirling, C.E. and Lee, A. (1980) [^{3}H]Oubain Autoradiography of Frog Retina. *J. Cell Biol.* **85**, 313-324.

Strapazon, E., and Steck, T.L. (1976) Binding of Rabbit Muscle Aldolase to Band 3, the Predominant Polypeptide of the Human Erythrocyte Membrane. *Biochemistry* **15**, 1421-1424.

Strapazon, E., and Steck, T.L. (1977) Interaction of Aldolase and the Membrane of Human Erythrocytes. *Biochemistry* **16**, 2966-2971.

Stryer, L. (1986) Cyclic GMP Cascade of Vision. *Annu. Rev. Neurosci.* **9**, 87-119.

Stryer, L. (1988) in *Biochemistry*. W.H. Freeman and Co., New York.

Stryer, L. (1991) Visual Excitation and Recovery. *J. Biol. Chem.* **266**, 10711-10714.

Szél, A., Takács, L., Monostori, E., Diamantstein, T., Vigh-Teichmann, I., and Röhlich, P. (1986) Monoclonal Antibody-Recognizing cone Visual Pigment. *Exp. Eye Res.* **43**, 871-883.

Thomson, M.J., and Richards, J.F. (1977) Ornithine Decarboxylase and Thymidine Kinase Activity in Tissues of Prolactin-treated RAts: Effect of Hypophysectomy. *Life Sciences* **22**, 337-344.

Thorens, B., Charron, M.J. and Lodish, H.F. (1990) Molecular Physiology of Glucose Transporters. *Diabetes Care* **13**, 209-218.

Thorens, B., Sarkar, H.K., Kaback, H.R., and Lodish, H.F. (1988) Cloning and Functional Expression in Bacteria of a Novel Glucose Transporter Present in Liver, Intestine, Kidney, and *B*-Pancreatic Islet Cells. *Cell* **55**, 281-290.

Tombes, R.M. and Shapiro, B.M. (1985) Metabolite Channeling: A Phosphorylcreatine Shuttle to Mediate High Energy Phosphate Transport Between Sperm Mitochondrion and Tail.

Toyoda, N., Robinson, F.W., Smith, M.M., Flanagan, J.E., and Kono, T. (1986) Apparent Translocation of Glucose Transport Activity in Rat Epididymal Adipocytes by Insulin-like Effects of High pH or Hyperosmolarity. *J. Biol. Chem.* **261**, 2117-2122.

Vidaver, G.A. (1966) Inhibition of Parallel Flux and Augmentation of Counter Flux Shown by Transport Models Not Involving a Mobile Carrier. *J. Theoret. Biol.* **10**, 301-306.

Wald, G. (1968) Molecular Basis of Visual Excitation. *Science* **162**, 230-239.

Wald, G. and Brown, P.K. (1953) The Molecular Extinction of Rhodopsin. *J. Gen. Physiol.* **37**, 189-200.

Wallimann, T., Wegmann, G., Moser, H., Huber, R., and Eppenberger, H.M. (1986) High Content of Creatine Kinase in Chicken Retina: Compartmentalized Localization of Creatine Kinase Isoenzymes in Photoreceptor Cells. *Proc. Natl. Acad. Sci. U.S.A.* **83**, 3816-3819.

Walmsley, A.R. (1988) The Dynamics of the Glucose Transporter. *TIBS* **13**, 226-231.

Wang, C. (1987) The D-Glucose Transporter is Tissue-specific. *J. Biol. Chem.* **262**, 15689-15695.

Wang, C.-S., and Alaupovic, P. (1980) Glyceraldehyde-3-phosphate Dehydrogenase from Human Erythrocyte Membranes. Kinetic Mechanism and Competitive Substrate Inhibition by Glyceraldehyde-3-phosphate. *Arch. Biochem. Biophys.* **205**, 136-145.

Wensel, T.G. and Stryer, L. (1990) Activation Mechanism of Retinal Rod Cyclic GMP Phosphodiesterase Probed by Fluorescein-labeled Inhibitory Subunit. *Biochemistry* **29**, 2155-2161.

Wheeler, G.L. and Bitensky, M.W. (1977) A Light-activated Cyclic GMP Phosphodiesterase. *Proc. Natl. Acad. Sci. U.S.A.* **74**, 4238-4242.

Wheeler, T.J. and Hinkle, P.C. (1981) Kinetic Properties of the Reconstituted Glucose Transporter from Human Erythrocytes. *J. Biol. Chem.* **256**, 8907-8914.

Whitesell, R.R. and Gliemann, J. (1979) Kinetic Parameters of Transport of 3-O-Methylglucose and Glucose in Adipocytes. *J. Biol. Chem.* **254**, 5276-5283.

Wilden, U. and Kuhn, H. (1982) Phosphodiesterase Activation by Photoexcited Rhodopsin Is Quenched When Rhodopsin Is Phosphorylated and Binds the Intrinsic 48-kDa Protein of Rod Outer Segments. *Biochemistry* **21**, 3014-3022.

Winkler, B.S. (1972) The Electroretinogram of the Isolated Rat Retina. *Vision Res.* **12**, 1183-1198.

Winkler, B.S. (1981a) Glycolytic and Oxidative Metabolism in Relation to Retinal Function. *J. Physiol.* **77**, 667-692.

Winkler, B.S. (1981b) The Intermediary Metabolism of the Retina: Biochemical and Functional Aspects. In *Biochemistry and Physiology of the Eye*. R.E. Anderson (ed.), 227-242, American Academy of Ophthalmology, San Francisco.

Winkler, B.S. (1987) In Vitro Oxidation of Ascorbic Acid and Its Prevention by GSH. *Biochim. Biophys. Acta* **925**, 258-264.

Winkler, B.S., DeSantis, N., and Solomon, F. (1986) Multiple NADPH-Producing Pathways Control Glutathione (GSH) Content in Retina. *Exp. Eye Res.* **43**, 829-847.

Wisloki, G.B. and Sidman, R.L. (1954) The Chemical Morphology of the Retina. *J. Comp. Neurol.* **101**, 53-91.

Wong, S. and Molday, R.S. (1986) A Spectrin-like Protein in Retinal Rod Outer Segments. *Biochemistry* **25**, 6294-6300.

Woodruff, M.L., Bownds, M.D. (1979) Amplitude, Kinetics, and Reversibility of a Light-induced Decrease in Guanosine 3',5'-Cyclic Monophosphate in Frog Photoreceptor Membranes. *J. Gen. Physiol.* **73**, 629-653.

Yamazaki, A., Sen, I., Bitensky, M., Casnellie, J.E., and Grrengard, P. (1980) Cyclic GMP-specific High-affinity, Noncatalytic Binding Sites on Light-activated Phosphodiesterase. *J. Biol. Chem.* **255**, 11619-11624.

Yamazaki, A., Hayashi, F., Tatsumi, M., Bitensky, M.W. and George, J.S. (1990) Interactions between the Subunits of cyclic GMP Phosphodiesterase in *Rana Catesbiana* Rod Photoreceptors. *J. Biol. Chem.* **265**, 11539-11548.

Yau, K.-W. and Baylor, D.A. (1989) Cyclic GMP-activated Conductance of Retinal Photoreceptor Cells. *Annu. Rev. Neurosci.* **12**, 289-327.

Yau, K. -W., Haynes, L.W. and Nakatani, K. (1988) Study of the Phototransduction Mechanism in Rods and Cones in *Proceedings of the Retina Rsearch Foundation Symposium*. D.M.-K. Lam (ed.), 41-58, Portfolio Publishing Company, Inc. Texas.

Yau, K. -W. and Nakatani, K. (1984) Electrogenic Na-Ca Exchange in Retinal Rod Outer Segment. *Nature* **311**, 661-663.

Yau, K. -W. and Nakatani, K. (1985) Light-induced Reduction of Cytoplasmic Free Calcium in Retinal Rod Outer Segment. *Nature* **313**, 252-255.

Yee, R. and Liebman, P.A. (1978) Light-activated Phosphodiesterase of the Rod Outer Segment. Kinetics and Parameters of Activation and Deactivation. *J. Biol. Chem.* **253**, 8902-8909.

Yeltman, D.R. and Harris, B.G. (1982) Fructose-bisphosphate Aldolase from Human Erythrocytes. *Methods Enzymol.* **90**, 251-254.

Yokishima, S. and Hagins, W.A. (1970) Ionic Basis of Dark Current and Photocurrent of Retinal Rods. *Biophys. J.* **10**, 60a.

Yu, J., and Steck, T.L. (1975) Associations of Band 3, the Predominant Polypeptide of the Human Erythrocyte Membranes. *J. Biol. Chem.* **250**, 9176-9184.

Zoccoli, M.A. and Lienhard, G.E. (1977) Monosaccharide Transport in Protein-depleted Vesicles from Erythrocyte Membranes. *J. Biol. Chem.* **252**, 3131-3135.

Zuckerman, R., Buzdygon, B., Philip, N., Liebman, P., Sitaramayya, A. (1985) Arrestin: An ATP/ADP Exchange Protein that Regulates cGMP Phosphodiesterase Activity in Retinal Rod Disk Membranes (RDM). *Biophys. J.* **47**, 37a.